

IDENTIFYING AND ASSESSING WINDBREAKS IN FORD COUNTY, KANSAS USING
OBJECT-BASED IMAGE ANALYSIS

by

MIKE W. DULIN

B.S., KANSAS STATE UNIVERSITY, 2007

A THESIS

submitted in partial fulfillment of the requirements for the degree

MASTER OF ARTS

Department of Geography
College of Arts and Sciences

KANSAS STATE UNIVERSITY
Manhattan, Kansas

2009

Approved by:

Major Professor
Dr. J.M. Shawn Hutchinson

Abstract

Windbreaks are a valuable resource in conserving soils and providing crop protection in western Kansas and other Great Plains states. Currently, Kansas has neither an up-to-date inventory of windbreak locations nor an assessment of their condition. The objective of this study is to develop remote sensing and geographic information system methods that rapidly identify and assess the condition of windbreaks in Ford County, Kansas. Ford County serves as a pilot study area for method development with the intent of transferring those methods to other counties/regions in Kansas and the Great Plains. A remote sensing technique known as object-based classification was used to classify windbreaks using color aerial photography acquired through the 2008 National Agricultural Imagery Program. Object-based classification works by segmenting imagery where areas with similar spectral, shape, and textural properties are grouped into vectors (*i.e.*, objects) that are later used as the basis for image classification. Using this technique, 355 windbreaks, totaling nearly 1,012 acres (410 hectares), were identified in Ford County. When compared to a spatial dataset of confirmed windbreak locations generated via a heads-up digitizing process, the location of windbreaks identified using object-based classification results agreed approximately 81% of the time. Mean textural and spectral values were then combined and used to place identified windbreaks into three condition categories (good, fair, and poor) using a manual classification approach. Analysis showed the area of windbreaks in good condition to be 170 hectares, with the remaining 171 hectares of windbreaks falling in the fair or poor classes. Methods detailed in this study proved successful at rapidly identifying windbreak location and for providing useful condition class results for windbreak renovation and restoration planning.

Table of Contents

List of Figures	v
List of Tables	vii
List of Equations	ix
List of Equations	ix
Acknowledgements	x
Dedication	xi
CHAPTER 1 - Introduction	1
Purpose and Objectives	3
Applied and Academic Contribution	6
CHAPTER 2 - Literature Review	8
Windbreaks	8
Previous Windbreak Assessments	9
Remote Sensing	12
Object-based Classification Concepts	14
Object-based Classification Implementation	21
CHAPTER 3 - Study Area	25
CHAPTER 4 - Data and Methods	32
Imagery	32
Image Preprocessing	33
Image Segmentation and Merging	36
Attribute Value Extraction	40
Image Classification	42
Object-based Classification Accuracy Assessment	46
Moving from Test Site to County	48
Windbreak Extraction	52
Windbreak Condition Assessment	53
Acreage Calculations	57
Ground Truth Data Collection	58

Highly Erodible and Impaired Soils Layer	59
CHAPTER 5 - Results and Discussion	62
Segmentation Results.....	62
Classification Accuracy	63
Windbreak Classification Accuracy	66
Windbreak Condition Assessments	69
Windbreaks in Highly Erodible and Impaired Areas.....	79
CHAPTER 6 - Conclusions	81
CHAPTER 7 - References	87
Appendix A - 2001 National Land Cover Dataset Landcover Codes and Descriptions.....	96
Appendix B - Feature Attribute Description.....	97
Appendix C - Attributes Selected For Classification.....	101
Appendix D - Procedures for using the ENVI Zoom 4.5 <i>Feature Extraction Module</i>	103

List of Figures

Figure 1. Field windbreak located 20 miles east of Dodge City, Kansas.	1
Figure 2. Field windbreak located approximately 25 miles east of Dodge City Kansas.	2
Figure 3. Classification diagram used by Read (1958) to assess the condition of windbreaks. ..	11
Figure 4. A visual example of the segmentation process.....	16
Figure 5. Differences between the main and first-order lines of an object.....	19
Figure 6. Ford County study area with Kansas Forest Service districts highlighted.....	25
Figure 7. Landcover/Landuse classes in Ford County.....	27
Figure 8. Graph of population change in Ford County, 1870-2009.....	29
Figure 9. Five year precipitation averages for Ford County, 1895-2006.....	30
Figure 10. Five year mean temperatures for Ford County, 1895-2006.	31
Figure 11. Workflow sketch of the methods used in this research.	33
Figure 12. Comparison of the Ford County 2008 NAIP image at 1 and 6 meter pixel size.....	36
Figure 13. Location of Ford County test site.	37
Figure 14. Screenshot of the ENVI Zoom 4.5 Feature Extraction Module and viewing portal. .	38
Figure 15. Screenshot of the band thresholding operation used to eliminate areas not required for windbreak classification.....	41
Figure 16. Classified landuse/landcover map of the features generated in Ford County using object-based classification.	51
Figure 17. Highly erodible and impaired soils in Ford County, Kansas.	60
Figure 18. Segmented image of vegetative features in Ford County (1:235,000 scale).	62
Figure 19. Portion of the segmented image of vegetative features for Ford County (1:60,000 scale).	63
Figure 20. Images displaying accurate windbreak border assignment and an inaccurate border assignment.....	66
Figure 21. Example of a fragmented windbreak classified by NRCS as a single unit, but as two distinct units by object-based classification.....	68
Figure 22. Box-and-whisker plot illustrating the overlap in NDVI values across windbreak condition classes for field-surveyed windbreaks.....	72

Figure 23. Box-and-whisker plot illustrating the variation in textural values across windbreak condition classes for field-surveyed windbreaks. 76

Figure 24. Example of windbreak classified during a field survey as being in good condition but in poor condition when using the standard deviation classification technique..... 79

Figure 25. Example of a fair condition windbreak containing several areas that need renovation activities. 80

List of Tables

Table 1. Common windbreak tree species in Ford County, Kansas.	9
Table 2. Total area of each landuse/landcover class in Ford County (Source: 2001 NLCD).....	28
Table 3. Historic population change in Ford County, Kansas.	28
Table 4. Annual precipitation for Ford County, 2000-2008.	30
Table 5. Custom landuse/landcover classes developed based on expert knowledge of the features remaining in the Ford County image after band thresholding.	44
Table 6. Discrete Capability Index overall interval types.....	45
Table 7. Example of a populated error matrix with generic variables.	48
Table 8. Parameter settings used to classify the Ford County 2008 NAIP image.	49
Table 9. Final landuse/landcover categories used in the Ford County classification.	50
Table 10. Number of training sites selected for each landuse/landcover class in Ford County. .	50
Table 11. Software processing times required for each step in the classification of the Ford County NAIP image using object-based methods.	52
Table 12. Windbreak condition class evaluation guide.	58
Table 13. Windbreak attributes used to place windbreaks into condition classes.	59
Table 14. Classification error matrix for the Ford County test site.	64
Table 15. Error matrix compiled from a random distribution of sample points for the Non-Windbreak (NWB) and Windbreak classes.	65
Table 16. Comparison of windbreak acres for the NRCS and object-based classification products.....	67
Table 17. Error matrix for windbreak condition assessment based on average green reflectance and a quantile classification scheme.	69
Table 18. Error matrix for windbreak condition assessment based on average green reflectance and a natural breaks classification scheme.	70
Table 19. Error matrix for windbreak condition assessment based on average green reflectance and a standard deviation (SD) classification scheme.	71

Table 20. Error matrix for windbreak condition assessment based on average NDVI values and a quantile classification scheme.....	73
Table 21. Error Matrix for windbreak condition assessment based on average NDVI values and a natural breaks classification scheme.	73
Table 22. Error matrix for windbreak condition assessment based on average NDVI values and a standard deviation (SD) classification scheme.	73
Table 23. Error matrix for windbreak condition assessment based on mean texture values and a standard deviation (SD) classification scheme.	76
Table 24. Error matrix for windbreak condition assessment based on average condition index values and a standard deviation (SD) classification scheme.....	77
Table 25. Windbreak area by condition class.	78
Table 26. Total area of Ford County windbreaks located on highly erodible and impaired soils by condition class.....	79

List of Equations

Equation 1. Full Lambda-Schedule algorithm for segment merging.....	39
Equation 2. Method used to distinguish between classes by DCI interval type.	45
Equation 3. The Fitzpatrick-Lins equation.	47
Equation 4. The Cohen Kappa statistic.....	49
Equation 5. Normalized Difference Vegetation Index (NDVI).....	55
Equation 6. Formula to calculate area (m ²) for each windbreak condition class.....	57
Equation 7. Formula to convert area to acres from square meters.....	57
Equation 8. Formula to convert acres to hectares.	57
Equation 9. Implementation of the Fitzpatrick-Lins equation.	64

Acknowledgements

I would like to thank Dr. J.M. Shawn Hutchinson (Department of Geography, Kansas State University) for a tremendous amount of input and advice pertaining to this manuscript. I would also, like to thank Dr. Hutchinson for giving me the opportunity to work in the Geographic Information Systems and Spatial Analysis Laboratory (GISSAL) in the Department of Geography at Kansas State University. The valuable work experience I received in GISSAL made this project possible and finally got me a job working for Uncle Sam at the Army Corps of Engineers.

Dr. John Harrington Jr. and Dr. Douglas Goodin, who served as my two additional committee members, deserve special thanks for all of their advice and guidance which helped lead to the completion of this manuscript.

Funding for this research was provided from the Kansas Forest Service (KFS) through a USDA State and Private Forestry FY 2008 Western Competitive Grant. Thanks to Robert Atchison (KFS) this grant was successfully funded for years 2008-2010.

Finally, I would like to thank my fiancée Danielle White for her understanding, patience, and love as I had to dedicate more time to my work than her. Thanks for sticking with me Danielle!

Dedication

This thesis is dedicated in loving memory to the late Pamela Dulin (Dec. 31, 1949 – July 22, 2005). You were a wonderful mother and are greatly missed. It was through your guidance and dedication as a mother that my college education was made possible.

CHAPTER 1 - Introduction

Windbreaks, also known as shelterbelts, are a valuable resource in conserving soil and providing crop protection in western Kansas, as well as many other Great Plains states (Brandle *et al.*, 2004). Many of these windbreaks were planted to reduce wind erosion during the Dust Bowl era of the 1930's (Read 1958). The Society of American Foresters (SAF) defines a windbreak as “a strip of trees or shrubs maintained mainly to alter wind flow and microclimates in the sheltered zone, usually farm buildings.” SAF also defines a shelterbelt as a “strip of trees or shrubs maintained mainly to alter wind flow and microclimates in the sheltered zone, usually agricultural fields” (R. Atchison 2008, pers. comm.). Brandle *et al.*, (2004) provide a much simpler definition “Windbreaks or shelterbelts are barriers used to reduce wind speed.” In this study, the Brandle *et al.*, (2004) definition will be used as both farmstead and field windbreaks are objects of interest. Figures 1 and 2 are photos of multi-row windbreaks commonly found throughout the Ford County study area.

Figure 1. Field windbreak located 20 miles east of Dodge City, Kansas.



Figure 2. Field windbreak located approximately 25 miles east of Dodge City Kansas.



Currently, Kansas has neither an up-to-date inventory of windbreak locations nor an assessment of their condition. In this study, methods are applied to identify the location and assess the condition of windbreaks in Ford County, Kansas using remote sensing (RS) and geographic information system (GIS) techniques. The most recent study in Kansas was completed in 1992, when the U.S. Department of Agricultural (USDA) Natural Resource Conservation Service (NRCS) determined there were approximately 78,000 windbreaks in the state (R. Atchison 2008, pers. comm.). Most natural resource professionals agree that field windbreaks are a declining resource in Kansas and that few new ones are being established, yet there is little good science available to efficiently document windbreak location, size, or condition. Still, the 1997 NRCS Natural Resource Inventory (NRI) suggests that wind continues

to erode 1.8 million acres (728,434 ha) of cropland in Kansas at rates that exceed tolerable limits (around 1.3 tons/acre/year) (R. Atchison 2008, pers. comm.).

Sorenson and Marotz (1977) expressed concerns that windbreaks in Kansas were beginning to be removed over 3 decades ago. Many of the windbreaks planted in western Kansas were planted during the Dust Bowl era when Congress passed the Prairie States Forestry Act (PSFA) (Croker 1991). The Act called for the planting of millions of trees and tens of thousands of shelterbelts in an attempt to prevent eolian erosion and to create jobs for a destitute Great Plains economy (Read 1958). Bates (1924) pointed out that, before the Dust Bowl, the lack of windbreaks in the Great Plains was a “severe handicap” to agricultural land. It is now timely to build upon previous work of the NRCS and additional shelterbelt research projects to develop methods for the rapid identification of windbreak location and an assessment their condition..

Purpose and Objectives

The main purpose of this research is to work in conjunction with the Kansas Forest Service (KFS) to develop GIS and RS methods to identify the location, size, and condition of windbreaks in Ford County, Kansas. In addition, it is the purpose of this research to determine how well automated classification schemes match with ground truth data of windbreak condition. Once a satisfactory method of classification has been obtained, the same or similar methods can be used in future research to locate and assess windbreaks in other western Kansas counties and across the Great Plains.

This project has three primary goals:

- 1) To rapidly classify windbreaks using object-based classification on County Composite Mosaic (CCM) aerial imagery,
- 2) To develop a secondary classification to assess windbreak condition (good, fair, poor) and determine the number of acres/hectares that exist in each class, and
- 3) To identify windbreaks located on highly erodible and impaired soils.

To achieve these goals a remote sensing technique known as object-based classification was used to classify windbreaks from 2008 National Agriculture Imagery Program (NAIP) imagery. Attributes from four spectral bands (blue, green, red, and near-infrared) present in the NAIP imagery were used in the classification process. Object-based classification takes into account size, shape, and context as well as spectral information of features identified for classification (Baatz *et al.*, 2004). These non-spectral classification criteria are crucial for accurate classification of windbreaks for two reasons. First, windbreaks are usually linear strips of tree plantings. A riparian area could easily share similar spectral reflectance characteristics as a windbreak making it difficult to distinguish between the two features without considering some shape criteria in the classification. Second, some object-based classification software packages allow for the isolation of features of interest. This option means that based on certain shape and spectral parameter settings, one can eliminate features in the image that are not of interest before beginning the classification process, resulting in more efficient classification and image processing times.

Traditionally, foresters determine windbreak condition using measures of tree density and/or porosity. In addition, windbreak condition can also be based on how well it is functioning as a wind restraint. A dense windbreak is capable of blocking more wind from the sheltered

zone while a sparsely-planted windbreak provides less wind resistance over the same area. Read (1958) developed condition classification criteria that are still widely accepted and used (R. Atchison pers. comm. 2008). Read's classification approach requires field crews to visit each windbreak and look through it horizontally to determine density. In this study, windbreak condition is assessed using a vertical view provided by aerial photographs. If assessment results generated by analysis of aerial photography compare well with ground-based assessments, many hours of field surveying could be replaced with digital image processing for condition assessments.

The mean spectral reflectance brightness values (BV) of windbreak features in the green band (band 2) of windbreaks were used to determine windbreak condition. The average BV of a windbreak should correlate well with vegetation density and tree cover within a given stand. Dense windbreaks appear as dark linear features with few gaps where bare soil and grass is visible through the tree canopy. Such windbreaks should be in relatively good condition and have a lower average BV as compared to a less dense windbreak with multiple or large gaps in the stand.

Normalized Difference Vegetation Index (NDVI) was also calculated from the NAIP image to perform a second condition assessment and then be compared with results from the BV-based assessment. As a measure of greenness, average NDVI values for a windbreak should be a good measure of vegetation abundance and health. A third, and final, condition assessment was performed using a condition index based on both mean textural values and BV's using a linear scaling model suggested by Booyesen (2002).

In addition to knowing the location and associated condition of windbreaks, Kansas foresters are also interested in understanding more about the soils on which they are found. To

achieve the third goal of this project, a geospatial data layer of highly erodible and impaired soils was obtained from Hutchinson *et al.*, (2008). This layer was composed of agricultural crop land and soils with a wind erodibility index (WEI) of 87 or greater. Identifying windbreaks in these vulnerable areas can assist foresters in prioritizing windbreak renovation projects and new areas for future plantings.

Applied and Academic Contribution

Results from this research will assist foresters in Kansas as they plan for future windbreak renovations and identify sites for new plantings. In addition, this research may serve as a catalyst for future research that places a monetary value on the ecosystem services provided by windbreaks. Within the academic realm of geography this research helps answer one of the most common questions in the discipline, ‘where?’(Pattison 1963; Golledge 2002; Cutter *et al.*, 2004). Cutter *et al.*, (2004) identify ten “Big Questions in Geography” that are meant to work as guides in helping bring geographic research to the public in meaningful and useful ways. Research from this project addresses two of these questions:

- 1) “How has the earth been transformed by human action?” and
- 2) “What role will virtual systems play in learning about the world?”

Prior to the 1930’s few, if any, windbreaks existed in Kansas or the Great Plains (Crocker 1991). Identifying windbreaks will contribute to the understanding of how humans have modified the landscape in the interest of soil loss prevention. Additionally, use of RS and GIS methods is likely to promote better understanding of ‘what’ we can identify ‘where’ on the landscape. Understanding the capabilities and limits of virtual systems is a fundamental element

when determining the scenarios for which these systems can be effectively used to extracting valid information from real-world imagery.

CHAPTER 2 - Literature Review

Windbreaks

Windbreaks provide a number of environmental benefits for semi-arid regions throughout the world. Windbreaks provide protection from wind for cattle, crops, and soil as well as homes and other structures (Kort and Stefner 2007; Brandle *et al.*, 2004). Stoeckeler and Williams (1949) reported many farmers throughout the Great Plains encountered a drastic reduction in winter fuel expenses after planting windbreaks to protect their homes.

Windbreaks first appeared on the landscape in Scotland during the mid-1400's after Scottish Parliament urged planting to assist in soil loss prevention on agricultural lands (Brandle *et al.*, 2004; Droze 1977). The first major planting of windbreaks in the United States occurred during the 1930's. Due to Dust Bowl conditions, U.S Congress authorized the Prairie States Forestry Project (PSFP) to assist with planting of shelterbelts to minimize wind erosion and decrease the number and intensity of dust storms (Brandle *et al.*, 2004; Droze 1977; Read 1958). Many of the dust storms common to Kansas were the result of severe drought, mismanaged agricultural land, and "suit case farming" practiced by transient farmers (Saloutos 1969 pg. 1). The PSFP provided jobs for an economically distressed population and resulted in the planting of over 200 million trees and shrubs totaling 18,600 miles in length (Read 1958). Between 1935 and 1942, the PSFP was successful in planting shelterbelts on 30,000 farms stretching from the Canadian border of North Dakota south to the Texas Panhandle (Read 1958). Windbreaks planted in western Kansas consisted mainly of the species listed in Table 1.

Controversy arises, however, when dealing with the total number of trees actually planted by the PSFP. Croker (1991) stated that only 145 million trees were planted by the PSFP between

1935 and 1942, which is not consistent with the numbers given by Read (1958). Though the numbers do not match, there is little argument that the PSFP was “One of the greatest projects ever attempted by man to improve the environment of our planet” (Crocker 1991 pg. 4).

Table 1. Common windbreak tree species in Ford County, Kansas.

Scientific Name	Common Name
<i>Prunus angustifolia</i>	Sand Hill plum
<i>Prunus americana</i>	American Plum
<i>Prunus virginiana</i>	Choke Cherry
<i>Fraxinus pennsylvanica</i>	Green Ash
<i>Populus deltoides</i>	Eastern Cottonwood
<i>Ulmus pumila</i>	Siberian Elm
<i>Celtis occidentalis</i>	Hackberry
<i>Gleditsia triacanthos</i>	Honey Locust
<i>Quercus macrocarpa</i>	Bur Oak
<i>Gymnocladus dioica</i>	Kentucky Coffee Tree
<i>Juniperus scopulorum</i>	Rocky Mountain Juniper
<i>Juniperus virginiana</i>	Eastern Red Cedar
<i>Pinus ponderosa</i>	Ponderosa Pine
<i>Pinus sylvestris</i>	Scotch Pine
<i>Pinus nigra</i>	Austrian Pine

Previous Windbreak Assessments

In 1938, the first windbreak survey in the United States was conducted to assess the survival rate of windbreaks as a whole and not just the individual health of trees planted during the PSFP. Results showed that 61% of all species planted survived (Read 1958). Factors cited for the failure of the remaining 39% of plantings included poor agricultural practices, insects, rodents, and improper planting strategies (Read 1958). While this survey reported a fairly high survival rate for plantings, it did not take into consideration the condition of surviving windbreaks.

In forestry terms, windbreak condition is determined based on how well it is functioning rather than solely on the health of individual trees. Function ratings are based on the number of

gaps (*i.e.*, porosity) in a windbreak (Cornelis and Gabriels 2005). Porosity can be measured as a ratio between the open area and the total area of a windbreak (Cornelis and Gabriels 2005; Jensen 1954).

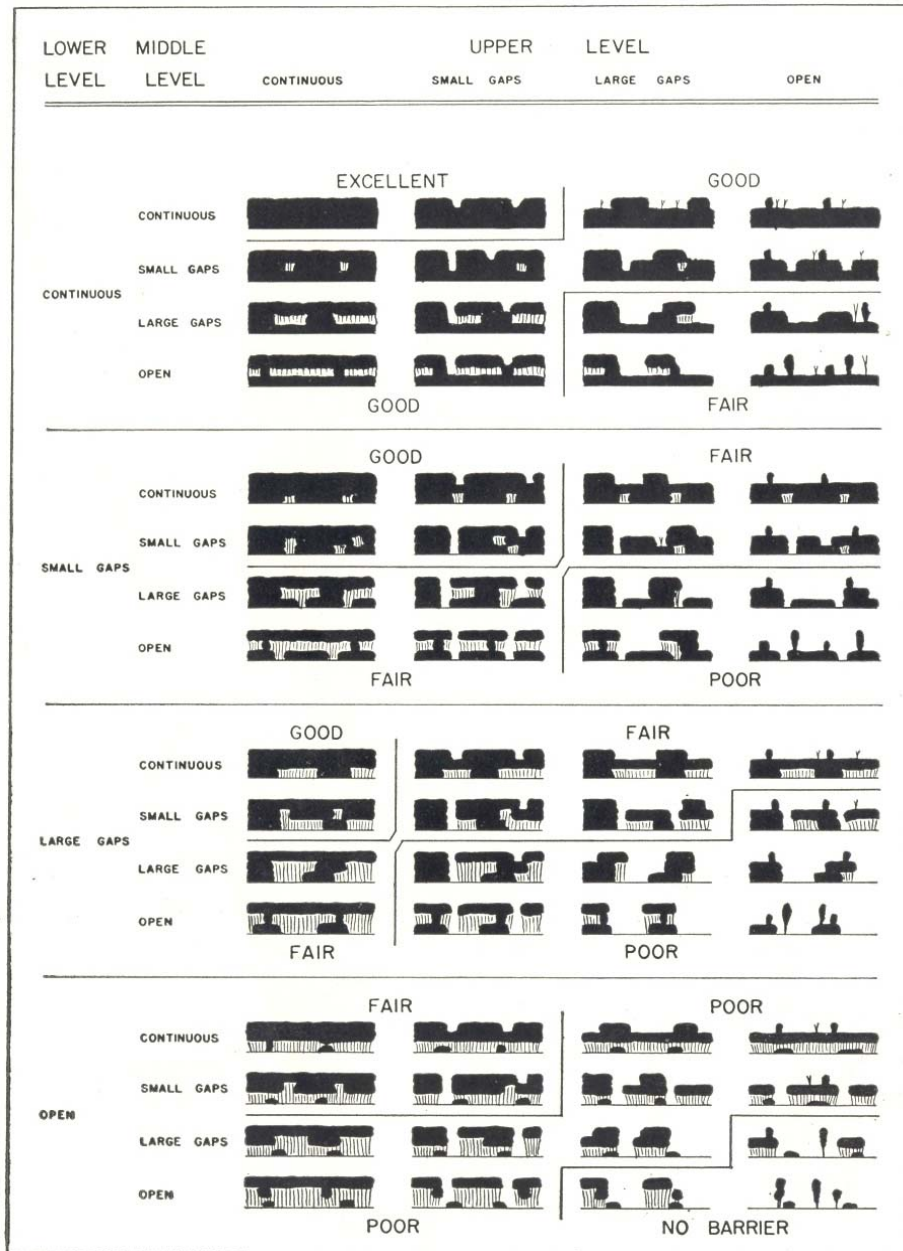
A second survey was conducted in 1944 to assess PSFP-planted windbreaks. By this time, the plantings ranged in age from 4 to 7 years (Read 1958). Samples included over 1,000 windbreaks spanning from North Dakota to Texas with 78% of them being rated in good condition or higher (Read 1958). Read (1958) explains that the criteria for classifying a windbreak as “good” was based only on “survival and the potential of producing a barrier”.

In 1954, Read (1958) conducted another survey that re-examined many of the same windbreaks (938 or 1,079) sampled ten years earlier. His research took into consideration survival, height, diameter at breast height (DBH), vigor, crown spread, and continuity of trees for each species. In addition, Read (1958) also developed four classes (good, fair, poor, or destroyed) into which windbreaks could be placed based on their “effectiveness”, which is now considered to be “function” (Figure 3). Good windbreaks in the Read (1958) study exhibited moderate but continuous density throughout the stand. Windbreaks in the poor class generally had low density with sparsely separated or clumped trees. Read (1958) reported that 42% of the windbreaks surveyed were in good or excellent condition, 31% were classified as fair, 19% classified as poor, and the remaining 8% had been removed (Ticknor 1989).

More recently, the 1992 NRCS Natural Resource Inventory (NRI), the last assessment conducted in Kansas, identified 78,000 windbreaks in the state. These windbreaks covered a total of 114,000 acres and extended a collective length of 20,000 miles. Of those windbreaks surveyed, 13% were found to be in excellent condition, 38% good, 34 % fair and 15% poor (United States Department of Agriculture 1994). In producing the 1992 NRI, NRCS adopted

many of the same criteria for classifying windbreaks as those used by Read (1958). Read's classification scheme remains the most widely accepted and used method of rating windbreaks in the field (R. Atchison 2008 pers. comm.).

Figure 3. Classification diagram used by Read (1958) to assess the condition of windbreaks.



Recently, Wiseman *et al.*, (2007) used object-based image analysis using very-high resolution (VHR) imagery to identify and assess windbreaks. Segmentation methods were used on VHR images to create a spatial polygon file which was then used to extract windbreaks via Structured Query Language (SQL) queries within a GIS. A total of 27 sample windbreaks were selected throughout a study area located approximately 150 kilometers east of Winnipeg, Manitoba, Canada. Of these 27 windbreaks, 26 were classified correctly when compared to ground truth data. Wiseman *et al.*, (2007) also used spectral properties from the red, green, and blue bands to determine windbreak density and shape characteristics along with expert knowledge to extract windbreak vectors from their segmented data.

Remote Sensing

Remote sensing is commonly used for the identification, extraction, and classification of landuse/landcover types (Koch *et al.*, 2007). Biophysical remote sensing techniques have also been proven useful in monitoring vegetation biomass, soil moisture, surface temperature, and surface texture (Jensen 1983). At the simplest level, remote sensing can be thought of as the process of extracting data from real world imagery (Quattrochi *et al.*, 1989). Geographic remote sensing requires that users understand the nature of the imagery they are working with (*i.e.*, knowing what landcover features they are looking at) and the drivers or physical processes that determine why particular features or cover types are located where they are (Quattrochi *et al.*, 1989).

Remote sensing methods take advantage of advanced sensors to capture images of particular features or geographic areas. The process of gathering remotely-sensed imagery has been around for over 150 years (Jensen 2007). In 1858, the first aerial image was captured by the Frenchman Nadar from a tethered balloon (Jensen 2007). Modern sensors are capable of

capturing imagery at multiple angles, various spatial resolutions, and using most areas of the electromagnetic spectrum. These advanced sensors can be found on satellites orbiting the earth, onboard terrestrial aircraft, and even contained within portable units that users can take to the field to capture detailed information about the earth's surface (Rostoker *et al.*, 1995; Moran *et al.*, 1997; Diner *et al.*, 1999; Landgrebe 2003; Jensen 2007).

Imagery collected through remote sensing is not only used for visual interpretation, but also to extract relevant thematic information through classification and to analyze various biophysical properties of vegetative land cover (Jensen 2005). Extracting thematic information from imagery is typically accomplished through 'supervised' or 'unsupervised' classification approaches (Jensen 2005; Richards and Xiuping 2005; Schowengerdt 2007).

In a supervised classification, known ground truth points are selected as training sites for a predefined number of thematic classes. These training sites are then used in classification algorithms to group like clusters of homogeneous pixels into their respective class (Jensen 2005; Richards and Xiuping 2005). In unsupervised classifications, algorithms are used to group like pixels into categories with little, or no, prior knowledge of the thematic types present in the imaged area (Duda *et al.*, 2001; Jensen 2005). Once the unsupervised classification scheme groups like pixels, the user then labels the groups or classes according to their corresponding information class as determined from expert knowledge or ground truth data (Famiglietti *et al.*, 1999; Jensen 2005).

Both supervised and unsupervised classification methods have traditionally been accomplished on a per-pixel basis. Per pixel classifications takes into account only the spectral value of a single pixel, which limits its capability to identify 'features' and process VHR data (Jensen 2005). More recently, object-based classification methods have been gaining in

popularity. Object-based classifications group homogeneous pixels through a segmentation process and convert them to multi-pixel shapes which later become the basis for classification (Blashke *et al.*, 2004; Jensen 2005). Objects created during segmentation provide not only spatial information, but also have spectral and textural properties of the objects associated with them (Baatz *et al.*, 2004). For example, each segmented object will have an associated mean pixel value for each electromagnetic waveband as an attribute which can be used later during classification.

Object-based Classification Concepts

Object-based classification is not a new idea. While the approach has been known since the 1970's, a lack of computing power has prevented its widespread use until very recently (Rutherford and Rapoza 2008). Traditional pixel-based classification only takes into account position, size, and value of individual pixels in remotely-sensed imagery (Jensen 2005). Object-based classification takes into account not only the position, size, and spectral characteristics of individual objects, but also shape and context as a fourth category to delineate between individual landscape features, or objects (Blaschke *et al.*, 2004). Essentially, object-based classification allows a classification scheme to be based on the shape of objects or features rather than simply the spectral reflectance of single pixels. The main purpose of object oriented-image analysis is to extract or identify "real world objects" that are "proper in shape and proper in classification" (Baatz *et al.*, 2004).

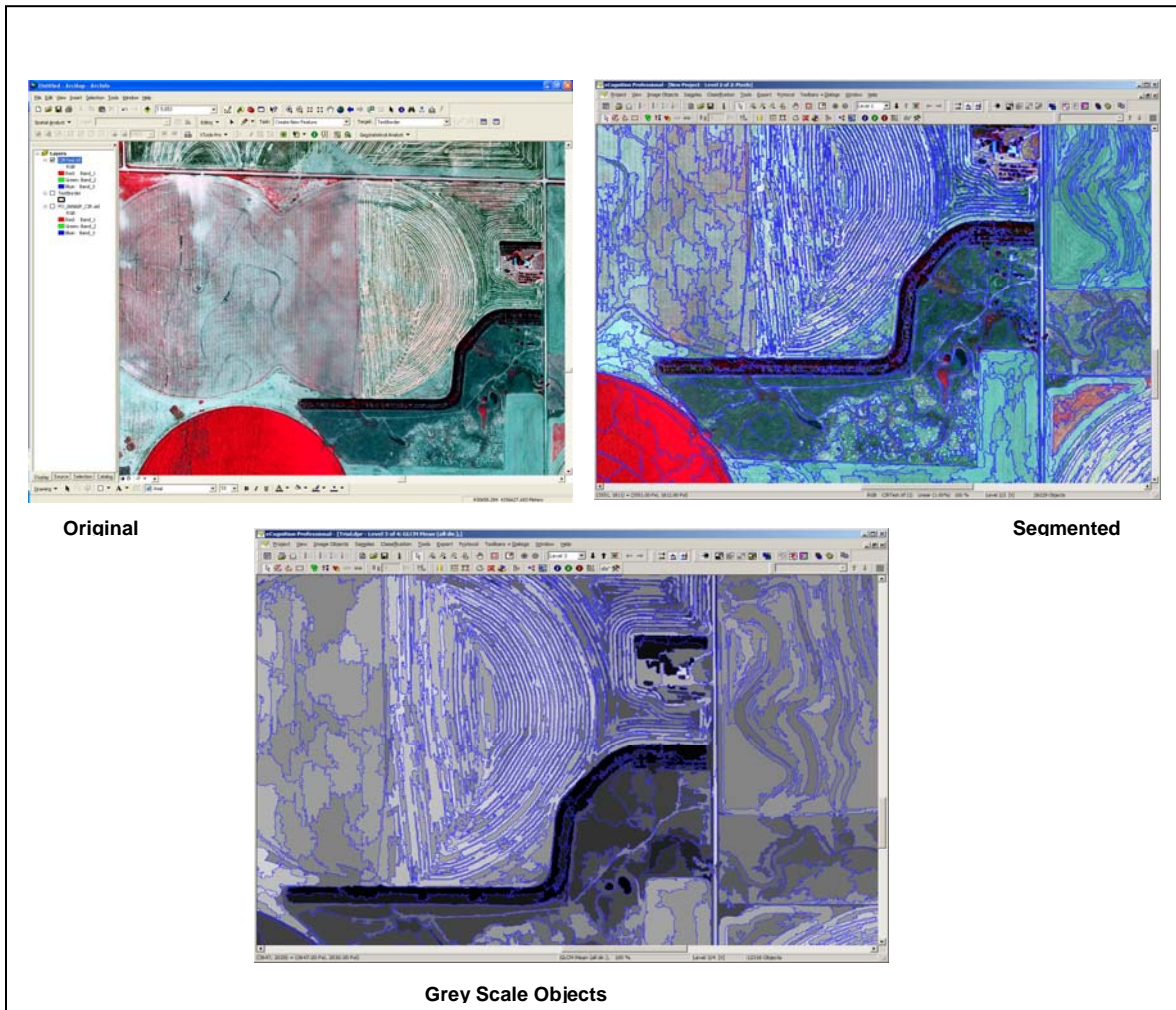
Object-based classification depends on a critical process called segmentation. Segmentation groups similar pixels together to create object vectors. Conceptually, segmentation methods are used to divide an image into homogeneous objects or regions for extraction and classification (Koch *et al.*, 2007). However, a "general segmentation method,

which performs well in many contexts, does not exist” (Kermad and Chehdi 2002 pg. 542). This means that a general scale parameter setting, which determines the size of objects to be created, does not exist to segment all desired objects all the time in remotely-sensed images. In the context of this study, if the scale-based segmentation parameter is set too high, the image may be segmented into very large polygons that encompass much more area than the features of interest (*e.g.*, windbreaks). Alternatively, if the scale parameter is set too low, then the image could be segmented the component pieces of a feature of interest (*e.g.*, individual trees in a windbreak) and fail to capture the entire feature as one object. Figure 4 is provided to facilitate visualization of a segmented aerial image.

In order to overcome the issues surrounding scale-based segmentation parameter settings, many parameter values need to be tested to determine the optimal segmentation size(s) based on the type of object(s) a user wants to classify (Rutherford and Rapoza 2008). This approach introduces some subjectivity into the segmentation process but little has been done to generalize segmentation parameters in the interest of isolating any given set features.

There are three basic and accepted approaches to performing image segmentation: Pixel, edge, and region (Blaschke *et al.*, 2004). Pixel-based approaches assign a label to continuous patches of pixel cells. Edge-based methods attempt to identify edges between regions and assign labels to boundaries between regions where a pixel value change occurs. According to Robinson *et al.*, (2002), the edge-based approach works fastest because it incorporates only the scale parameter into the segmentation process. Region and pixel-based segmentation methods incorporate compactness (ratio of pixels in the perimeter length) and smoothness (jagged edges vs. smooth edges) into the segmentation algorithm which slows down processing time (Kermad and Chehdi 2002; Jensen 2005).

Figure 4. A visual example of the segmentation process.



Region-based techniques are subdivided into three categories: Region growing, region merging, and region splitting (Batz *et al.*, 2004). Seed points are used to start this region-based process. Next, neighboring pixels are joined to the original seed point until a specific size threshold is met. After this, the process starts over with a new set of seed points (Blaschke *et al.*, 2004). Kermad and Chehdi (2002) suggest that an integrated segmentation approach will yield the best results, especially when edge- and region-based approaches are combined. Often, a bottom-up region-merging segmentation approach beginning with an individual pixel has proven

quite successful. This approach, referred to as the fractal net evolution approach (FNEA), is inherent in the eCognition (Definiens, Muchen Germany) digital image segmentation software (Huang and Zhang 2008).

The ENVI Zoom 4.5 *Feature Extraction Module* (ITT Visual Information Solutions, Boulder, Colorado), which was used in this research, uses an edge-based algorithm developed by Robinson *et al.*, (2002) to segment imagery. However, little research has been published using this software due to its recent availability (ITT Visual Information Solutions 2008). The edge-based algorithm is intended to work very fast because it requires only one parameter input (scale level) (ITT Visual Information Solutions 2008). Robinson *et al.*, (2002) algorithm was developed to detect edge features then merge neighboring regions based on similar measures of spectral values as scale parameter increases.

Expert knowledge, or knowledge-based image interpretation, is a strategy in which a user determines the proper segmentation and classification parameters based on his/her knowledge of the objects they wish to classify (Rutherford and Rapoza 2008; Benz *et al.*, 2004). For example, users can look at an image and determine if the segmentation parameters did or did not adequately capture the objects of interest. Benz *et al.*, 2004 (pg. 241) list four key points to employ the best knowledge-based image interpretation techniques:

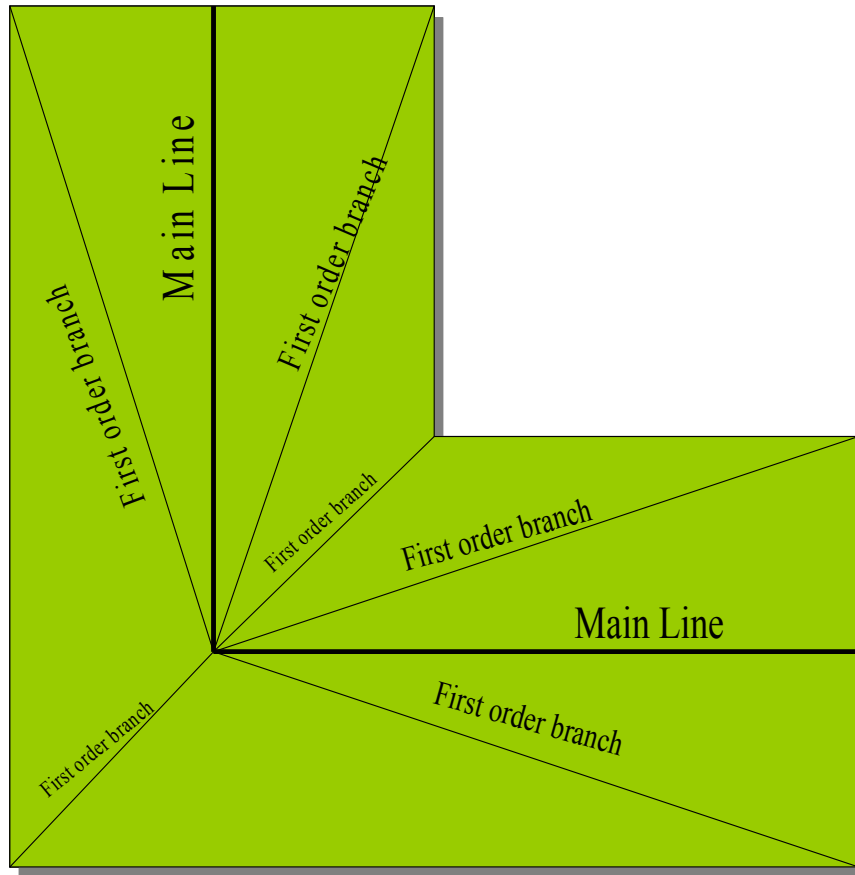
1. Understanding sensor characteristics,
2. Understanding the appropriate scale of analysis,
3. Identification of typical context and hierarchical dependencies,
4. Consideration of inherent uncertainties of the whole information extraction system, starting with the sensor, up to fuzzy concepts for the requested information.

Complementary to expert knowledge, is the ability of object-based classification to account for the compactness, smoothness, and linearity of various objects (Tian and Chen 2007; Baatz *et al.*, 2004). Linearity can be represented by three different object feature measures: (1) Length/width of object, (2) length/width of main line, and (3) length/width of main line plus long branches of first order” (Tian and Chen 2007). Tian and Chen (2007) suggest that using length/width of main line is far superior to length/width of object because it can capture the true linearity of objects. Figure 5 illustrates a generic main line and first order lines of a generic object. Baatz *et al.*, (2004) mentions, however, that relying too much on shape information may reduce the quality of segmentation and advises users to emphasize spectral information while incorporating shape information only when necessary.

Rectangular fit is another important criterion that can be used to capture the linear nature of windbreaks. According the ENVI Feature Extraction Module User’s Guide (ITT Visual Information Solutions 2008), rectangular fit can be used to eliminate circular and radically ‘jagged’ features from any class when deemed necessary by the user.

Scale is also an important factor when setting segmentation parameters. In remote sensing “a certain scale is always presumed by pixel resolution” but “objects of interest often have their own inherent scale” (Benz *et al.*, 2004 pg. 241). For example, while a windbreak may not be visible on a LANDSAT 5 image with 30 meter spatial resolution, it would be visible on VHR imagery with a spatial resolution of 1 meter. Though related, scale and spatial resolution do have distinct differences. Resolution refers to the “average area dimension a pixel covers on the ground,” where as scale measures the “magnitude or the level of aggregation (and abstraction) on which certain phenomenon can be described” (Benz *et al.*, 2004 pg. 245).

Figure 5. Differences between the main and first-order lines of an object.



Once desired segmentation parameters have been determined, the next step in gathering useful information from an image is to place segmented objects into classes. Classifying objects simply means labeling certain image objects using category class names (Baatz *et al.*, 2004). Classes, in turn, are established by placing like objects into a user-defined set of categories (Baatz *et al.*, 2004). Fuzzy classification strategies, commonly referred to as fuzzy logic, assign a measure of membership to each pixel or object and have become increasingly popular when classifying objects (Wang 1990; Jager and Benz 2000; Blaschke *et al.*, 2004). Fuzzy logic can also be used to assign certain objects or shapes to an individual class. Membership values fall

between 0.0 and 1.0, with 0.0 indicating no membership exists with any given class and 1.0 means full membership (Baatz *et al.*, 2004).

Jager and Benz (2000) suggest the fuzzy logic approach has great value when compared with ground truth data collected for accuracy measures because it takes into account mixed pixel issues by assigning a degree of membership to each relevant category. Certainly, fuzzy logic would be useful for identifying windbreaks as such objects will frequently have mixed pixels due to their narrow linear character that can result in frequent overlap of forest pixels with neighboring grasses or other landcover types. Also, many windbreaks are planted in distinct rows that permit soil and grasses to be visible within them in addition to gaps caused by the presence of dead trees.

Using a supervised classification strategy, multiple objects can be selected as training areas for each class to be established. Various shape, contextual, spectral, and other spatial attributes, such as length and area, can then be calculated for and assigned to training sites to determine what other objects in the image fit into the predetermined classes best (Baatz *et al.*, 2004). Image processing software used in this research project incorporates both a supervised classification strategy and a rule-based classification strategy. The rule-based classification strategy can be used to isolate features of interest while eliminating irrelevant features and works by allowing the user to define certain criteria that objects must possess in order to be placed in a given class. It is essentially a singular classification that eliminates all but one particular set of objects.

This process is accomplished by first eliminating pixels that do not contain spectral values inherent to the features of interest. Second, shape and contextual based criteria can be used to further eliminate features not desired in the final output (ITT Visual Information

Solutions 2008). Recently, similar rule-based techniques have been used to identify urban features such as rooftops and buildings (Huang and Zhang 2008).

Once desired objects have been classified, they can be imported into a GIS as a vector or raster dataset for further analysis (Wiseman *et al.*, 2007). According to Tian and Chen (2007), however, vectors exported from certain image processing platforms sometimes contain no spatial reference. This prevents a GIS from recognizing the actual size, spatial extent, or location of the data. To address this issue, Tian and Chen (2007) developed a custom tool that allowed them to set the spatial reference. Spatial reference definitions did not appear to be an issue with research done using more modern image processing software (Radoux and Defourny 2007; Huang and Zhang 2008; Rutherford and Rapoza 2008).

Object-based Classification Implementation

Traditional methods of classification using remotely-sensed images have become time consuming and inefficient given the development of automated classification techniques (Drăgut and Blaschke 2006). In fact, even traditional pixel-based classification techniques are being replaced with object-based classification due to its increased accuracy and versatility. Whiteside and Ahmad (2005) found that object-based image analysis produced 78% accuracy while pixel-based approaches yielded 69.1% in a land cover classification comparison in northern Australia. Koch *et al.*, (2007) classified landuse and landcover at a study site within the interior Atlantic forest of Paraguay in an attempt to monitor Hantavirus dynamics. Their research showed that object-based classification produced 84% overall accuracy while the per-pixel approach yielded only 43% overall accuracy (Koch *et al.*, 2007). Koch *et al.*, (2007) also reported that the Kappa metric calculated from their results was significantly higher for the object-based classification results compared to that of the per-pixel results. Cohen's Kappa is a statistic used to measure

how much better the classification worked compared to random chance assignment of features to classes (Jenson 2005). Higher percentage accuracy for object-based classifications was a common trend throughout all of the literature reviewed for this research. The topic of accuracy assessment is addressed in detail by Jäger and Benz (2000) and Jenson (2005 pg. 506-509).

Object-based classification can be used for a variety of image analysis objectives. Commonly, object-based classification is used when classifying land cover, however, it is certainly not limited to that function. Baatz *et al.*, (2006) used object-based classification for high content screening of fluorescent cell images at a microbiological level. Geomorphologists such as Drägut and Blaschke (2006) have used object-based classification to identify landform elements and created a reproducible methodology that could be applied to a number of study sites. Most recently, researchers have been using an object-based approach to classify urban areas which are inherently hard to classify due to the diverse range of spectral values that are typically present (Huang and Zhang 2008; De Roeck *et al.*, 2009; Bernad *et al.*, 2009). In fact, De Roeck *et al.*, (2009) were able to produce a Kappa value of 0.84 when classifying urban fringe areas, meaning that their classification scheme worked 84% better than a random assignment of features to classes.

Relevant to this project is a study conducted by the Agriculture and Agri-Food Canada (AAFC) Prairie Farm Rehabilitation Administration (PFRA) Shelterbelt Centre in Indian Head, Saskatchewan. Similar to the KFS, the AAFC PFRA had no spatial data regarding the location of windbreaks, or their condition, within their area of responsibility. It was determined that traveling across the country to visit individual windbreaks would be too costly and time consuming. Therefore two main objectives were established for their research: (1) “Can high resolution imagery be used to generate an accurate inventory of shelterbelts across a vast

landscape?” and (2) “Can shelterbelts be identified by species from high resolution imagery?” (Wiseman *et al.*, 2007 pg. 2). Wiseman *et al.*, (2007) randomly selected 27 individual windbreaks for ground truth comparisons with windbreak features they extracted from aerial imagery. They did not classify windbreaks after segmenting their image but, instead, chose to export the vector-based polygon geometries into a GIS immediately after segmentation and isolate windbreaks from the rest of the polygons using standard query language (SQL) statements. Rather than classify the image, they used a set of shape and length SQL queries to pick out windbreaks from the rest of the segmented polygons. Using this technique, 26 of the 27 ground truth windbreaks were successfully identified. Wiseman *et al.*, (2007) reported that shape attributes were most useful in identifying whole windbreaks, while spectral information produced better results for individual species classification. While their results seem accurate, it should be understood that Wiseman *et al.*, (2007) did not employ a conventional classification strategy. Rather they used a technique more closely related to a process referred to as feature-based classification (Bernad *et al.*, 2009).

In this scenario, features of interest are extracted from the rest of the polygons and placed into their own category or file. This means that there are no 1's and 0's, like in a binary classification, but just 1's indicating the feature exists or “no data”. It should be understood that accuracy results from a single feature extraction such as this cannot be compared to results generated from a Kappa metric because they represent different measures. The Kappa metric is used to measure how much better a classification scheme worked compared to the random assignment of features to classes. Weisman *et al.*, (2007) tried only to classify windbreaks that they knew to exist. The issue with their accuracy measure appears to be, that outside of the 27

windbreaks they visited in the field, they did not document whether any other windbreaks in their study area were correctly identified.

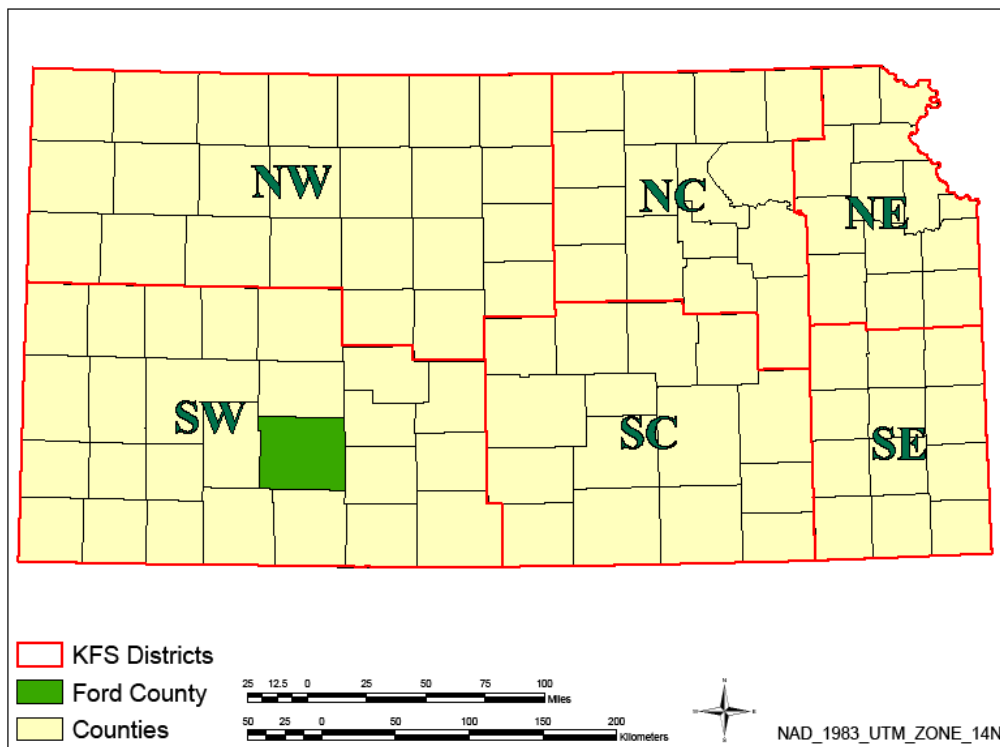
It has been noted that, in image classification, as more classes are developed the better the chances are of distinguishing between them (Jensen 2007). The idea is that more classes will eliminate confusion between features by reducing generalization that can occur when using too few classes. For example, if windbreaks were the only class selected for features that contain trees, then the all trees in the image would be placed into the windbreak class. However, if classes were developed for windbreaks, riparian zones, and larger forest stands, various algorithms can be used to place each “tree” feature in their correct respective classes based on other properties such as shape, size, and spectral reflectance.

Object-based classification has proven to be a useful technique in classifying land cover in a variety of scenarios. Often, object-based classification has shown its usefulness in classifying entire images and for single feature extraction. Using certain spatial and spectral criteria, it is the objective of this research to isolate windbreaks from all other land cover features and assess their condition using different spectral and textural properties. By taking advantage of the unique ability of object-based classification to classify features based on their shape, windbreak features should be easily distinguished from all other landcover features that share similar spectral properties. In addition, using this automated technique it should help decrease the amount of time required to inventory windbreaks by eliminating much of the field survey methods employed by Read (1958). While a variety of windbreak surveys have been conducted in the past, none performed in Kansas have ever attempted to extract windbreaks from aerial imagery at the county level.

CHAPTER 3 - Study Area

Ford County, Kansas was selected as the study area for this research project and will serve as the pilot county for the development of remote sensing and GIS methods to classify windbreaks (Figure 6). The methods tested in Ford County, if successful, will then be applied to a multi-county area in southwest Kansas, including the counties of Clark, Gray, Haskell, Hodgeman, Meade, and Seward. These counties are located in the Southwestern District of the KFS and selected for analysis in the Conserving, Renovating & Establishing Working Field Windbreaks (CREFW) grant that funded this research. The CREFW was accepted for funding via the State and Private Forestry FY 2008 Western Competitive Grant Application.

Figure 6. Ford County study area with Kansas Forest Service districts highlighted.



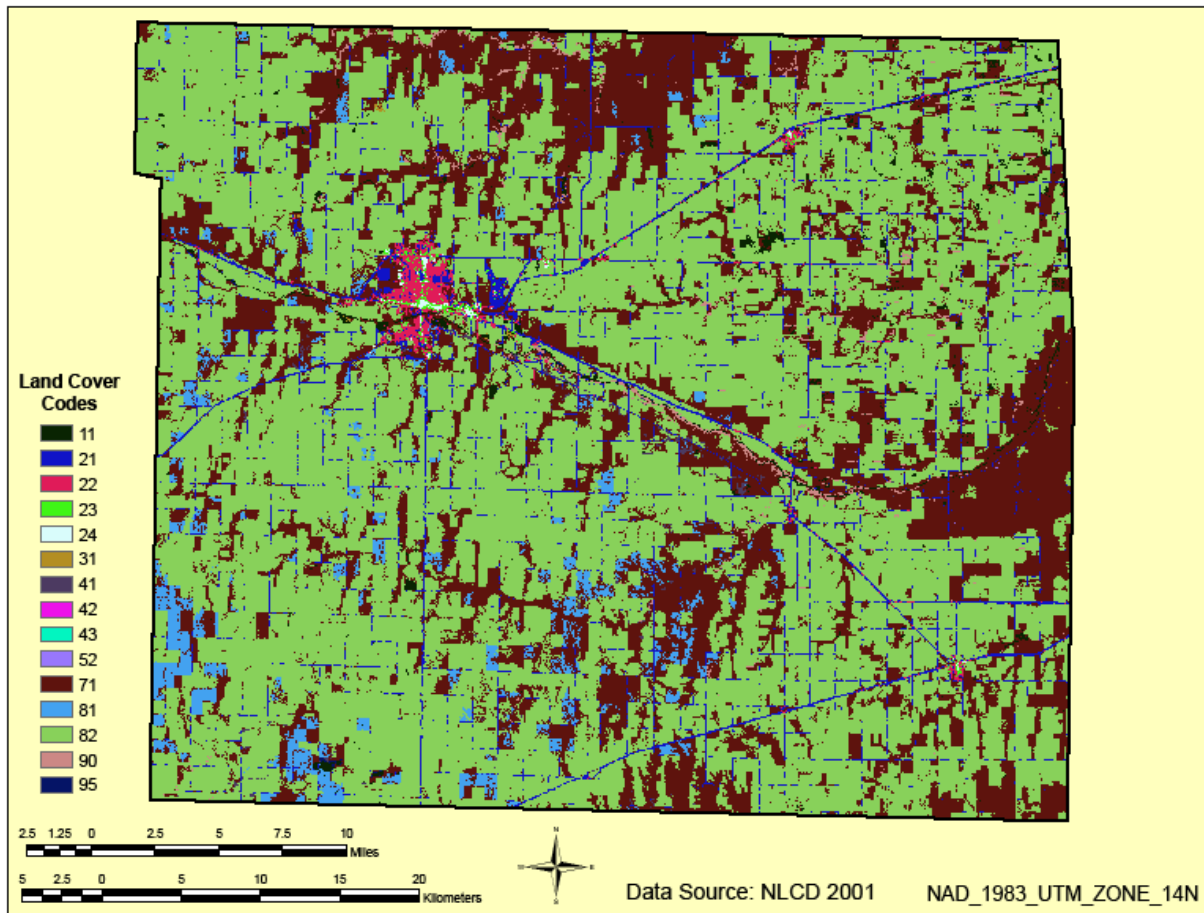
Ford County is home to more than 800 acres of windbreaks, some of which were planted during the PSFP (1930's-1940's). In addition, the Natural Resource Conservation Service (NRCS) provided an independently developed GIS-friendly spatial data file for windbreaks identified using a 'heads-up digitizing' process that will be used to assess the accuracy of the classification techniques applied in this project (R. Temat 2008, pers. comm.).

Ford County is located in southwest Kansas and spans an area of 2,850 km². Landcover within the county is dominated by agricultural cropland, while mixed or short grass prairies make up the majority of native vegetation (Goodin *et al.*, 2002 pg. 46). Figure 7 shows a map of Ford County landcover based on the 2001 National Landcover Dataset (NLCD). Land use related to the cattle industry also makes up a major part of the landscape with many areas being used as grazing land, livestock feed production, and large scale feedlots (Harrington 2001). A detailed breakdown of current landuse/landcover types in Ford County is shown in Table 2. Appendix A gives a description of the NLCD land cover types and associated cover codes.

Much of the county's agricultural cropland remains bare soil after harvest, which usually occurs in mid- to late June. The lack of crop residue makes it extremely susceptible to wind erosion throughout much of the year. During the period between harvest and next planting, windbreaks sometimes provide the only protection against soil loss (Brandle *et al.*, 1982).

Another important landcover feature in the study area is the lengthy riparian area bordering the Arkansas River. This forest corridor stretches approximately 65 km from the northwest to east-central border of the county. Eastern cottonwood (*Populus deltoides*) is the dominant tree species found in the riparian area, as well as in many of the older windbreaks (R. Atchison pers. comm. 2009).

Figure 7. Landcover/Landuse classes in Ford County.



Dodge City is the major urban center in Ford County and is home to 77% of the county's residents (Harrington *et al.*, 2003). Current population estimates from the U.S. Census Bureau (2009) shows this percentage holding steady, with Dodge City comprising 25,737 out of the county total population of 33,340. Table 3 shows historic population estimates from 1870 to the present (U.S. Census Bureau and National Historical GIS (NHGIS)). Drastic population spikes occurred between 1900-1930 as well as from 1960-2000. These population spikes are illustrated in Figure 8. Population booms in the 1930's and 1960's are due to the "Green Revolution", an era in which advanced in agricultural technology made farming an appealing and profitable career choice (Evenson and Gollin 2003).

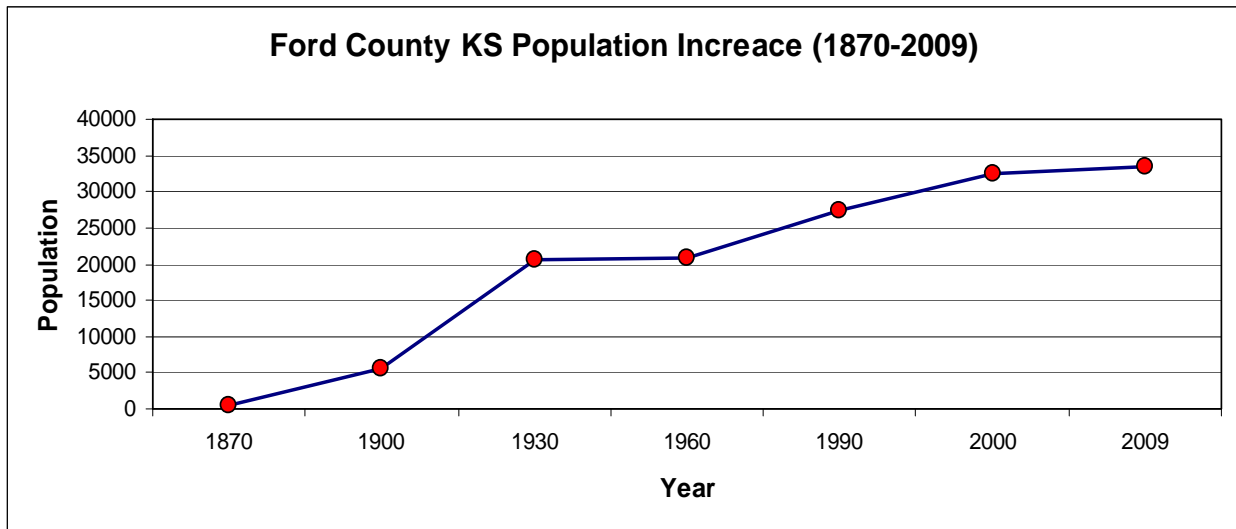
Table 2. Total area of each landuse/landcover class in Ford County (Source: 2001 NLCD)

COVER TYPE	COVER CODE	ACRES	HECTARES	% OF TOTAL
Open Water	11	19,021.2	7697.6	0.9%
Developed, Open Space	21	87,027.9	35,218.9	3.9%
Developed, Low Intensity	22	13,818	5,591.9	0.6%
Developed, Medium Intensity	23	3,377.2	1,366.7	0.2%
Developed, High Intensity	24	1,550.3	627.4	0.1%
Barren Land (Rock/Sand/Clay)	31	557.5	225.6	0%
Deciduous Forest	41	5,343.3	2,162.3	0.2%
Evergreen Forest	42	12.7	5.1	0%
Mixed Forest	43	19.1	7.7	0%
Shrub/Scrub	52	69.1	27.9	0%
Grassland/Herbaceous	71	564,014.8	228,248.6	25.4%
Pasture/Hay	81	55,236.9	22,353.5	2.5%
Cultivated Crops	82	1,455,024.7	588,827.6	65.6%
Woody Wetlands	90	11,644.5	4,712.2	0.5%
Emergent Herbaceous Wetlands	95	492.4	199.3	0%
Total		2,217,209.4	897,272.8	100%

Table 3. Historic population change in Ford County, Kansas.

Year	Population	Year	Population
2009	33,340	2001	32,281
2008	33,293	2000	32,565
2007	33,077	1990	27,463
2006	32,751	1960	20,938
2005	32,876	1930	20,647
2004	32,654	1900	5,497
2003	32,558	1870	427
2002	32,164		

Figure 8. Graph of population change in Ford County, 1870-2009.

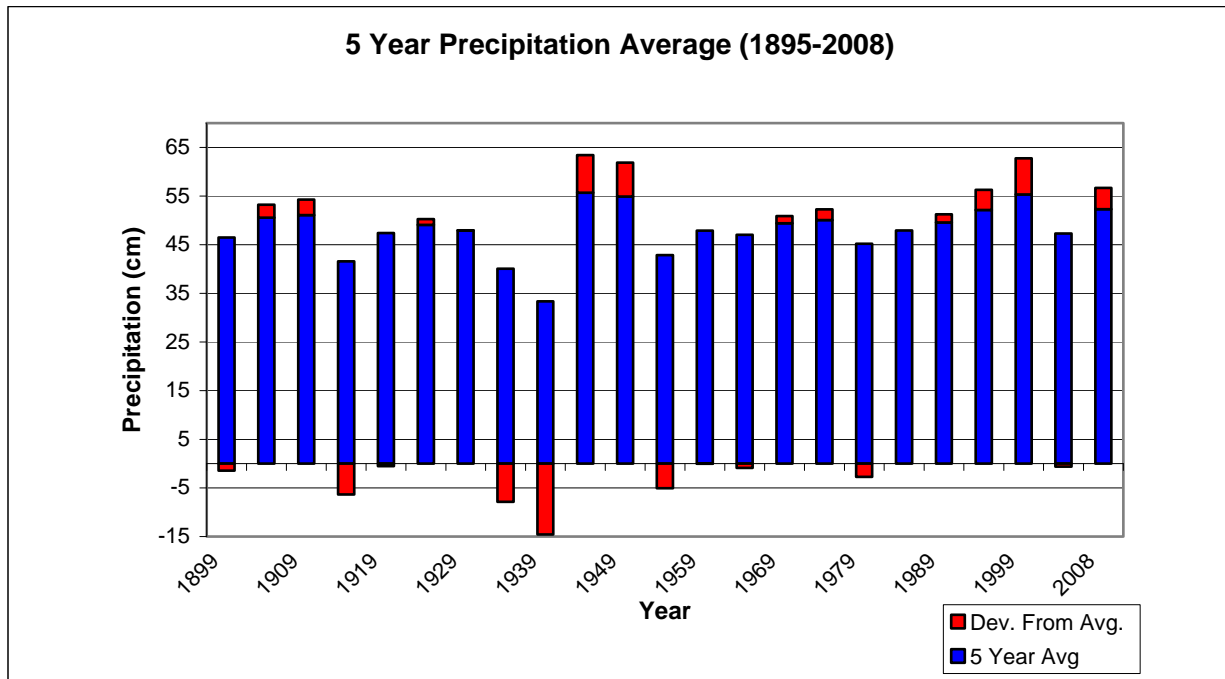


Ford County has a semi-arid climate characterized by high winds, low yearly precipitation (> 58 cm) and extreme weather events. Table 4 lists average annual precipitation values for the county dating back to 2000. Figure 9 is a graph of five-year mean precipitation totals plus the deviations from the long term average (47.9 cm) taken from the Dodge City weather station and date as far back as 1895. Periods of drought during the 1930's are easily visible in Figure 9 as precipitation deviates well below the long term mean. In a tree ring chronology study under taken by Woodhouse and Overpeck (1998), it was determined that the severity of droughts during the 1930's and 1950's were equal to or slightly less than droughts experienced thousands of years ago. This study indicates that severe drought has consistently plagued the study area for hundreds of years, with some drought periods lasting for decades or longer (Woodhouse and Overpeck 1998).

Table 4. Annual precipitation for Ford County, 2000-2008.

Year	Precipitation (in)	Precipitation (cm)
2000	23.3	59.3
2001	17.5	44.4
2002	17.8	45.3
2003	19.1	48.4
2004	23.5	59.7
2005	25.2	64.1
2006	24.6	62.4
2007	27.2	69.1
2008	22.7	57.6

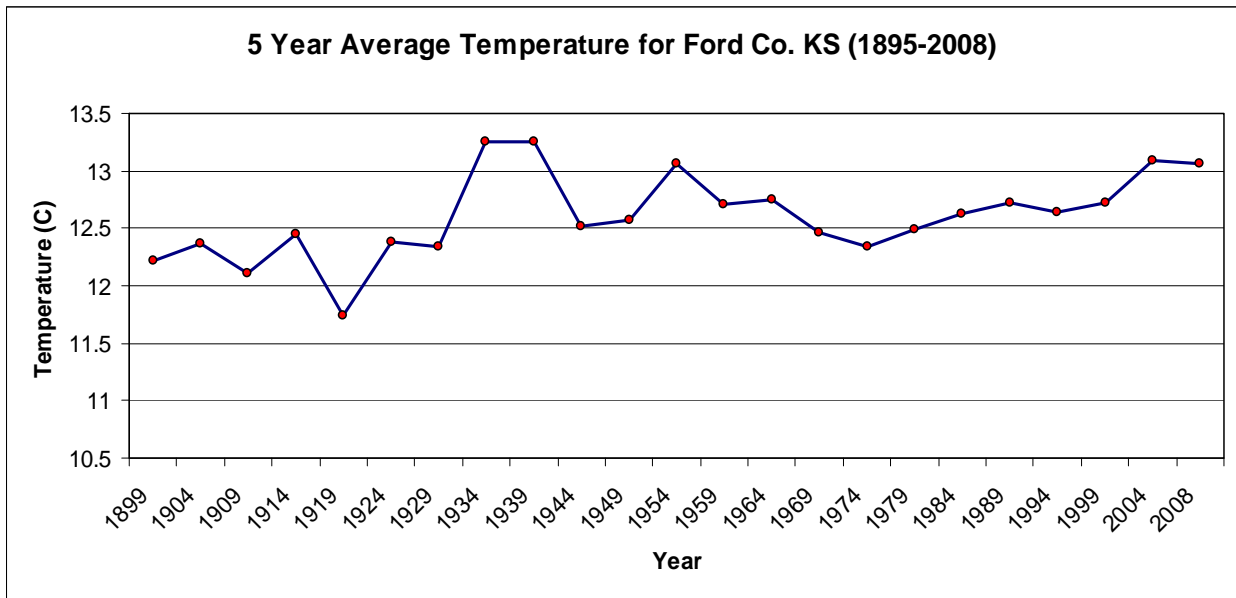
Figure 9. Five year precipitation averages for Ford County, 1895-2006.



Blizzards are common events during winter months, while drought often strikes during the summer months. Severe winds, tornados, and thunderstorms accompanied with hail are also very common in the spring (Flora 1948). The National Climactic Data Center (2009) reported 73

documented tornado touchdowns between 1950-2008. Mean monthly temperature variations range from -1° to $+27^{\circ}$ C (Goodin *et al.*, 1995; Harrington *et al.*, 2003). Figure 10 is graph of historic annual mean temperatures ranging from 1875-2008. This data was collected from the Dodge City weather station and made available by the Kansas Board of Agriculture.

Figure 10. Five year mean temperatures for Ford County, 1895-2006.



High winds accompanied by severe weather events (*e.g.*, blizzards) are common to the area and have the potential to cause significant damage to shelterbelts. Winter ice storms in 2007 caused major widespread damage to windbreaks in the area due to the combined impact of accumulated ice and winds which broke limbs and, in some instances, brought down entire trees (R. Atchison. pers comm. 2009).

CHAPTER 4 - Data and Methods

Imagery

The image used in this study was acquired through the 2008 National Agricultural Imagery Program (NAIP). NAIP imagery has a spatial and radiometric resolution of 1 m and 8 bits, respectively (United States Department of Agriculture 2008). Each image is multispectral in nature, and contains spectral data from four bands of the electromagnetic spectrum: Blue (band 1), green (band 2), red (band 3), and near-infrared (NIR) (band 4). Documentation was not available with the NAIP image that described the specific wavelengths recorded in each band. The NAIP image used here was collected during the crop-growing months of 2008.

Individual multispectral NAIP images are processed into Compressed County Mosaics (CCMs), with a compression ratio of 1:15, and distributed to the public in the JPEG 2000 (.jp2) format (Adkins 2008). The 2008 NAIP CCM for Ford County was downloaded from the Kansas Geospatial Community Commons (<http://www.kansasgis.org>). The image is delivered to the public with a maximum of 10% cloud cover, georectified (North American Datum 1983 Universal Transverse Mercator Zone 14 North) and with atmospheric corrections already made (Mathews and Davis 2007). Because little cloud cover was observed in the Ford County image, it was determined that the few clouds that did exist would not introduce significant error into later windbreak classification efforts.

One great advantage of using the 2008 NAIP imagery is that it can be downloaded for free as compared to similar 1 m resolution imagery which can cost over \$25.00 U.S. dollars per km² (M. Kallas, 2008 pers. comm.). Because the area of Ford County is 2,850 km², the total cost associated with purchasing imagery could easily be \$71,250, making it unaffordable for this and other projects.

The remainder of this chapter outlines methods used to process the NAIP image, perform object-based classification, assess windbreak condition, and calculate the area of windbreaks found on highly erodible soils. Figure 11 diagrams a general workflow of the methods used in this research.

Figure 11. Workflow sketch of the methods used in this research.

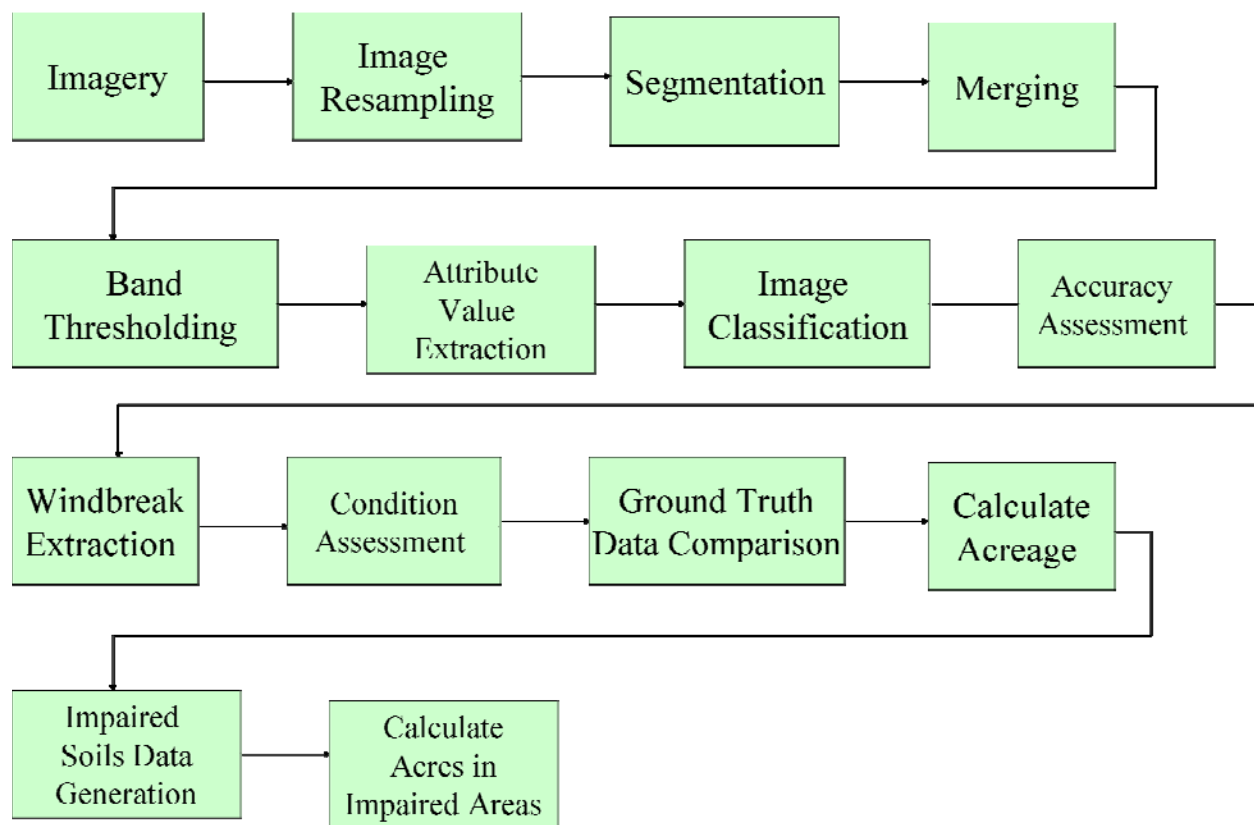


Image Preprocessing

Most GIS software packages are compatible with the .jp2 compressed file format. However, the digital image processing software program used in this study, ENVI Zoom 4.5 *Feature Extraction Module* (ITT Visual Information Solutions, Boulder, CO), did not recognize

the .jp2 format. Because of this, the original .jp2 CCM for Ford County was converted to the TIFF format (based on a lossless compression technique) to make it universally compatible with the all image processing and GIS software packages used here.

Image resampling was performed next and the process of geometrically transforming an image and is commonly used to enhance the visual characteristics of an image for display purposes (Parker *et al.*, 1983; Dodgson 1992). Image resampling can also be used to decrease the spatial resolution of an image by enlarging the dimensions of individual pixels through resampling techniques such as nearest neighbor, bilinear interpolation, and cubic convolution filtering. This process is sometimes referred to as spatial down-sampling (Parker *et al.*, 1983; ITT Visual Information Solutions 2008).

The advantage of using fine spatial resolution imagery comes at the cost of enormous file sizes which can significantly slow computer-based processing methods. Dodgson (1992) suggests that image resampling should be done when, (1) collecting the imagery at different resolutions is not an option, and (2) when it is possible to recapture the imagery but resampling requires no additional monetary input and would result in faster processing. Here we cannot have NAIP personnel re-fly Ford County to capture imagery with less spatial resolution and faster processing times are obviously desired. The original .jp2 NAIP image was approximately 14.5 GB which exceed the 4 GB limit to convert to a .tiff file (Geospatial Data Abstraction Library 2009).

Based on Dodgson (1992) suggestions it was confirmed that resampling the original imagery was indeed the best option. Though information is lost in this process, it will not impact this research. For example, a data reduction step such as resampling would not be appropriate if individual tree species were to be classified. Here, however, the objective is to identify entire

windbreaks, so image resampling is actually beneficial by both reducing file sizes and by transforming windbreaks into areas of more homogeneous pixels rather than isolated pixels representing single trees within a windbreak.

The Nearest Neighbor (NN) resampling technique was used because of its speed and simplicity (Parker *et al.*, 1983, OverWatch Textron Systems 2008). The Feature Analyst Reference Manual (OverWatch Textron Systems 2008) also suggests that the NN resampling technique be used when linear features, like windbreaks, are of particular interest.

Resampling factors of 2, 4, 6, 8, and 10 were all performed to determine an optimal solution to the .tiff conversion issue. Resampling the image at factors of 2 and 4 did not decrease the original .jp2 file size sufficiently to allow for file conversion. In addition, when resampling factors of 8 and 10 were used windbreaks in the imagery appeared to lose most, if not all, spatial integrity. Pixels comprising small windbreaks were averaged in with surrounding grasslands and all digital information regarding them was lost. Furthermore, when resampling factors of 8 and 10 were used, several large field windbreaks were averaged into a single row of pixels which would have prevented an accurate assessment of their condition in later classification steps.

Resampling the image by a factor of 6 reduced the .jp2 file size enough to permit for .tiff conversion while maintaining much of the spatial integrity of field and farmstead windbreaks. Figure 12 illustrates a sample of the original and resampled image that was used for segmentation and classification.

Figure 12. Comparison of the Ford County 2008 NAIP image at 1 and 6 meter pixel size.

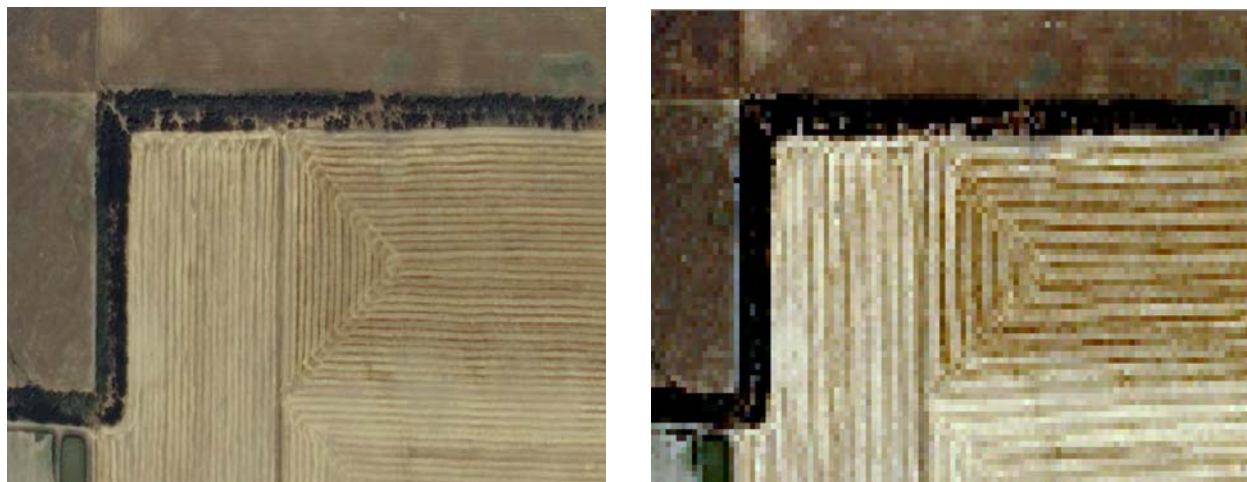


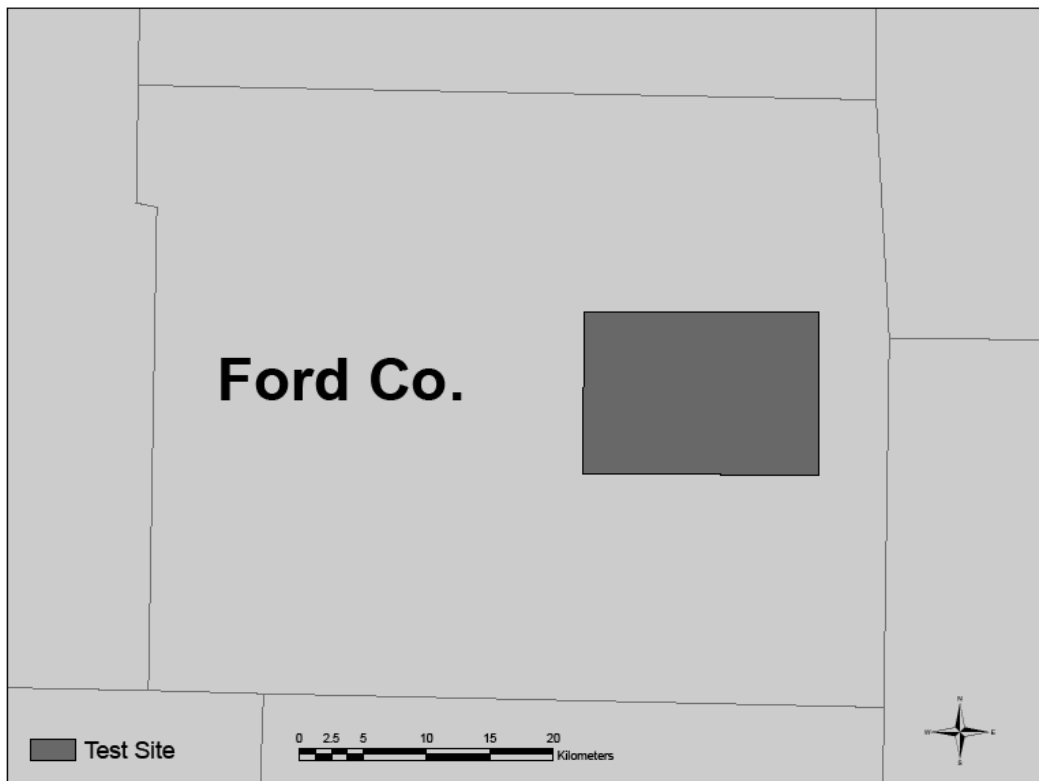
Image Segmentation and Merging

Several segmentation methods are available that can be used to isolate homogeneous pixels into proper objects. In a preliminary segmentation test for this project conducted as part of a class assignment, a bottom-up region merging approach was used to segment imagery within a test site in Ford County. Using this approach, and a minimum distance classifier, an overall accuracy of 53.2% was achieved for a landuse/landcover classification. For this research, an edge-based segmentation method and Support Vector Machine (SVM) classifier was applied to determine whether improved accuracy was possible.

Segmenting imagery can be a time-consuming activity depending on the processing power of the computer hardware being used to operate the segmentation software. Because of this, an area of just over 240 km² was extracted from the resampled imagery to develop segmentation and classification parameters to be applied later to the entire CCM of Ford County (Figure 13). Developing parameter settings using a smaller image file allows for faster processing times and eliminates much of the need for lengthy “trial and error” experimentation

on the much larger CCM file. The test site was selected because it contained most of the windbreak ground truth data collected for accuracy assessment. In addition, this particular area was noted as having a particularly high number of windbreaks (> 30) compared to other areas of the county.

Figure 13. Location of Ford County test site.

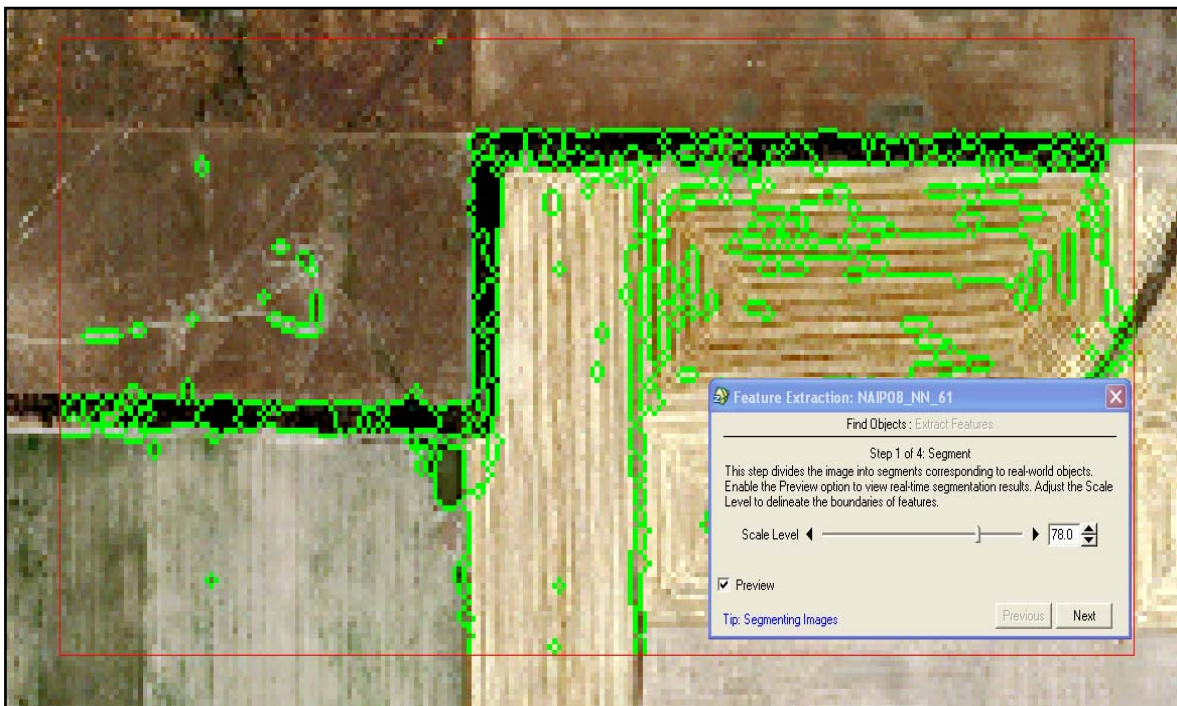


Segmenting an image relies heavily on a trial-and-error approach where the user evaluates the performance of several different scale parameter settings in order to determine which performs best. The ENVI Feature Extraction Module User's Guide (ITT Visual Information Solutions 2008) suggests users should implement the highest scale level that properly defines the boundaries of features of interest. The image processing software used in this research provided a viewing portal in which different segmentation parameters could be set

and the results then viewed “on the fly” prior to segmenting the entire image to determine if the segments are satisfactory. The viewing portal is mobile, meaning users can move the portal to any region of the image and view a sample of what segments would result.

Scale level is an area measure that determines the ‘size’ of objects to be created. Scale parameter values range from 0.0-100.0 with segments decreasing in size as they move closer to 0.0. After viewing several scale parameters in the viewing portal, it was determined that a scale parameter of 78 adequately delineated large homogeneous regions within windbreaks throughout the image (Figure 14). Higher scale parameters appeared to create larger objects that encompassed more landuse/landcover types than just windbreaks. Lower parameters values began to create borders around individual trees within windbreaks.

Figure 14. Screenshot of the ENVI Zoom 4.5 Feature Extraction Module and viewing portal (outlined in red).



Using a scale level of 78, an edge-based segmentation algorithm was used to segment the entire Ford County image. The edge-based segmentation algorithm works faster than other approaches, such as bottom-up region merging, because it requires only one parameter input (scale level). Though the scale level of 78 adequately defined segments between the windbreak and surrounding landcover, several small segments within the windbreak remain. To correct for this issue, a technique called segment merging was used to group small segments of similar spectral, spatial, and textural values to create even larger segments containing similar values.

Segment merging is based on a Full Lambda-Schedule algorithm created by Robinson *et al.*, (2002) (Equation 1). Merging of objects occurs when the algorithm identifies a set of neighboring objects with similar spatial and spectral properties. The merge which groups shapes into even larger objects uses the same Equation 1 as the segmentation process and has a range of threshold lambda values between 0.0 - 100.0. After experimenting with a wide variety of lambda values it was determined that a value of 50 properly merged segments within windbreaks while keeping them isolated from neighboring landuse/landcover types.

Equation 1. Full Lambda-Schedule algorithm for segment merging.

$$t_{i,j} = \frac{\frac{|O_i| * |O_j|}{|O_i| + |O_j|} * \|u_i - u_j\|^2}{length(\partial(O_i, O_j))}$$

where,

O_i = region i of the image,

O_j = region j of the image,

u_i = average value in region i ,

u_j = average value in region j ,

$\|u_i - u_j\|$ = Euclidean distance between spectral values of regions i and j , and

$Length(\partial(O_i, O_j))$ = length of the common boundary of O_i and O_j .

In addition to segmenting and merging objects, an additional technique called thresholding was used to eliminate objects containing mean spectral values that were not essential for identifying windbreaks. With thresholding, a histogram of regional mean values are calculated and displayed with the option to set upper and lower value limits which will remain in the image for later classification. For this project, the only landuse/landcover type of concern is the vegetation within windbreaks, so elimination of impervious features such as roads, houses, bare soil, and parking lots makes the process of defining classes of remaining vegetation types much simpler. Note that spectral values from bare earth that were captured within objects considered to be windbreaks were not eliminated. The thresholding process only eliminated large contiguous areas of bare soil, grasses, roads, etc. The processing time required to classify remaining objects is less and should be more accurate by reducing any confusion in the data between impervious and vegetative features.

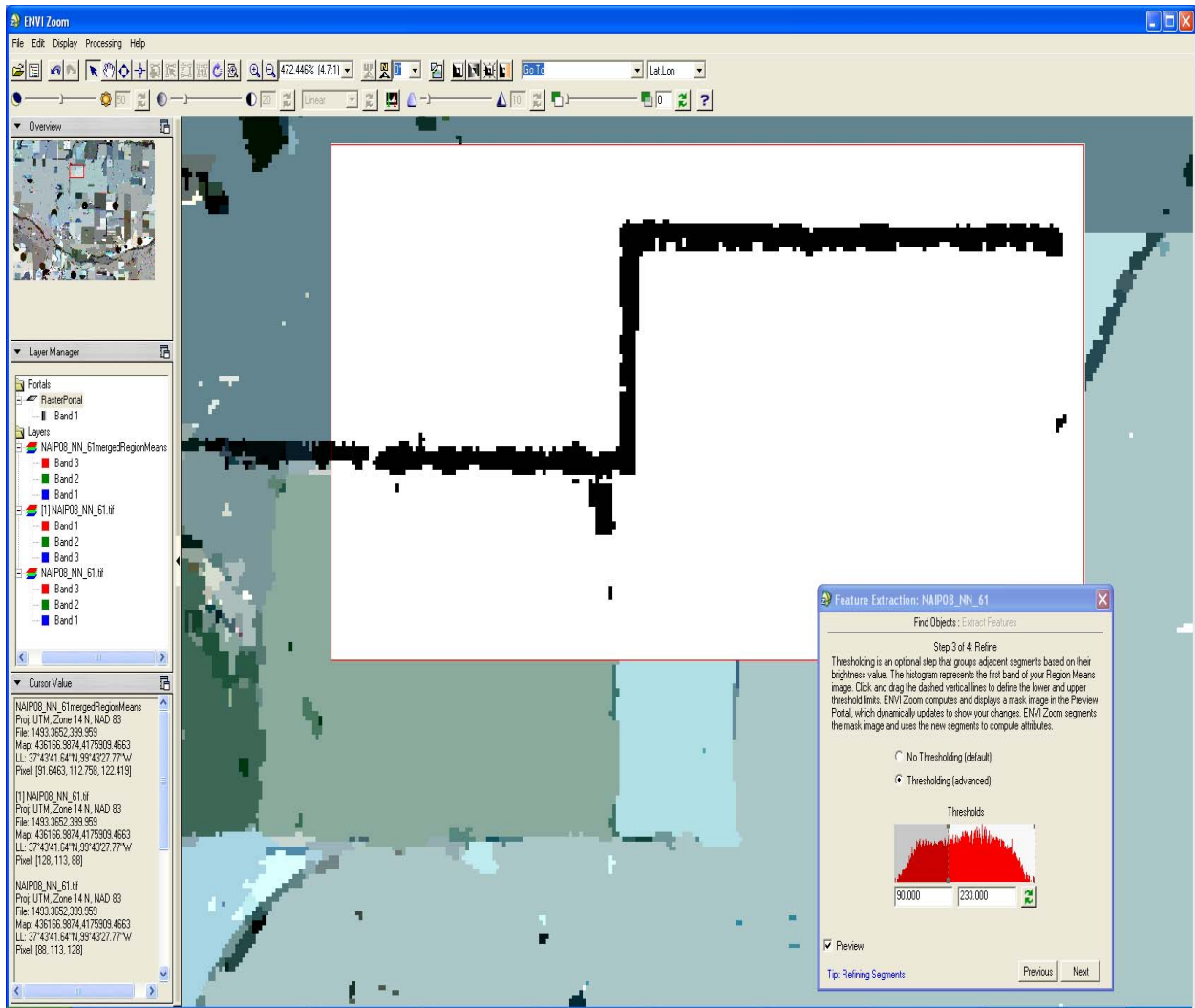
Several band threshold parameters were tested and viewed throughout the Ford County image using the viewing portal previously mentioned. Visual analysis showed a minimum band threshold of 90 eliminated most impervious features. No upper limit was placed on the band threshold parameters to prevent the potential elimination of any tree cover. Using these threshold parameters all region mean values in the image below 90 were masked from future analysis (Figure 15). After thresholding, several non-windbreak landuse/landcover types (*e.g.*, riparian areas and cropland) remain in the image.

Attribute Value Extraction

After thresholding has been used to eliminate unwanted regions of the image, attributes must be computed for the remaining features. Attributes calculated for later use in classification included those related to spatial geometry (area, length, roundness, etc.), spectral characteristics

(pixel BV's within objects), texture (measures of pixel variance and range), and band ratio (hue, saturation, and intensity of pixel values within objects). A detailed listing all attributes calculated, accompanied with a definition and the equation used to calculate the individual attributes, can be found in Appendix B.

Figure 15. Screenshot of the band thresholding operation used to eliminate areas not required for windbreak classification.



In the object-based classification software used here (ENVI Zoom 4.5 *Feature Extraction Module*) object attributes are calculated for the purpose of classification only. Any classification

results produced within the software will not include attribute information pertaining to the attributes identified in Appendix B. This can pose a problem for later classifications or classification enhancements/modifications performed in a GIS later using these same attributes. To overcome this problem, objects must be exported immediately after the “calculate attributes” operation and before classifying them based on landcover type within the software. This will ensure that a shapefile (spatial data file) of objects with spatial, spectral, textural, and band ratio attributes exists.

When objects are finally delineated into their appropriate landcover classes they can be exported to shapefile format however, the only attribute associated with this export will be ‘landcover class.’ Once classified objects have been exported, a spatial query (*i.e.*, “select by location”) can be performed in a GIS to select objects from the original segmented shapefile (the one containing attribute information) that intersect or overlay known landcover classes in the exported landcover class shapefile (the one containing no attribute information). If this is accomplished properly, the objects selected from the original segmentation shapefile can then be used to classify landcover features based on their attribute information identified in Appendix B.

Image Classification

Object classification was the next step following the export of segments and their associated attributes. Two classification approaches were considered for extraction of windbreaks. The first was a rule-based classification strategy where the user develops a set of rule-based algorithms, or guidelines, to eliminate all features except those of interest for extraction. Rule-based classifications within the software used here were developed as a binary classification tool for the extraction of an individual feature type (*e.g.*, houses, buildings, roads, etc.).

After much experimentation with this approach, it was found that windbreaks shared far too many spectral and spatial characteristics with other vegetated features such as riparian areas, ditches, and some crop fields to be completely isolated into their own class using the algorithms provided in the object-based image classification software. Because of this it was decided to use a traditional supervised classification strategy in order to isolate windbreaks from the other landuse/landcover features in the Ford County image.

Supervised classification requires selection of training sites, or objects of known identity, which are then used in the classification algorithm to place objects of an unknown feature type into the training class with which it is most similar. First, a set of classes have to be developed based on what cover types are known to be in the image. Much consideration was given to building on the Anderson *et al.*, (1976) Level I and II classification schemes. However Level I was much too generalized to incorporate a windbreaks class, and Level II was too detailed to derive windbreaks from multiple tree species classes. In fact, while the trees planted in a windbreak are indeed a type of landcover, a windbreak in its entirety is a landuse because they were planted on the land to be ‘used’ as a wind restraint. Because of this, the remaining feature types were inspected to build a set of custom classes based on suggestions by Jensen (2005) and Baatz *et al.*, (2004). Manual inspections of the objects remaining in the image after band thresholding resulted in the identification of four remaining landcover types within the test site (Table 5).

The ENVI Zoom Feature Extraction User’s Manual (ITT Visual Information Solutions 2008, pg. 33) comments that the more accurate results are obtained when using more training sites. However they do not specify an upper value to the number of training sites. Instead, they state that “an overwhelming number of training samples will cause poor performance during

classification and previewing results.” Several different combinations of training site numbers by cover type were tested via visual inspection. It was determined that 15 training sites for crops, riparian areas, and windbreaks along with 25 tree stand samples yielded the best results.

Table 5. Custom landuse/landcover classes developed based on expert knowledge of the features remaining in the Ford County image after band thresholding.

Cover Type	Description
Crops	Live row crops including live crops on center pivot irrigation land.
Tree Stands	Individual stands of trees/shrubs not linear in nature and not near water features.
Riparian	Long irregularly shaped stands of trees bordering water features.
Windbreaks	Linear strips of trees planted near farm houses and crop fields likely to have gagged edges conforming to the shape of outer edge trees.

Once training sites were established, the next process was to select the appropriate attributes for classifying the remaining features. An algorithm established by ITT Visual Information Solutions (2007) was used to automatically select attributes for classification. This algorithm uses a Discrete Capability Index (DCI) to establish the significance level (0.0 - 1.0) of an attribute’s capability to distinguish between multiple classes based on 6 distinct types of attribute signature overlap (Table 6). For example, a Type 1 interval has no overlap between classes while Type 6 intervals have full overlap.

Using the “Auto Select Attributes” function, Equation 2 was used to calculate the significance of each attribute based on its ability to distinguish between classes at each interval type. If an attribute has the significance level to fully distinguish among 2 classes it receives a value of 1.0, which would be the case for Type 1 and 2 intervals. Once the significance values of attributes were calculated, the DCI was used to determine the largest intervals that could discern

one class from all other classes. Attributes used to classify the remaining features in the test site are listed in Appendix C.

Table 6. Discrete Capability Index overall interval types (ITT Visual Information Solutions 2007).

Type 1: Interval 1 is before Interval 2 without Overlap: ██████
Type 2: Interval 2 is before Interval 1 without Overlap:	██████
Type 3: Interval 1 is before Interval 2 with Overlap: ██████ ██████
Type 4: Interval 2 is before Interval 1 with Overlap:	██████
Type 5: Interval 1 contains Interval 2: ██████ ██████
Type 6: Interval 2 contains Interval 1:	██████

Equation 2. Method used to distinguish between classes by DCI interval type.

$$significance = 1 - \frac{nf}{nn}$$

where:

nf = the number of feature points falling in the interval overlap range

nn = the total number of training points that belong to that class.

The final step in object-based image classification, (using ENVI Zoom 4.5 *Feature Extraction Module*) requires a choice between two classification algorithms that operate on the selected attributes in Appendix C: K Nearest Neighbor algorithm and Support Vector Machine (SVM). The K Nearest Neighbor classifier considers n number of neighbors to classify objects based on Euclidean distance between n neighbors. SVM uses a training set of “instance-label” pairs to map vectors into a possibly infinite dimension of space by the function Φ (Hsu *et al.*,

2008). The SVM algorithm then uses optimization methods to divide numeric attributes into upper and lower margins based on a set number of hyperplanes that split the data into their respective classes (Huang and Zhang 2008; Hsu *et al.*, 2008).

The SVM classifier was used in this project. Two issues prevented use of K Nearest Neighbor: (1) Misleading results would likely result given that very large areas were masked out after applying a band threshold to the Ford County image, and (2) windbreaks are distributed in a non-uniform manner across the study area landscape such that nearby similar features can't reliably be classified as windbreaks.

Use of the SVM classifier requires selection of a kernel type to operate the classifier. Typically there are four kernel types from which to choose: (1) Linear, (2) polynomial, (3) radial basis function (RBF), and (4) sigmoid (Hsu *et al.*, 2008). Because the RBF kernel type has been noted for working most efficiently in a variety of classification experiments (Hsu *et al.*, 2008 and ITT Visual Information Solutions 2008), it was selected here.

Object-based Classification Accuracy Assessment

A wide variety of accuracy assessments can be applied to classification results obtained from remotely sensed data. Before moving on to classify the entire study area, accuracy measures needed to be performed on the classification results from the test site. Little ground truth data had been obtained within the test site area making it difficult to compare those classification results to ground truth measurements. In order to measure the accuracy of the object-based classes, several ground truth points would have needed to be collected before the classes were generated. Based on suggestions by Jäger and Benz (2000), Jensen (2005), Koch *et al.*, (2007), and Rutherford and Rapoza (2008) random samples within each class were generated in order to create a classification error matrix, including values for user, producer, and

overall accuracies. The proper number of random samples were determined using the Fitzpatrick-Lins (1981) equation (Equation 3) derived from the Binomial Probability Theory (Jensen 2005).

Equation 3. The Fitzpatrick-Lins equation.

$$N = \frac{Z^2 * p * q}{E^2}$$

where:

p = expected percent accuracy of the whole classification

q = 100 - *p*

E = allowable error

Z = 2 from the standard normal deviate of 1.96 for the 95% two-sided confidence level.

In addition to calculating overall accuracy, the Cohen's Kappa metric was calculated to determine to determine the agreement between the object-based classifications and the reference data located in the major diagonal of the confusion matrix and the random chance of agreement which is specified in the row and column totals (Jensen 2005).

Once random samples were generated within each class, the error matrix was populated by inspecting the underlying landcover class of each random point. Expert knowledge, or knowledge based interpretation, of landcover/landuse features was used to determine if the object-based classification classes matched the actual landcover/landuse visible in the 2008 NAIP imagery. Because the windbreak category was the only class for which accuracy was relevant, a 2x2 error matrix of non-windbreak and windbreak classes was constructed. Table 7 is an example of a populated error matrix.

Table 7. Example of a populated error matrix with generic variables.

	Variable 1	Variable 2
Variable 1	179	4
Variable 2	3	17
Column Total	182	21

Producer and user accuracies for each class were calculated once the error matrix was populated. Producer accuracy, which is a statistic representing the probability of a reference object being classified correctly, was then calculated for each class by dividing the number of correctly classified objects by the column totals (Jensen 2005). User accuracy, or the probability that an object classified in the object-based results corresponds with the actual underlying landcover, was calculated by dividing the correct number of sampled objects by the row total (Jensen 2005). Finally, overall accuracy of the error matrix was calculated by dividing the major diagonal values total by the total number of samples. Finally, the Kappa metric (Equation 4) was calculated to measure the accuracy between the object-based classes, reference (ground truth) data and random chance agreement. Jensen (2005) states that to show strong agreement, the Kappa statistic needs to be greater than 80.0%. Values ranging from 79.9 to 40.0 are considered to have moderate agreement, while any value less than 39.9 shows weak agreement.

Moving from Test Site to County

Results from image resampling, segmentation, merging, thresholding, and RBF-based classification produced, after visual inspection, accurate results in the Ford County test site for the four established classes. The same parameters and algorithms were then used to classify the entire CCM for Ford County (Table 8).

Equation 4. The Cohen Kappa statistic.

$$\hat{K} = \frac{N \sum_{i=1}^K x_{ii} - \sum_{i=1}^K (X_{i+} * X_{+i})^2}{N^2 \sum_{i=1}^K (X_{i+} * X_{+i})}$$

where:

N = total observations

$\sum_{i=1}^K X_{ii}$ = sum of the major diagonal

$\sum_{i=1}^K (X_{i+} * X_{+i})$ = sum of the row total * the column total for each class.

Table 8. Parameter settings used to classify the Ford County 2008 NAIP image.

Parameter or Classification Setting	Value
Segmentation Parameter	78.0
Merge Factor	50.0
Band Threshold	90.0-255.0
Classification Algorithm	SVM

Segmented objects with attribute information contained in Appendix B were exported for later classification using spectral information. This file will be referred to as “Ford Co. Segments.” As noted earlier, the software package used here did not export attribute information in a shapefile after it had been classified. Object primitives established during the segmentation and merging process were exported for later classification based on their attribute information.

After band thresholding, two additional classes were added to the Ford County classification to reduce confusion when placing landuse/landcover features into their correct classes (Table 9). These features, manicured landscapes (including golf courses and lawns) and

ditches, were not present in the Ford County test site. Both lawns and golf courses were placed into the manicured landscape category because they shared very similar spectral properties.

Table 9. Final landuse/landcover categories used in the Ford County classification.

LULC Type	Description
Crops	Live row crops including center pivot irrigation land
Tree Stands	Individual stands of trees/shrubs not linear in nature and not near water features
Riparian	Long irregularly shaped stands of trees bordering water features
Windbreaks	Linear Strips of trees planted near farm houses and crop fields likely to have gaged edges conforming to the shape of outer edge trees
Manicured Landscape	Vegetative features such as Golf Courses and Lawns under apparent human management
Ditches	Extremely long linear features running parallel to roads and rail road tracks containing few trees and smooth edges

As compared to the test site, the segmentation process for Ford County as a whole resulted in thousands more objects that had to be placed into the six landuse/landcover classes. Since there was an increase in the number of objects for the entire county, more training sites were used as compared to that with the test site (Table 10).

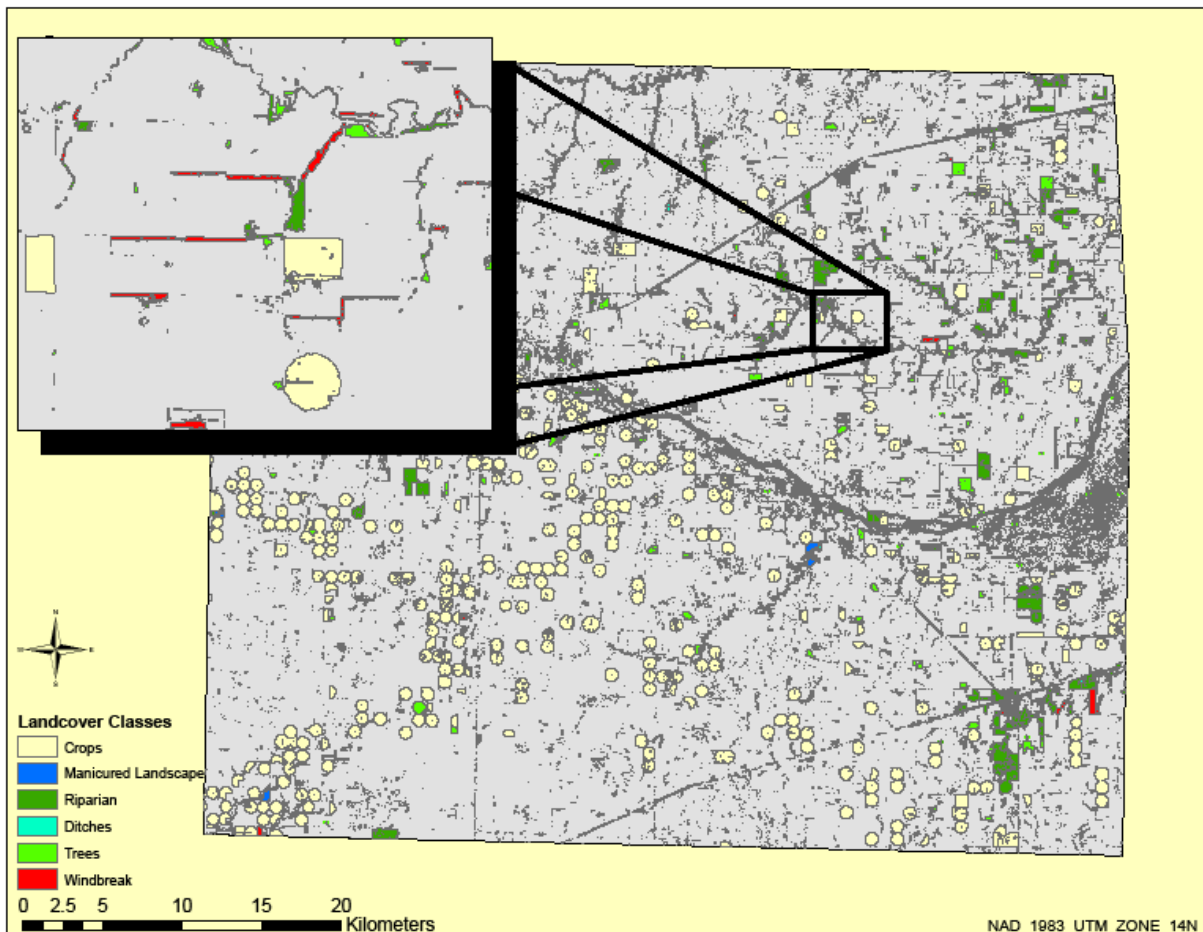
Table 10. Number of training sites selected for each landuse/landcover class in Ford County.

Cover Type	Number of Training Sites
Crops	35
Tree Stands	50
Riparian	20
Windbreaks	45
Manicured Landscape	6
Ditches	15

The final step in classifying the remaining objects in Ford County again required the use of the SVM RBF algorithm. Hsu *et al.*, (2008) state that the RBF algorithm works just as well, if

not better than, the three other kernel types when dealing with a large number of data points (*i.e.*, attributes of objects). For the purpose of consistency, and based on the suggestions of Hsu *et al.*, (2008), the RBF algorithm was used to classify the objects in Ford County. The original classified vectors, prior to any manual cleanup or accuracy assessment, are shown in Figure 16. The ‘windbreak’ Landcover class was assigned a Class ID of “WB” in the attribute table. The data in Figure 16 is used for display purposes of what the RBF classification algorithm generated but is not yet a final result.

Figure 16. Classified landuse/landcover map of the features generated in Ford County using object-based classification.



The speed with which windbreaks could be classified was an issue of concern in this research. The KFS wanted a method that reduced the time needed to identify windbreak locations as compared to the heads-up digitizing technique that required many hours to inventory windbreaks using aerial photographs. The amount of time required for the various computational steps required to generate the classification results is listed in Table 11. These time measures are only for software processing time and do not include user decision times.

Table 11. Software processing times required for each step in the classification of the Ford County NAIP image using object-based methods.

Step	Time (Minutes)
Segmentation	5.1
Merging	22
Thresholding	4.2
Extract Features	18
Classify Features	7
Total	56.4

Windbreak Extraction

The windbreak class was extracted from the original classification results by selecting Class ID “WB” and exporting it as a single shapefile. The windbreaks in this shapefile contained no attribute information (*e.g.*, spectral, spatial, textural, or band ratio) and is referred to as Windbreaks NA (NA= No Attributes). Once the windbreaks were isolated into their own file with no other landuse/landcover types present, a manual editing session was used to remove any features that were misclassified as a windbreak. The windbreak class was placed over the original 2008 NAIP CCM of Ford County and carefully inspected to remove any misclassified features by manually editing the shapefile within a GIS

Windbreak Condition Assessment

The second objective of this research was to assign identified windbreaks to distinct condition classes. Members of the Kansas Forest Service (KFS) determined that establishing three classes (good, fair, and poor) would best suit their needs for future windbreak renovation planning and policy reporting. Wiseman *et al.*, (2007) stated that using average spectral reflectance of windbreaks correlated well with ground truth observations. Building off of this work, average spectral reflectance of the green band (Band 2) of the 2008 Ford County NAIP image was used to estimate windbreak condition classes. In this assessment mean BV's were obtained from the 6 m resampled imagery of Ford County. The rationale behind using Band 2 was that average green reflectance values would correlate well with windbreak density, a common criteria used to rate windbreak condition. The principle here is that that darker BV's (lower reflectance) will correlate with dense (good) windbreaks having few gaps or snags and those which are functioning well. It should be noted that windbreaks are rated based on how well they are functioning as a wind restraint and not solely the health of individual trees within the stand (Kort and Stefner 2007). Brighter (higher) BV's will correlate well with poor condition windbreaks containing gaps and snags. Less dense (poor) windbreaks will have areas of bare earth showing through from a vertical view and result in higher average BV's. A dense (good) windbreak will have little to no bare earth showing through and lower mean BV's. Areas of bare earth within windbreaks were not removed during the thresholding process because they had already been factored into the windbreak vectors during the 'merge' process. This ensured that measuring the mean spectral reflectance of windbreak objects would still reflect any gaps or breaks in the barrier.

In order to classify windbreaks based on their average green reflectance, windbreaks were extracted from the "Ford Co. Segments" shapefile that contained this attribute information.

Windbreaks were extracted using a spatial query (*e.g.*, “select by location”) that identified features that intersected the Windbreak NA feature class. Once windbreaks were selected from the Ford Co. Segments shapefile they were exported to another shapefile called “WB Vectors BVS” (Windbreak Vectors Brightness Values).

Three classification strategies were used to place windbreaks into the good, fair and poor categories. First, a quantile, or equal frequency, scheme was used in a GIS to place windbreaks into the three condition classes in an automated fashion. A quantile classification works by “dividing the total number of data values by the number of classes and ensures that each class contains the same number of data values” (Chang 2006, pg 179). Second, a natural breaks method was used to place windbreaks into the three classes in a similar automated fashion. Natural breaks classification works by implementing the Jenk’s optimization formula which places data into classes based on natural groups within the data set (Chang 2006). Finally, a statistical classification scheme was developed by assigning every value that was less than one standard deviation from the mean to the good class and every value that was one standard deviation higher than the mean to the Poor class. All values falling between ± 1 standard deviation of the mean were placed into the Fair category. As mentioned earlier, good condition windbreaks will have few gaps which would allow soil or grasses to show through the canopy and raise the overall average BV of the windbreak as a whole. Poor windbreaks, on the other hand, will contain many gaps where high BV’s from bare soil and grasses will increase the mean BV of the windbreak being classified.

The Normalized Difference Vegetation Index (NDVI) was also evaluated as a means to assess overall windbreak condition. NDVI is an indexed measure of greenness with values ranging from 0.0 - 1.0 (Liu and Huete 1995). The closer to 1.0 a NDVI value the healthier the

vegetation is supposed to be with vegetation health decreasing as the values near 0.0. NDVI was developed by Rouse *et al.*, (1974) and is a measure of the greenness of the earth's surface that frequently correlates well with vegetation properties such as aboveground biomass, leaf area index, and percent cover (Cihlar *et al.*, 1991). It is calculated using data from the red and NIR bands of remotely-sensed data (Equation 5). In the context of this study, object with high NDVI values (greener surfaces) are considered to contain more and healthier vegetation.

Equation 5. Normalized Difference Vegetation Index (NDVI).

$$NDVI = \frac{(NIR - redband)}{(NIR + redband)}$$

Using the zonal statistics function within a GIS, NDVI values were obtained for ground truth windbreaks that had been field surveyed to determine their condition class. Mean NDVI values were calculated for these windbreaks to determine proper class breaks between the good, fair, and poor class categories.

Jensen (2007) notes that one of the major weaknesses of NDVI is that it is “very sensitive to canopy background variations” and can be artificially high with darker canopy backgrounds. Darker areas in an NDVI image often contain areas of soil and dry grasses. Because of this, porous windbreaks with large caps in the canopy (*i.e.*, those likely to be in the poor windbreak condition class) might have higher average NDVI values resulting in placement in a better condition class.

In addition to average green reflectance values and NDVI, spectral texture was also evaluated as a means to measure windbreak condition. Often, when objects of different landcover types share similar spectral properties, textural measures can serve as a means to

distinguish between the two. Jensen (2005) states that the higher (coarser) a textural value is then the brighter it will appear. This means that windbreaks with coarse mean textural values will likely have a wide variation of values within them that likely signify the presence of gaps and snags which are characteristic of windbreaks in the poor condition class. Conversely, good condition windbreaks with few gaps or snags will have low mean textural values.

A texture image was calculated using a 3 x 3 moving window from the 2008 NAIP image of Ford County. Mean texture values were obtained for each windbreak using the zonal statistics function within a GIS. As with the green BV and NDVI-based assessments, textural values were classified using three classification strategies to place each windbreak into the good, fair, or poor condition class category and poor categories.

A fourth, and final, approach involving a combination of texture and green reflectance was also used to produce accurate assessments of windbreak condition. Because the BV's associated with texture and green reflectance images of windbreaks in good and poor condition classes are inversely related (*e.g.*, poor condition windbreaks likely have both high green reflectance textural values) should correlate well with poor condition windbreaks it was thought that combining the two would increase the likelihood of distinguishing between condition class and make class breaks more discernable. In this step mean BV's were obtained from the original 1m 2008 NAIP imagery using zonal statistics within a GIS. Texture and BV's were then added together within a GIS to form their own attribute. Raw values of texture and BV's had a wide range of values (4.4 - 232.3) so based on suggestions from Booyesen (2002) it was decided to use a linear scaling transformation to index the values into a more manageable distribution. Using Booyesen (2002) linear scaling model texture and BV's were indexed to values between 0.0 - 10, with the idea that windbreak health/function would decline as values move towards 10.

Acreage Calculations

To determine the amount of acres/hectares in each condition class the geospatial data layer containing the condition index information was converted to a 1 m raster. After the file was converted to a raster it was reclassified so that all values in the good category received a new value of 1, windbreaks in fair condition received a value of 2, and windbreaks in poor condition received a value of 3.

In order to calculate the total acreage of each class, the total area in square meters of each class had to first be determined. Because each pixel covers an area of 1 m², total area in square meters was calculated shown in Equation 6. Square meters were converted to acres using a conversion factor of 0.000247105381 as shown in Equation 7. Acres were then converted to hectares using Equation 8.

Equation 6. Formula to calculate area (m²) for each windbreak condition class.

$$TotalArea(m^2) = 1 * N$$

where:

N = the total number of pixels in each class.

Equation 7. Formula to convert area to acres from square meters.

$$TotalArea(Acres) = TotalArea(m^2) * 0.000247105381$$

Equation 8. Formula to convert acres to hectares.

$$TotalHectares = TotalAcres * 0.404685642$$

Ground Truth Data Collection

Remote sensing accuracy assessments usually, if not always, require the use of ground truth data for comparison purposes. For this study, ground truth data was needed to both quantify the performance of the object-based windbreak classification and the accuracy of estimated windbreak condition assessments. The location and condition of 34 windbreaks in Ford County were cataloged during a series of field surveys conducted during June 2008. This was approximately the same time period during which the 2008 NAIP image used in this study was collected.

Published in the Great Plains Initiative Inventory Project Field Guide 1.0 (2008), foresters have developed a set of criteria that are used when performing field surveys of windbreaks. In the field, foresters record the category (Table 12) where the majority of the condition descriptions listed in Table 13 apply. While conducting condition assessments, foresters walk (or drive) the length of each windbreak and observe them from a distance of 1/8 of a mile (approximately 200 m) to identify gaps.

Table 12. Windbreak condition class evaluation guide (GPIIP Field Guide 1.0 2008).

Condition Class	Description
Good	Meets at least 7 of the attributes listed (one needs to be less than 25% mortality)
Fair	Has 5-6 of the attributes listed (one needs to be less than 25% mortality)
Poor	Has less than 5 of the attributes listed an/or more than 25% mortality

Using the criteria outlined in Tables 12 and 13, 9 of 34 windbreaks (26%) surveyed were determined to be in poor condition as they met less than 5 of the listed attributes. A total of 16 (47%) and 9 (26%) windbreaks were determined to be in the fair and poor classes, respectively.

Table 13. Windbreak attributes used to place windbreaks into condition classes (GPIIP Field Guide 1.0 2008).

Less than 25% of the trees are dead
Continuous barrier, no gaps (missing trees)
50% density of greater
No smooth bromegrass or fescue sod present
Majority of the tree crowns are healthy with less than 25% of the trees showing insect, disease or herbicide damage
None to very little livestock activity in the planting
Tree regeneration is present
Trees are expected to live another 20 years

Many of the surveyed windbreaks (between 10-15) were located on private property where permission to access the windbreak locations had not been granted to access the land in order to measure spatial properties using a GPS. Since accurate GPS-derived coordinates for these windbreak locations could not be obtained, a geospatial data layer of windbreak locations was created via heads-up digitizing using the 2008 NAIP image for Ford County.

Condition classes were assigned as attributes to each windbreak in the attribute table based on findings from the field surveys. Average green (band 2) spectral reflectance, NDVI, and textural values were also added as attributes and used later as the basis for the GIS-generated condition class results (*e.g.*, quantile, natural breaks, and standard deviation classifications).

Mean spectral reflectance values for the windbreaks surveyed in the field were obtained by using zonal statistics derived from the NAIP image. NDVI and texture values were calculated using the zonal statistics function in a GIS from the NDVI and texture images.

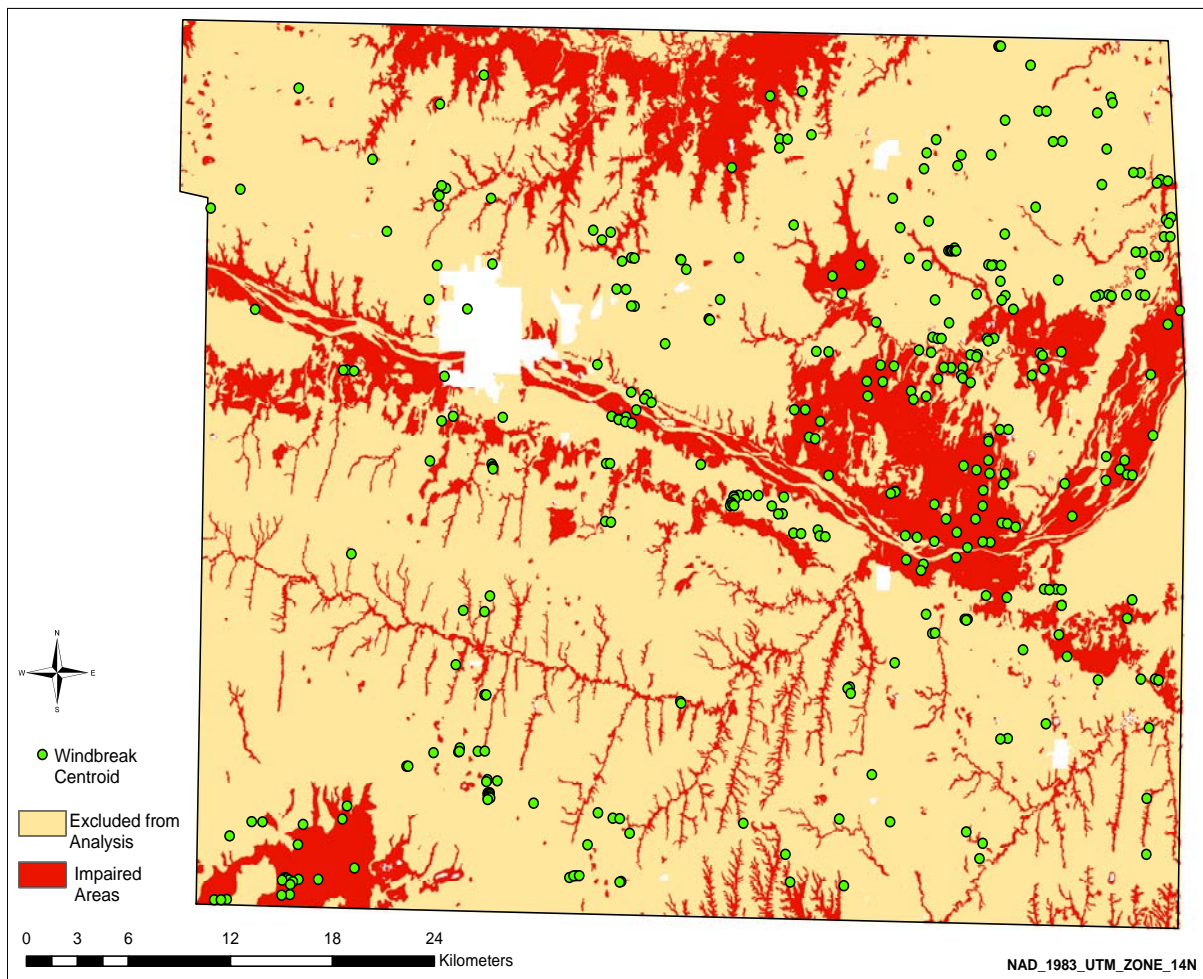
Highly Erodible and Impaired Soils Layer

Staff members from the KFS requested that the number of windbreak acres present on erodible soils be calculated as part of this project. To accomplish this task, a raster dataset of highly erodible and impaired soils was obtained from Hutchinson *et al.*, (2008). This dataset was

produced using data from the State Soil Survey Geographic (SSURGO) and the Kansas GAP landcover dataset and identified areas of cultivated lands with a wind erodibility index (WEI) of 87 or greater.

Ford County was extracted from the soils layers using an ‘extract by mask’ function with a vector-based feature class of the county boundary serving as the mask (Figure 17). Hutchinson *et al.*, (2008) excluded incorporated areas from their analysis, but only one Ford County windbreak was located in an area containing no information related to erodible or impaired soils.

Figure 17. Highly erodible and impaired soils in Ford County, Kansas.



The highly erodible or impaired soils raster for Ford County was converted from its original 30 m cell size to a 1 m resolution to match the grain of the windbreak condition class grid which was converted to a 1m raster to calculate total condition acres in a previous step. Each windbreak condition class was isolated into separate binary grids with representing the presence (value = 1) or absence (value = 0) of windbreaks in a given condition class. Next, each windbreak class was added separately to the erodible/impaired soils grid using a raster calculator function to determine pixel counts of each class in an impaired area. Pixel counts for each class were then converted to square meters, acres, and hectares (Equations 6-8).

CHAPTER 5 - Results and Discussion

Segmentation Results

As noted earlier, object-based classification relies almost entirely on the segmentation process where objects are created by grouping like or similar pixels into polygons or ‘shapes.’ Using the segmentation parameters discussed previously, 51,202 objects were generated within Ford County. These objects are displayed at a scale of 1:235,000 in Figure 18. Areas in white contain no data as they were masked out during the thresholding process. A larger-scale view (1:60,000) of several segmented objects within the study area is shown in Figure 19.

Figure 18. Segmented image of vegetative features in Ford County (1:235,000 scale).

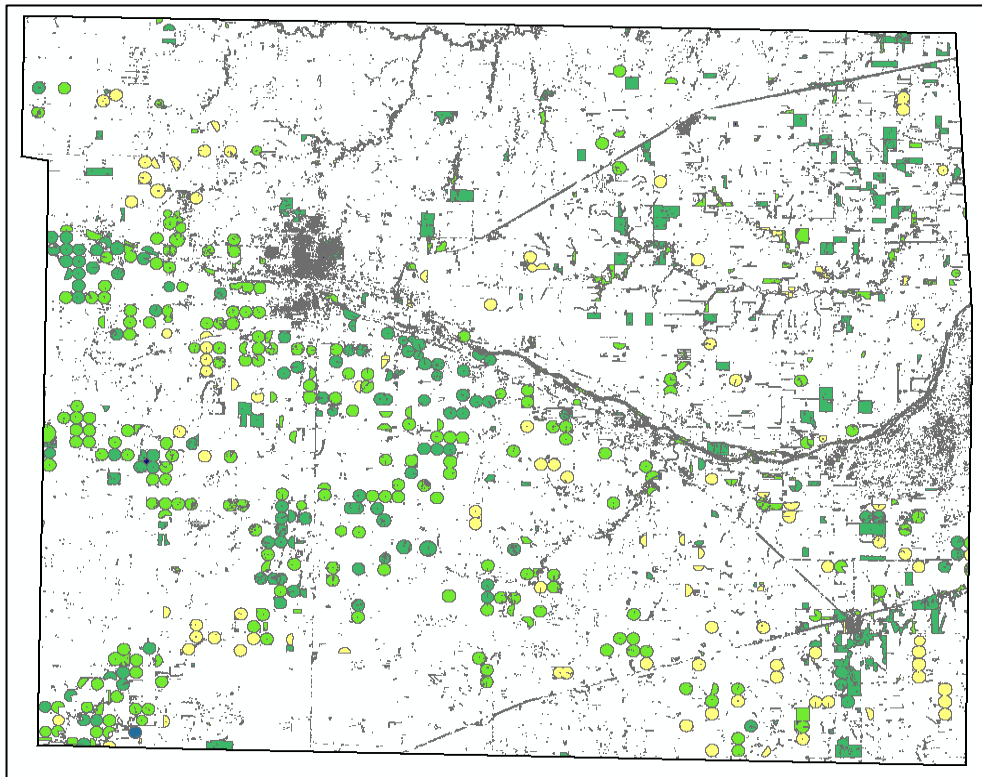
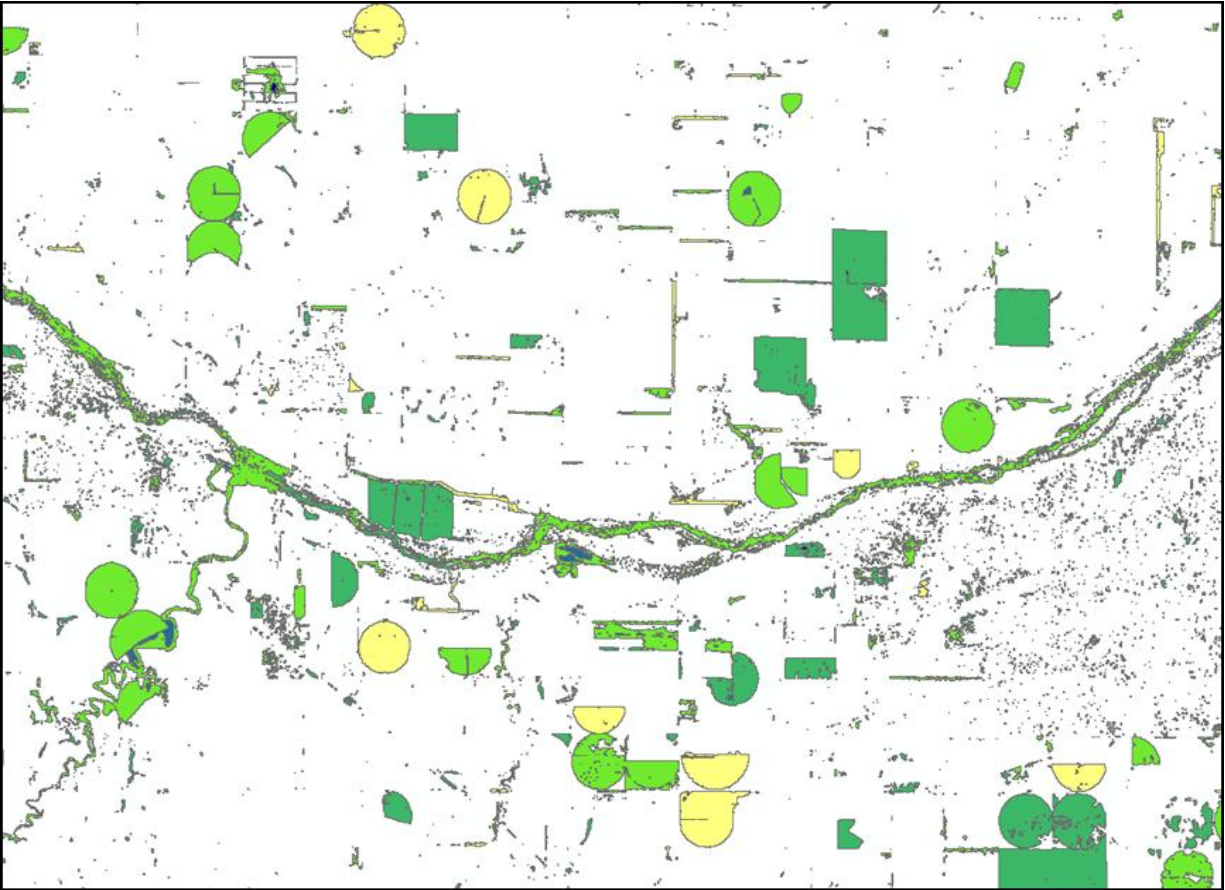


Figure 19. Portion of the segmented image of vegetative features for Ford County (1:60,000 scale).



Classification Accuracy

After segmenting the imagery objects were classified and placed into their respective landuse/landcover categories. Accuracy of the object-based classification was measured by creating an error matrix (Table 14) and calculating the Kappa metric. The error matrix combines all non-windbreak classes into one class labeled NWB (non-windbreak). First however, the proper number of samples had to be determined using Fitzpatrick-Lins (1981) equation derived from Binomial Probability Theory (Jensen 2005). Equation 9 shows the allowable error, expected accuracy and number of sample points used in this research. Given the needs of the forest service in regards to windbreak renovation planning it was decided by members of the

KFS that an allowable error of 15% would be acceptable for this research. 203 sample points were generated using the random sample generator within a GIS. Given the small size of the test site it was determined that stratified random sampling would not be necessary and that the Fitzpatrick-Lins (1981) equation would suffice.

Equation 9. Implementation of the Fitzpatrick-Lins equation.

$$N = \frac{2^2 * 85 * 15}{5^2} = 203$$

Table 14. Classification error matrix for the Ford County test site.

	NWB	Windbreak	Row Total	User Accuracy
NWB	179	4	183	97.8%
Windbreak	3	17	20	85%
Column Total	182	21	203	
Producer Accuracy	98.35%	80.95%	Overall Accuracy	96.6%
			Kappa	81%

Given that the current classification scheme had a very good overall accuracy of 96.6% and a strong Kappa statistic, it was determined that the parameters used to classify landcover/landuse features in the test site would be appropriate for classifying the entire county.

After classifying the entire Ford County image, an additional error matrix was compiled to measure the user, producer, and overall classification accuracy (Table 15). Ford County contained over 51,000 objects, so the random sample size was increased from 203 to 300. Congalton (1991) and Congalton and Green (1999) suggest that each class have at least 50 random points when dealing with large areas (*i.e.*, 1 million ha or more), so each class was assigned 50 random points in order to construct the error matrix. As with the test site, all non-windbreak features were placed into the single (NWB) category.

Table 15. Error matrix compiled from a random distribution of sample points for the Non-Windbreak (NWB) and Windbreak classes.

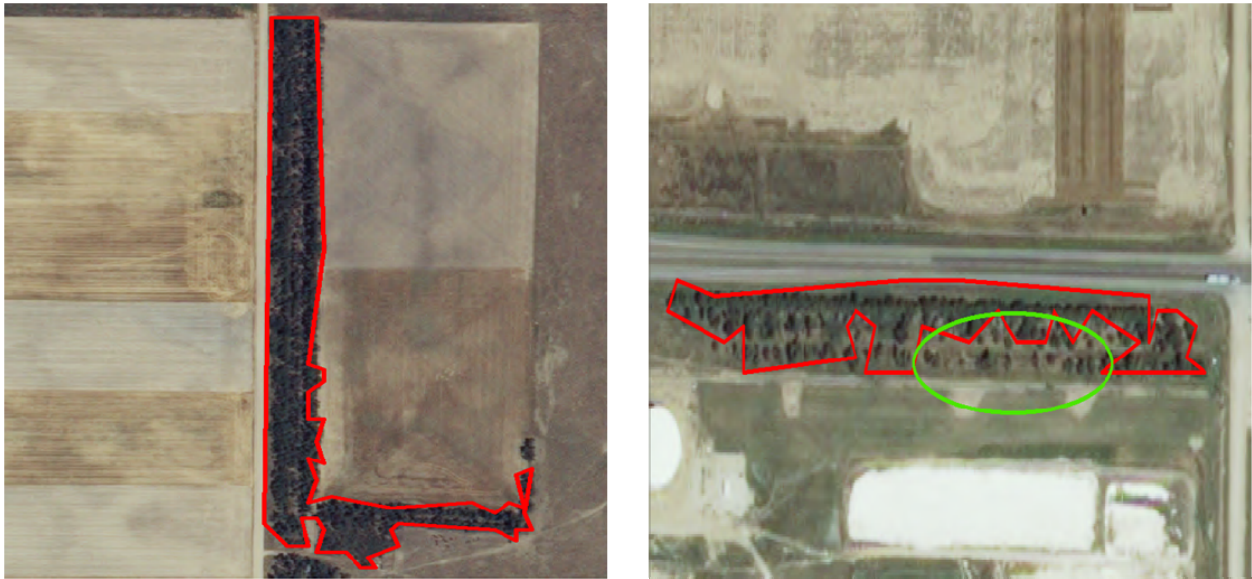
	NWB	Windbreak	Row Total	User Accuracy
NWB	247	22	269	91.8%
Windbreak	3	28	31	90.3%
Column Total	250	50	300	
Producer Accuracy	98.8%	56%	Overall Accuracy	91.7%
			Kappa	64.6%

Using the same object-based classification parameter settings as in the test site, an overall accuracy of 91.7% was obtained with a corresponding Kappa metric of 64.6%. While producer accuracy appeared fairly low (56%) for the windbreak class, the user accuracy was quite high at just over 90%. In addition, both producer and user accuracy for the non-windbreak category were both over 90%.

While the overall classification accuracy of approximately 92% is very good, the proper boundaries of the windbreak objects were often inconsistent with that of the actual windbreak features on the ground. When observing the object-based results over the original 1 m NAIP imagery it was evident that some windbreaks were not captured in their entirety. Because the down-sampled 6 m image was being used for segmentation and windbreak classification, the segmentation process had difficulty recognizing very poor condition areas where snags, gaps, and soil was visible in between trees within a larger windbreak feature. This is due to the drastic change in spectral reflectance values between a dense area in a windbreak and a degraded area. Figure 22 displays a subset of the Ford County image where the segmentation process defined the border of a dense windbreak very well compared to another site where an inaccurate border was identified for a degraded windbreak. The green oval in the photo on the right of Figure 22 illustrates an area in which the true border of the windbreak was not defined correctly during

segmentation. This may be corrected, to a degree, by incorporating a smoothing technique on a set of manually selected features without altering boundaries of properly defined windbreaks.

Figure 20. Images displaying accurate windbreak border assignment and an inaccurate border assignment.



Windbreak Classification Accuracy

Approximately 150 objects (23%) were removed from the windbreak class during a manual editing session within a GIS. Several riparian areas, ditches and some cropland were misclassified as windbreaks. However, removal of these objects was a simple process requiring less than 30 minutes, as such errors were easy to visually detect. These misclassified features had to be removed in order to accurately report the total number of windbreaks (355) in the study area. Most of the features removed were fairly small (12 m^2 or less) so they did not take up a significant portion the overall total area of the windbreak class.

In order to perform an accuracy assessment of the windbreak class by itself, several known windbreak locations were needed for comparison. A geospatial dataset of 137 known windbreaks was obtained from the USDA NRCS for comparison with windbreaks derived by object-based classification. It is important to note that while this project attempted to classify every windbreak within Ford County, the NRCS dataset was created using a ‘heads-up’ digitizing approach for only those windbreaks considered ‘significant’ (Table 16).

Table 16. Comparison of windbreak acres for the NRCS and object-based classification products.

Statistic	NRCS	Object-based Classification
Mean	2.42	0.86
Minimum	.24	0.007
Maximum	11.71	3.95
Standard Deviation	1.39	0.99
Total	821.3	1,011.9

The large difference in maximum values between the NRCS and object-based classification results is likely due to some fragmentation within windbreaks classified using the object-based approach. For example, it is likely that the NRCS digitized a single feature based on an extremely long windbreak with fragments in it due, perhaps, to bisecting roads. While a human can subjectively make the decision to classify a fragmented, or multi-part, windbreak into one singular unit, object-based classification methods classify each part as separate object primitives. This is one weakness of the object-based method when trying to capture singular features that contain very dynamic attributes.

Making careful visual inspections of the object-based classification results and the NRCS data it was confirmed that the NRCS data did not account for fragmented windbreaks but rather made the decision to classify them as singular units (Figure 21). The NRCS windbreak polygon

outlined in red in Figure 21 is located in central Ford County and was the largest windbreak inventoried, measuring 11.7 hectares (28.9 acres) in area.

Though there is a large difference in the number of windbreaks as reported by NRCS and classified in this study, a comparison of total windbreak area should be similar. In fact, a difference of only 190 acres was found to exist between the two datasets.

Figure 21. Example of a fragmented windbreak classified by NRCS as a single unit, but as two distinct units by object-based classification.



A simple percentage match comparison was performed to test how well the object-based windbreak classification results agreed spatially with the NRCS data. Using the spatial query

capability within a GIS, all windbreaks classified using the object-based method that intersected NRCS windbreaks were selected. Results showed that 111 of the 355 (81%) object-based features coincided with the 137 NRCS windbreaks.

Windbreak Condition Assessments

Each of the classified windbreak features were placed into one of three condition classes (good, fair, and poor) based on the average green (band 2) reflectance computed for each feature. A quantile classification method was the first technique used to place windbreaks into the 3 classes. An error matrix (Table 17) was created to determine how accurately the quantile classification scheme could automatically place windbreaks into the correct condition class when compared to field survey assessments.

Table 17. Error matrix for windbreak condition assessment based on average green reflectance and a quantile classification scheme.

Surveyed Condition Class	Quantile Classification Condition Class			Row Total	User Accuracy
	Good	Fair	Poor		
Good	4	6	0	10	40%
Fair	4	7	5	17	41.2%
Poor	0	4	4	8	50%
Column Total	8	17	9	34	
Producer Accuracy	50%	41.2%	44.4%	Kappa = 9.7%	
				Overall Accuracy= 44.1%	

Using the quantile classification scheme an overall accuracy of 44.1% was obtained. The Kappa statistic showed that the classification was not significantly better than random assignment of condition classes. Because of this, quantile classification was abandoned as a means to classify average green reflectance.

A natural breaks classification was the second approach used to place windbreaks into the three condition classes. An error matrix (Table 18) was created to compare results with ground truth data in similar fashion to the quantile classification assessment.

Table 18. Error matrix for windbreak condition assessment based on average green reflectance and a natural breaks classification scheme.

Surveyed Condition Class	Natural Breaks Classification Condition Class			Row Total	User Accuracy
	Good	Fair	Poor		
Good	6	3	0	9	66.7%
Fair	5	10	5	22	40.9%
Poor	0	3	2	5	40%
Column Total	11	16	7	34	
Producer Accuracy	54.6%	62.5%	28.6%	Kappa= 18.8%	
				Overall Accuracy=52.9%	

Results from the natural breaks classification yielded a stronger measure of overall accuracy (52.9%) than the quantile classification and an improvement in the Kappa metric (18.8%). The Kappa metric was still too low to show that the classification significantly worked better than the random assignment of condition classes. Wishing to improve the accuracy between ground truth condition and the GIS generated classifications, a standard deviation classification was implemented next.

The standard deviation classification was developed based on ± 1 standard deviation (14.7) from the mean green reflectance of each windbreak. Again, an error matrix (Table 19) was created to assess the accuracy of the statistical classification when compared to field survey results.

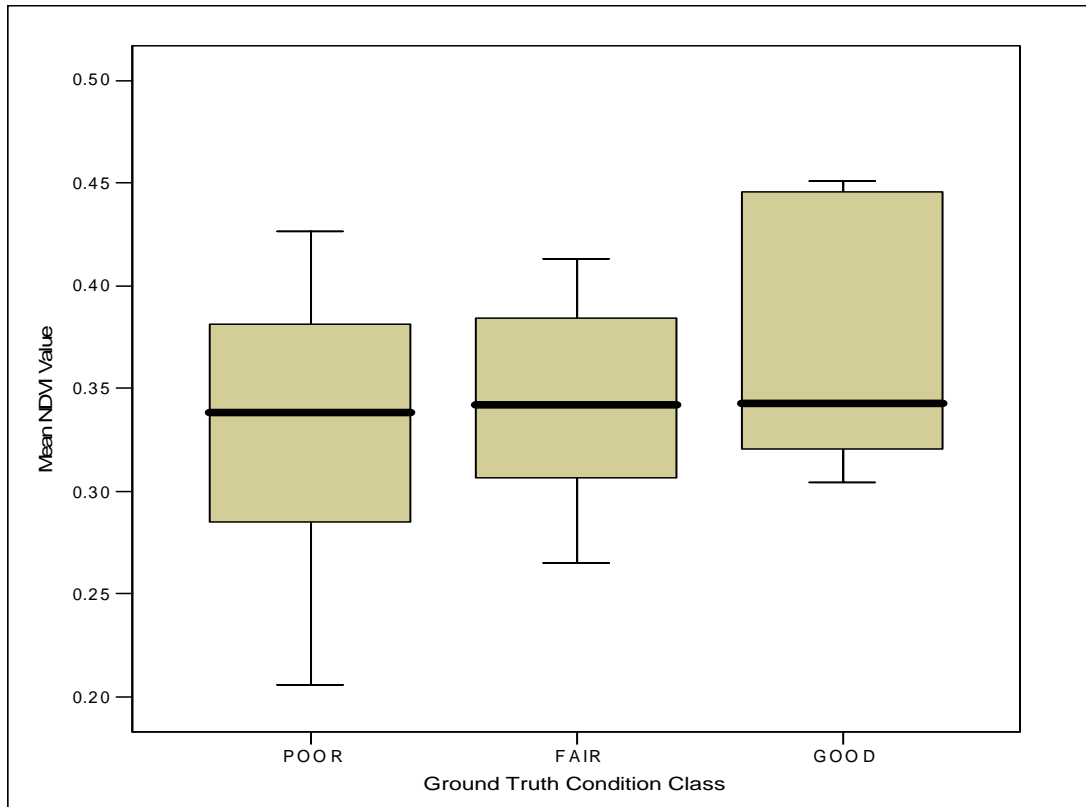
Table 19. Error matrix for windbreak condition assessment based on average green reflectance and a standard deviation (SD) classification scheme.

Surveyed Condition Class	SD Classification Condition Class				User Accuracy
	Good	Fair	Poor	Row Total	
Good	3	0	0	3	100%
Fair	2	10	3	15	66.7%
Poor	4	6	6	16	37.5%
Column Total	9	16	9	34	
Producer Accuracy	33.3%	62.5%	66.7%	Kappa = 31.5%	
				Overall Accuracy=55.9%	

The standard deviation classification produced much better results (55.9% overall accuracy) than the quantile or natural breaks classifications. The Kappa metric also showed improvement (31.5%) when using the standard deviation classification. User accuracy for the good condition class was discovered to be 100% while the producer accuracy was only 33.3%. Producer accuracy for the poor class was found to be approximately 67% showing much improvement compared to the results of the quantile and natural breaks classifications.

After evaluating the effectiveness of using average green reflectance to accurately determine windbreak condition class, the same classification strategies were implemented to place windbreaks into their respective condition classes based on the mean NDVI value of each windbreak feature. However, as can be seen in Figure 25 no clear break existed in the data. An extreme amount of overlap between the classes existed making it impossible to determine appropriate class breaks. In addition all the classes had similar overall mean NDVI values (good = 0.37, fair = 0.36, and poor = 0.33) denoted by the heavy black line running horizontally through the box plots in Figure 22.

Figure 22. Box-and-whisker plot illustrating the overlap in NDVI values across windbreak condition classes for field-surveyed windbreaks.



Despite the vast amount of overlap between NDVI values in the condition classes it was decided to use the quantile, natural breaks, and statistical classification schemes similar to those used in the condition assessments based on mean spectral reflectance of band 2. By doing this, a comparison could be made between the two classification variables (BV's vs. NDVI).

Tables 20 - 22 contain error matrices that compare field survey condition class assessments with those made based on average NDVI using a quantile, natural breaks, and standard deviation classification scheme.

Table 20. Error matrix for windbreak condition assessment based on average NDVI values and a quantile classification scheme.

Surveyed Condition Class	Quantile Classification Condition Class				User Accuracy
	Good	Fair	Poor	Row Total	
Good	3	7	2	12	25%
Fair	6	7	4	17	41.2%
Poor	0	2	3	5	60%
Column Total	9	16	9	34	
Producer Accuracy	33.3%	43.8%	33.3%	Kappa = 2.3%	
				Overall Accuracy=38.2%	

Table 21. Error Matrix for windbreak condition assessment based on average NDVI values and a natural breaks classification scheme.

Surveyed Condition Class	Natural Breaks Classification Condition Class				User Accuracy
	Good	Fair	Poor	Row Total	
Good	3	7	2	12	25%
Fair	6	7	4	17	41.2%
Poor	0	2	3	5	60%
Column Total	9	16	9	34	
Producer Accuracy	33.3%	43.8%	33.3%	Kappa = 2.3%	
				Overall Accuracy=38.2%	

Table 22. Error matrix for windbreak condition assessment based on average NDVI values and a standard deviation (SD) classification scheme.

Surveyed Condition Class	SD Classification Condition Class				User Accuracy
	Good	Fair	Poor	Row Total	
Good	3	4	1	8	37.5%
Fair	6	10	7	23	43.5%
Poor	0	2	1	3	33.3%
Column Total	9	16	9	34	
Producer Accuracy	33.3%	62.5%	11.1%	Kappa = 3.4%	
				Overall Accuracy= 41.2%	

Using the quantile classification to place windbreaks into the condition categories based on mean NDVI values resulted in an overall accuracy of approximately 38% and a very low Kappa metric of 2.3%. User accuracy was highest (60%) for the poor condition class while user accuracy for the good class was the lowest (25%). Given these results the natural breaks classification was tested next to monitor improvement or a reduction in accuracy..

After natural breaks classification, the exact same results were produced as when applying the quantile strategy. After observing no improvement in the classification accuracy it was determined a standard deviation classification should be done using ± 1 standard deviation (± 0.08) of the NDVI mean (0.33) to determine class breaks. In this scenario windbreaks + 1 standard deviation (0.4) would be placed in the good category and all values less than - 1 standard deviation (0.29) would be placed into the poor category. All values falling between ± 1 standard deviation of the mean would be placed into the fair category.

The standard deviation classification proved to be most accurate (41% overall accuracy) compared to the rest of the classification techniques using average NDVI values. However, the overall accuracy of the standard deviation classification using average NDVI values was still less than that which was achieved when using the same classification method but with average green reflectance values (56% overall accuracy).

Jensen (2007) reports that one of the weaknesses of NDVI is that it is extremely sensitive to background variations in the canopy and that, during periods of peak greenness, NDVI values can become oversaturated due to the large amount of leaf area. Huete and Liu (1994) found NDVI to be unreliable because of sensitivity to soil characteristics visible through the canopy, as well as the presence of dead vegetation. Better results from NDVI classifications might be

obtained with imagery taken at times other than peak greenness where NDVI values would be less inflated in poor and fair windbreaks because of smaller leaf areas.

Average windbreak texture was used as a third means to classify windbreak condition. Areas having high mean texture values have a vast amount of variation in values within the windbreaks indicating that gaps and snags are likely present. Conversely, good windbreaks that are functioning well would have low mean textural values as a result of few existing gaps and snags. Because the standard deviation classification performed best in tests using average green reflectance and NDVI, it was also used to classify average texture values into the three condition classes. In this scenario it was found that using break values ± 0.5 standard deviations from the mean (42.7) worked best. All windbreaks with a mean textural value less than -0.5 standard deviations (31.2) were placed in the good category while all windbreaks having a mean textural value greater than $+0.5$ standard deviations (54.2) from the mean were placed into the poor category. Figure 23 displays the difference in textural values for each condition class of the ground truth windbreaks. Table 23 represents the error matrix created comparing field survey and remote sensing condition class assessments.

Figure 23. Box-and-whisker plot illustrating the variation in textural values across windbreak condition classes for field-surveyed windbreaks.

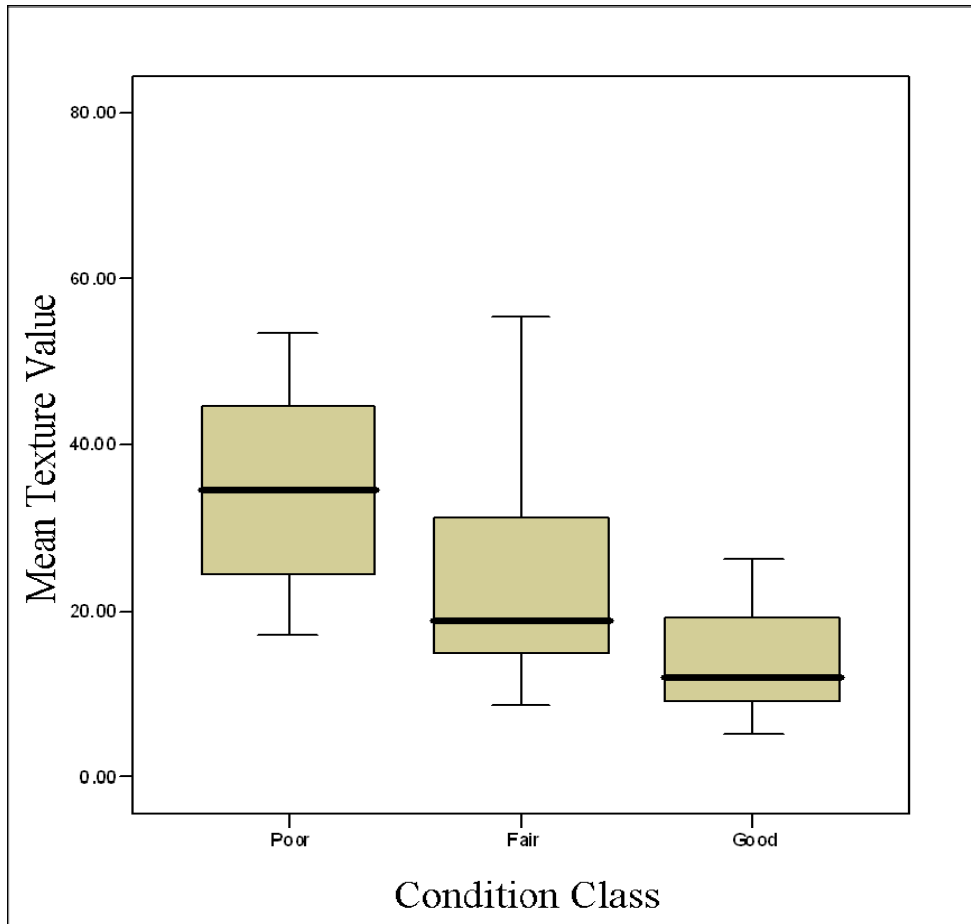


Table 23. Error matrix for windbreak condition assessment based on mean texture values and a standard deviation (SD) classification scheme.

Surveyed Condition Class	SD Classification Condition Class			Row Total	User Accuracy
	Good	Fair	Poor		
Good	5	4	0	9	55.6%
Fair	4	11	4	19	57.9%
Poor	0	1	5	6	83.3%
Column Total	9	16	9	34	
Producer Accuracy	55.6%	68.8%	55.6%	Kappa= 38.9%	
				Overall Accuracy=61.8%	

Using mean textural values to classify windbreak condition showed significant improvements over using mean NDVI and BV's. An overall accuracy of 61.8% and a Kappa metric of 38.9% was obtained using textural values. In addition, the poor condition class received a fairly high user accuracy of 83.3%. Still wishing to improve the overall accuracy of the condition classification, BV's and texture were combined to create a 'condition index' based on suggestions from Booyesen (2002). Table 24 displays the error matrix comparing the field survey data and condition index approach to class assessment.

Table 24. Error matrix for windbreak condition assessment based on average condition index values and a standard deviation (SD) classification scheme.

Surveyed Condition Class	SD Classification Condition Class				User Accuracy
	Good	Fair	Poor	Row Total	
Good	7	3	0	10	70%
Fair	2	12	4	18	66.7%
Poor	0	1	5	6	83.3%
Column Total	9	16	9	34	
Producer Accuracy	77.8%	75%	55.6	Kappa=53.3%	
				Overall Accuracy=70.6%	

By combining mean texture and average green reflectance of each windbreak, an overall accuracy of approximately 71% was achieved (Note: Average green reflectance here was calculated using the original 1 m resolution NAIP image). The Kappa metric also showed improvement (53%). This represents a 15% improvement in overall accuracy as compared to the results using only average green reflectance and a 30% improvement compared to results generated using average NDVI values. The areas of windbreaks in each condition class were

determined based on the condition index assessments due to the fact they exhibited the highest percent overall accuracy compared to all other condition classification attempts (Table 25).

Table 25. Windbreak area by condition class.

	Acres	Hectares
Good	313.1	126.7
Fair	528.6	213.9
Poor	170.2	68.9
Total	1011.9	409.5

A wide range of accuracy results were obtained from the condition assessments. It is important to consider the differences between classifying condition by viewing windbreaks horizontally from the ground versus viewing them from above using aerial imagery in order to understand the amount of error between ground truth condition classification and GIS generated classifications. For example, a windbreak may appear dense while viewing it from the ground, yet the canopy may have dead vegetation that could only be seen using a view from above. In this scenario, the field survey may conclude that the windbreak is in good condition, while the remote sensing assessment rates the same windbreak as poor (Figure 24). Similarly, a windbreak classified as poor in the field due to numerous gaps visible at ground level, may be assessed as good when using remote sensing methods that see only a continuous healthy and dense tree canopy.

Figure 24. Example of windbreak classified during a field survey as being in good condition but in poor condition when using the standard deviation classification technique.



Windbreaks in Highly Erodible and Impaired Areas

Procedures discussed in the Data and Methods section were used to calculate the total acres/hectares of each condition class in the study area. Table 26 contains the acreage and hectare data obtained for each condition class in highly erodible and impaired areas.

Table 26. Total area of Ford County windbreaks located on highly erodible and impaired soils by condition class.

	Acres	Hectares
Good	420.9	170.1
Fair	380.3	153.7
Poor	42.1	17
Total	843.3	340.8

Out of all the windbreak acres calculated, 340.8 hectares (843.3 acres) were identified as being located in an impaired area, while the Good condition class was determined to contain the most acres in any given number of disturbed areas. Foresters in Kansas are equally concerned with renovating both fair and poor windbreaks. The 170 hectares of fair and poor windbreaks will likely be the top priority yet given the nature of segmentation process; Poor areas within overall Fair windbreaks were able to be identified as well. Using this spatial data certain areas of windbreaks can be targeted for field inspections and renovation. Figure 25 gives an example of some poor areas identified within a windbreak considered to be in overall Fair condition. This information will certainly assist the KFS as they promote windbreak renovation throughout the study area.

Figure 25. Example of a fair condition windbreak containing several areas that need renovation activities.



CHAPTER 6 - Conclusions

The main purpose of this project was to assist the KFS with future windbreak renovation planning and reporting by creating a set of RS and GIS methods to rapidly identify and classify windbreaks. Object-based classification is a complicated technique that requires a vast amount of trial and error processes in an attempt to create optimal vector polygons of homogeneous groups of pixels. Those vectors or 'objects' are then used as the basis for classification taking into account their geometric, spectral, and textural properties as outlined in Appendix B. As discussed in the Data and Methods chapter a bottom-up region merging segmentation process was used with a minimum distance classifier within the Ford County test site in early attempts to segment and classify windbreaks. Using those methods an overall accuracy of just over 50% was achieved on the classification. Here it has been proven that the edge-based segmentation algorithm accompanied with the SVM classifier out performed those methods by generating just over 96% overall classification accuracy in the test site and approximately 91% overall accuracy in the entire county classification. In future research attempts could be made to possibly enhance the overall classification accuracy by adjusting the scale parameters of the edge-based algorithm in an incremental fashion then testing each parameter setting for accuracy after the classification algorithm ran.

Methods developed in this research are meant to serve as a stepping stone towards classifying windbreaks throughout the rest of western Kansas and potentially the Great Plains. The idea was to establish a universal yet dynamic set of criterion that could be slightly modified by novice GIS and RS users to inventory windbreaks in areas outside of Ford County. Depending on what county is being classified, additional classes may have to be developed to account for landcover features not encountered in Ford County. Some possible scenarios might

include adding an 'open water' class in a county that had several lakes. In addition, segmentation parameters, merge factors, and band threshold values will likely need to be modified based on the nature of windbreaks in other counties. Some counties may only contain small farmstead windbreaks less than 1 hectare which undoubtedly would require that the segmentation parameters be modified and reduced in order to capture the smaller features.

Windbreaks cover a relatively minuscule amount of land when compared to the total area of land within the study site making it difficult to determine proper segmentation parameters that will capture the homogeneity of windbreaks without over generalizing them. Windbreaks are also planted in an ever changing variety of shapes and sizes making the segmentation parameters particularly difficult to determine. Setting segmentation parameters too high will result in the exclusion of small farmstead windbreaks while setting parameters too low will cause over segmentation in large windbreaks and thereby will not grasp the overall homogeneity of the objects to be classified. This is one weakness of the object-based approach that always needs to be considered when classifying any given set of features. After much testing, it was confirmed that a segmentation parameter setting of 78.0 and a merge factor of 50.0 did a reasonable job isolating windbreaks while presumably excluding a minimal number of small farmstead windbreaks. It should also be noted that windbreaks are planted in a wide variety of tree species. Typically larger field windbreaks in the study area contained deciduous hardwood trees while smaller farmstead windbreaks contained coniferous species such as Eastern Red Cedar. Hardwood and coniferous trees ultimately reflect different spectral signatures making it difficult to place them in the same class even though they may share similar geometric properties. In addition, dense windbreaks containing hardwood trees will inherently have higher BV's potentially making them fall into the wrong condition class when in fact they are in good health.

Future research should account for this problem by establishing a coniferous and deciduous windbreak class. Separating windbreaks into two classes based on the majority of species composition would likely increase the accuracy of identifying windbreaks and condition assessments.

An overall classification accuracy of 91% and a Kappa of 64% was obtained for all the classes in Ford County, the real concern is how accurately were windbreaks identified? In this research windbreaks were extracted from all other feature types and isolated in their own single class geospatial dataset. A problem of particular concern then is how to determine if any windbreaks were left unclassified and not inventoried? In order to address this problem a comparison was done between an NRCS inventory and the object-based classification results. The NRCS data and the object-based results showed approximately an 81% spatial match yet the object-based results classified many windbreaks the NRCS missed. The problem arises when it is taken into account that this research attempted to classify 100% of the windbreaks in Ford County while the NRCS chose which windbreaks to inventory and ultimately did not capture 100% of the windbreaks in the county. The fact is a scientifically justifiable accuracy measurement cannot be performed until a dataset containing 100% of the windbreaks in Ford County has been created for spatial matching comparisons. Attempts could be made to generate random points throughout the study area with the prospect of one landing on an unclassified windbreak but because windbreaks take up such a small part of the landscape odds are astronomically stacked against that happening. Based on all the accuracy tests, it is safe to say that approximately 355 windbreaks totaling 409ha exist in Ford County with roughly 91% assurance. This means that the object-based results missed approximately 9% of the windbreaks in the county. However, it should be addressed that 355 windbreaks might be an overestimate, as

the object-based technique inventoried fragmented windbreaks as separate units. While a windbreak with a dividing feature in it such as a driveway should in all honesty be classified as one unit the object-based technique identifies something like a driveway as a dividing edge feature between two independent groups of like pixels. This is major weakness to the object-based approach compared to the 'heads-up' digitizing approach. In future research a logical expression should be developed to merge fragmented windbreaks that are within a certain distance of one another.

Another objective of this research was to assess the condition of identified windbreaks based on their mean BV's, NDVI, and textural values. Using spectral values from band 2, collected from the resampled 6m imagery, condition assessments were made and an overall accuracy of condition class compared to ground truth data was discovered to be around 56%. Based on the overall accuracy of the condition class measures we can say that the using the mean BV's of windbreaks to place windbreaks in their respective condition class works about 56% of the time. It is important to conclude here that discrepancies between ground truth condition assessments and condition assessments made using aerial imagery exist due to the nature in which the windbreaks are being viewed. A condition assessment on the ground is made by horizontally viewing through the windbreak to identify flaws while the GIS and RS assessment methods are done from a vertical view looking down. Viewing windbreaks vertically eliminates the possibility of seeing flaws that are easily identifiable on the ground such as damage from cattle or insect damage. That said, we can finally conclude that condition assessments made from vertical viewing using BV's are around 56% reliable. Higher percent condition assessment accuracy was desired, so NDVI and textural values were tested to determine if they would correlate more with the ground truth observations. Using NDVI values actually showed a

decrease in overall classification accuracy compared to the use of BV's. This is likely due to inflated NDVI values derived from a time of peak 'greenness.' Had the imagery used been captured in the fall or early spring results would have likely been more accurate as leaf area would not have caused an oversaturation in values.

Textural values calculated from the original 1m 2008 NAIP imagery proved to be more accurate (61% overall accuracy) when used for condition assessment than that of the BV's and NDVI. Noting that BV's from the 6m resampled imagery worked only 5% worse than texture values alone, the two variables were combined to create a condition index. First however, BV's were re-obtained from the original 1 meter 2008 NAIP imagery. Using this index, it was determined that condition assessments from the vertical view could be made with about 72% accuracy when compared to ground truth condition assessments. This confirms the hypothesis that textural values would correlate more significantly with ground truth assessments as compared to green spectral reflectance or NDVI alone.

After proving that the condition index performed more successfully than the other two assessments it was decided to use the resulting windbreak condition classes to determine how many hectares of each condition class existed in an area of highly erodible and impaired soils. Approximately 341 (83%) of the 409.5 hectares of windbreaks identified were found to exist in these impaired areas. Having discovered this, the hypothesis that over 50% of total windbreaks in Ford County existed in impaired areas, was confirmed.

It can be said that the object-based approach to classifying windbreaks confirmed the hypothesis that it would perform in a more rapid manner than 'heads-up' digitizing. The object-based approach took raw imagery and produced a windbreak classification within approximately one hour of processing time. This of course was after weeks of experimentation to implement

the optimal segmentation and classification parameters. The 'heads-up' digitizing process can take much longer based on the level of experience held by the user. In addition, the object-based approach eliminates much of the subjectivity encountered in a 'heads-up' digitizing environment. Hopefully, this research will be of great value to the KFS as they move forward with future windbreak inventory analysis and windbreak renovation/restoration programs. The idea is that by locating windbreaks using remote sensing and GIS methods that vast amounts of field survey time will be alleviated and more time can be spent renovating instead of dragging out long timely field surveys to locate and assess windbreaks individually.

CHAPTER 7 - References

- Adkins, Z. 2008. *Image Compression Information Sheet*. United States Department of Agriculture. http://www.fsa.usda.gov/Internet/FSA_File/compression_2006_updatep.pdf.
- Anderson, J.R., E.E., Hardy, J.T., Roach, and R.E. Witmer. 1976. A land use and land cover classification system for use with remote sensor data. *Geological Survey Professional Paper 964*. Washington, DC: United States Government Printing Office.
- Atchison R. 2008. (KFS Rural Forestry Coordinator). 2008. Personal communication. 06 March.
- Atchison R. 2009. (KFS Rural Forestry Coordinator). 2008. Personal communication. 05 May.
- Baatz, M. 2006. Object-oriented image analysis for high content screening: Detailed quantification of cells and sub cellular structures with the Cellenger software. *Cytometry Part A* 69(A):652-658.
- Baatz, M., U. Benz, S. Dehghani, M. Heynen, A. Höltje, P. Hofmann, I. Lingenfelder, M. Mimler, M. Sohlbach, M. Weber, and G. Willhauck. 2004. *eCognition Professional: User Guide 4*. Munich, Germany: Definiens-Imaging.
- Bates, C.G. 1924. The Windbreak as a farm asset. *Farmers Bulletin*: No. 1405. U.S. Department of Agriculture.
- Benz, U., P. Hofmann, G. Willhauck, I. Lingenfelder, M. Heynen. 2004. Multi-resolution, object-oriented fuzzy analysis of remote sensing data for GIS-ready information. *Journal of Photogrammetry & Remote Sensing* 58:239-258.
- Bernad, G.P., L. Denise., and P. Réfrégier. 2009. Hierarchical feature-based classification approach for fast and user-interactive SAR image interpretation. *IEEE Geoscience and Remote Sensing Letters* 6(1):117-121.

- Booyesen, F. 2002. An overview and evaluation of composite indices of development. *Social Indicators Research* 59(2):115-151.
- Blashke, Thomas, Charles Burnett, and Anssi Pekkarinen. 2004. Image segmentation methods for object-based analysis and classification. *Remote Sensing Image Analysis: Including the Spatial Domain*. Netherlands: Academic Publishers.
- Brandle, J.R., L. Hodges, and X.H. Zhou. 2004. Windbreaks in North American agricultural systems. *Agroforestry Systems* 61:65-78.
- Brandle, J.R., B.B. Johnson, and D.D. Dearmont. 1982. Field windbreak economics. *Proceedings of the 34th Annual Meeting of the Forestry Committee*. June 22-24. Dodge City, Kansas. 199-212.
- Chang, K.T. 2006. *Introduction to Geographic Information Systems* (3rd Edition). New York, NY: McGraw –Hill Companies, Inc.
- Cihlar, J., L. St.-Laurent, and J.A. Dyer. 1991. Relation between the Normalized Difference Vegetation Index and ecological variables. *Remote Sensing of Environment* 35:279-298.
- Congalton, R.G. 1991. A Review of assessing the accuracy of classifications of remotely sensed data. *Remote Sensing of the Environment* 37:35-46.
- Congalton, R.G. and K. Green. 1999. *Assessing the Accuracy of Remotely Sensed Data: Principles and Practices*. Boca Raton, FL: Lewis Publishers.
- Cornelis, W.M., and D. Gabriels. 2004. Optimal windbreak design for wind-erosion control. *Journal of Arid Environments* 61:315-332.
- Croker, Tom. 1991. *The Great Plains Shelterbelt*. Greeneville, TN: Artistic Printers.
- Cutter, S.L., R. Golledge, and W. Graff. 2004. The big questions in geography. *The Professional Geographer* 54(3):305-317.

- De Roeck, T., T. Van de Voorde., and F. Canters. 2009. Full hierarchic versus non-hierarchic classification approaches for mapping sealed surfaces at the rural-urban fringe using high-resolution satellite data. *Sensors* 9:22-45.
- Diner, J.D., G.P. Asner, R. Davies, Y. Knyazikhin, J.P. Muller, A.W. Nolin, B. Pinty, C.B. Schaaf, and J. Stroeve. 1999. New directions in earth observing: Scientific applications of multiangle remote sensing. *Bulletin of the American Meteorological Society* 80(11):2209-2228.
- Dodgson, N.A. 1992. *Image Resampling*. Technical Report: Number 261. Cambridge: University of Cambridge.
- Drăgut, L., and T. Blashke. 2006. Automated classification of landform elements using object-based image analysis. *Geomorphology* 81:330-344.
- Droze, W.H. 1977. *Trees, Prairies, and People: A History of Tree Planting in the Plains States*. Denton, TX: USDA Forest Service and Texas Woman's University Press.
- Duda, R.O., P.E. Hart, and D.G. Stork. 2001. *Pattern Classification* (2nd Edition). New York: John Wiley & Sons.
- Evenson, R.E., and D. Gollin. 2003. Assessing the impact of the green revolution, 1960 to 2000. *Science* 300(5620):758-762.
- Famiglietti, J.S., J.A. Devereaux, C.A. Laymon, T. Tsegaye, P.R. Houser, T.J. Jackson, S.T. Graham, M. Rodell, and P.J. van Oevelen. 1999. Ground-based investigation of soil moisture variability within remote sensing footprints during the Southern Great Plains 1997 (SGP97) Hydrology Experiment. *Water Resources Research* 35(6):1839-1851.
- Fitzpatrick-Lins, K. 1981. Comparison of sampling procedures and data analysis for a land-use and land-cover map. *Photogrammetric Engineering & Remote Sensing* 47(3):343-351.
- Flora, S.D. 1948. Climate of Kansas. *Report of the Kansas Board of Agriculture* 67(285) June.

- Geospatial Data Abstraction Library. 2009. *GTiff—GeoTIFF File Format*.
http://www.gdal.org/frmt_gtiff.html. Last updated May 2009.
- Golledge, R.G. 2002. The nature of geographic thought. *Annals of the Association of American Geographers* 92(1):1-14.
- Goodin D.G., J. Harrington Jr., B. Rundquist. 2002. Landcover change and associated trends in surface reflectivity and vegetation index in Southwest Kansas: 1972-1992. *Geocarto International* 17(1):45-52.
- Goodin D.G., J.E. Mitchell, M.C. Knapp, and R.E. Bivens. 1995. *Climate and Weather Atlas of Kansas: An Introduction*. Educational Series 12. Lawrence, KS: Kansas Geological Survey.
- Great Plains Initiative Inventory Project. 2008. *Data Collection Procedures, Field Guide Version 1.0*.
- Harrington J. Jr., D.E. Kromm, L.M.B. Harrington, D.G. Goodin, S.E. White. 2003. *Global Change and Southwestern Kansas: Local Emissions and Non-Local Determinants*. Global Change and Local Places: Estimation, Understanding, and Reducing Greenhouse Gases. Cambridge: Cambridge University Press.
- Harrington L.M.B. 2001. Attitudes toward climate change: major emitters in southwestern Kansas. *Climate Research* 16:113-122.
- Hsu, Chih-Wei., C-C, Chang, and C-J, Lin. 2008. *A Practical Guide to Support Vector Classification*. Department of Computer Science. National Taiwan University, Taipei 106, Taiwan. (<http://www.csie.ntu.edu.tw/~cjlin>).
- Huang, X. and L. Zhang. 2008. An adaptive mean shift analysis approach for object extraction and classification from urban hyperspectral imagery. *IEEE Transactions on Geoscience and Remote Sensing* 46(12):4173-4185.

- Huete, A.R., and H.Q., Liu. 1994. An error and sensitivity analysis of the atmospheric-and soil-correcting variants of the NDVI for the MODIS-EOS. *IEEE transactions on Geoscience and Remote Sensing* 32(4):897-905.
- Hutchinson, J.M.S., R. Atchison, M. Dulin, and R. Aslin. 2008. *Forest Stewardship Spatial Analysis Project: Methodology Report for Kansas*. Manhattan, KS: Kansas Forest Service.
- ITT Visual Information Solutions. 2007. *An Interval Based Attribute Ranking Technique*. An ITT-VIS White Paper. July.
- ITT Visual Information Solutions. 2008. *ENVI Feature Extraction Module User's Guide*. December Edition. Colorado Springs, CO.
- Jäger, G. and U. Benz. 2000. Measures of classification accuracy based on fuzzy similarity. *IEEE Transactions on Geoscience and Remote Sensing* 38(3):1462-1467.
- Jensen J.R. 1983. Biophysical remote sensing. *Annals of the Association of American Geographers* 73(1):111-132.
- Jensen J.R. 2005. *Introductory Digital Image Processing: A Remote Sensing Perspective* (3rd Edition). Upper Saddle River, NJ: Prentice-Hall.
- Jensen J.R. 2007. *Remote Sensing of the Environment: An Earth Resource Perspective* (2nd Edition). Upper Saddle River, NJ: Prentice-Hall.
- Jensen, M. 1954. The model law for phenomena in the natural wind. *Ingeniören* 2:121-128.
- Kallas, M. (Senior Sales Associate, MJ Harden: A GeoEye Company). 2008. Personal Communication. 08 May.
- Kermad, C.D. and K. Chehdi. 2002. Automatic image segmentation system through iterative edge-region co-operation. *Image and Vision Computing* 20:541-555.

- Koch, D.E., R.L. Mohler, and D. Goodin. 2007. Stratifying land use/land cover for spatial analysis of disease ecology and risk: An example using object-based classification techniques. *Geospatial Health* 2(1):15-28.
- Kort, J. and C. Stefner. 2007. *A Protocol for Shelterbelt Assessment Related to its Function. When Trees and Crops Get Together*. Proceedings of the 10th North American Agroforestry Conference, Québec City, Canada, June 10-13.
- Landgrebe, D.A. 2003. *Signal Theory Methods in Multispectral Remote Sensing*. Chapter 1: Introduction and Background. Ed. J.A. Kong. Toronto: John Wiley & Sons.
- Liu, H.Q. and A. Huete. 1995. A feedback based modification of the NDVI to minimize canopy background and atmospheric noise. *IEEE Transactions on Geoscience and Remote Sensing* 33(2):457-465.
- Mathews, L. and D. Davids. 2007. *The National Agriculture Imagery Program (NAIP): Options and Challenges*. Proceedings from the 2007 ESRI International Users' Conference. San Diego, CA, USA, June 18-22.
- Moran, M.S., Y. Inoue, and E.M. Barnes. 1997. Opportunities and Limitations for Image-Based Remote Sensing in Precision Crop Management. *Remote Sensing of the Environment* 61:319-346.
- National Climactic Data Center. 2009. U.S. Tornado Climatology. <http://www.ncdc.noaa.gov/oa/climate/severeweather/tornadoes.html>. Last updated 08 October 2008.
- OverWatch Textron Systems. 2008. *Feature Analyst Reference Manual: 4.2 for ArcGIS*. Missoula, MT: Visual Learning Systems.
- Parker, J.A., R.V. Kenyon, and D.E. Troxel. 1983. Comparison of Interpolating Methods for Image Resampling. *IEEE Transactions on Medical Imaging* MI-2(1):31-39.

- Pattison, W.D. 1963. The four traditions of geography. *Journal of Geography* 63(5):211-216.
- Quattrochi, D.A., S.J. Walsh, J.R. Jensen, and M.K. Ridd. 2003. *Remote Sensing*. Chapter 25 in *Geography in America*, Gaile, G. and C.J. Wilmot, eds. Oxford: Oxford University Press.
- Radoux, J. and P. Defourny. 2007. A quantitative assessment of boundaries in automated forest stand delineation using very high resolution imagery. *Remote Sensing of Environment* 110:468-475.
- Read, R. 1958. The Great Plains shelterbelt in 1954: Are-evaluation of field windbreaks planted between 1935 and 1942 and a suggested research program. *Great Plains Agricultural Council No. 16*.
- Richards, J.A., J. Xiuping. 2005. *Remote Sensing digital Image Analysis: An Introduction* (4th Edition). Berlin: Springer-Verlag.
- Robinson, D.J., N.J. Redding, and D.J. Crisp. 2002. *Implementation of a fast algorithm for segmenting SAR imagery*. Scientific and Technical Report, 01 January 2002. Australia: Defense Science and Technology Organization.
- Rostoker, G., J.C. Samson, F. Creutzberg, T.J. Hughes, D.R. McDiarmid, A.G. McNamara, A. Vallance Jones, D.D. Wallis, and L.L. Cogger. 1995. CANOPUA-A ground-based instrument array for remote sensing the high latitude ionosphere during the ISTP/GGS program. *Space Science Reviews* 71:743-760.
- Rouse, J.W., R.H., Haas, J.A., Schell, and D.W. Deering. 1974. *Monitoring Vegetation Systems in the Great Plains with ERTS*. Proceedings, Third Earth Resources Technology Satellite-1 Symposium, Greenbelt: NASA SP-351, 3010-3017
- Rutherford, P. and L. Rapoza. 2008. An evaluation of an object-oriented paradigm for landuse/landcover classification. *The Professional Geographer* 60(1):87-100.
- Saloutos, T., 1969. The New Deal and farm policy in the Great Plains. *Agricultural History* 43(3):345-356.

- Schowengerdt, R.A. 2007. *Remote Sensing: Models and Methods for Image Processing* (3rd Edition). Boston, MA: Academic Press.
- Sorenson, C.J., G.A. Marotz. 1977. Changes in shelterbelt mileage statistics over four decades in Kansas. *Journal of Soil and Water Conservation* 32(6):276-281.
- Stoeckeler, J.H., and R.A. Williams. 1949. Windbreaks and shelterbelts. *Year Book of Agriculture 1949* 191-199.
- Temat, R. (Supervisory District Conservationist, Natural Resource Conservation Service). 2008. Personal communication. 06 June.
- Tian, J. and D.M. Chen. 2007. Optimization in multi-scale segmentation of high-resolution satellite images for artificial feature recognition. *International Journal of Remote Sensing* 28(20):4625-4644.
- Ticknor, K.A. 1989. Federal perspective of windbreak renovation. *Windbreak Renovation, Great Plains Agriculture Council* 128:1-3.
- U.S. Census Bureau. 2009. American Fact Finder; Population Finder.
<http://factfinder.census.gov>
- United States Department of Agriculture (USDA). 2008. *National Agriculture Information Sheet*. http://www.fsa.usda.gov/Internet/FSA_File/naip_2007_infosheetpdf.pdf. Last accessed May 2009.
- United States Department of Agriculture (USDA). 1994. *Summary Report 1992 National Resources Inventory*. July
- Wang, F. 1990. Improving remote-sensing image-analysis through fuzzy information representation. *Photogrammetric Engineering and Remote Sensing* 56(8):1163-1169.
- Wiseman, G.S., J. Kort, D.J. Walker, J.S. Powers, and C.N. Stefner. 2007. *Quantification of Shelterbelt Characteristics Using High Resolution Imagery*. When Trees and Crops Get

Together. Proceedings of the 10th North American Agroforestry Conference, Québec City, Canada, June 10-13.

Whiteside T., and W. Ahmad. 2005. *A comparison of object-oriented and pixel-based classification methods for mapping land cover in northern Australia*. Proceedings of SSC 2005 Spatial Intelligence, Innovation and Praxis: The National Biennial Conference of the Spatial Sciences Institute. Melbourne: Spatial Sciences Institute. September

Woodhouse, C.A. and J.T. Overpeck. 1998. 2000 years of drought variability in the central United States. *Bulletin of the American Meteorological Society* 79(12):2693- 2714.

Appendix A - 2001 National Land Cover Dataset Landcover Codes and Descriptions

Taken from the 2001 National Landcover Dataset (NLCD) metadata published in 2007 by the U.S. Geological Survey, Sioux Falls, South Dakota.

NLCD 2001 Land Cover Class Definitions

11. Open Water - All areas of open water, generally with less than 25% cover of vegetation or soil.

12. Perennial Ice/Snow - All areas characterized by a perennial cover of ice and/or snow, generally greater than 25% of total cover.

21. Developed, Open Space - Includes areas with a mixture of some constructed materials, but mostly vegetation in the form of lawn grasses. Impervious surfaces account for less than 20 percent of total cover. These areas most commonly include large-lot single-family housing units, parks, golf courses, and vegetation planted in developed settings for recreation, erosion control, or aesthetic purposes

22. Developed, Low Intensity - Includes areas with a mixture of constructed materials and vegetation. Impervious surfaces account for 20-49 percent of total cover. These areas most commonly include single-family housing units.

23. Developed, Medium Intensity - Includes areas with a mixture of constructed materials and vegetation. Impervious surfaces account for 50-79 percent of the total cover. These areas most commonly include single-family housing units.

24. Developed, High Intensity - Includes highly developed areas where people reside or work in high numbers. Examples include apartment complexes, row houses and commercial/industrial. Impervious surfaces account for 80 to 100 percent of the total cover.

31. Barren Land (Rock/Sand/Clay) - Barren areas of bedrock, desert pavement, scarps, talus, slides, volcanic material, glacial debris, sand dunes, strip mines, gravel pits and other accumulations of earthen material. Generally, vegetation accounts for less than 15% of total cover.

41. Deciduous Forest - Areas dominated by trees generally greater than 5 meters tall, and greater than 20% of total vegetation cover. More than 75 percent of the tree species shed foliage simultaneously in response to seasonal change.

42. Evergreen Forest - Areas dominated by trees generally greater than 5 meters tall, and greater than 20% of total vegetation cover. More than 75 percent of the tree species maintain their leaves all year. Canopy is never without green foliage.

43. Mixed Forest - Areas dominated by trees generally greater than 5 meters tall, and greater than 20% of total vegetation cover. Neither deciduous nor evergreen species are greater than 75 percent of total tree cover.

52. Shrub/Scrub - Areas dominated by shrubs; less than 5 meters tall with shrub canopy typically greater than 20% of total vegetation. This class includes true shrubs, young trees in an early successional stage or trees stunted from environmental conditions.

71. Grassland/Herbaceous - Areas dominated by grammanoid or herbaceous vegetation, generally greater than 80% of total vegetation. These areas are not subject to intensive management such as tilling, but can be utilized for grazing.

81. Pasture/Hay - Areas of grasses, legumes, or grass-legume mixtures planted for livestock grazing or the production of seed or hay crops, typically on a perennial cycle. Pasture/hay vegetation accounts for greater than 20 percent of total vegetation.

82. Cultivated Crops - Areas used for the production of annual crops, such as corn, soybeans, vegetables, tobacco, and cotton, and also perennial woody crops such as orchards and vineyards. Crop vegetation accounts for greater than 20 percent of total vegetation. This class also includes all land being actively tilled.

90. Woody Wetlands - Areas where forest or shrubland vegetation accounts for greater than 20 percent of vegetative cover and the soil or substrate is periodically saturated with or covered with water.

95. Emergent Herbaceous Wetlands - Areas where perennial herbaceous vegetation accounts for greater than 80 percent of vegetative cover and the soil or substrate is periodically saturated with or covered with water.

Appendix B - Feature Attribute Description

Taken from “ENVI Feature Extraction Module User’s Guide (2008), ENVI Feature Extraction Preferences,” Copyright © ITT Visual Information Solutions.

Spatial Attributes

Attribute	Description
AREA	Total area of the polygon, minus the area of the holes. Values are in map units.
LENGTH	The combined length of all boundaries of the polygon, including the boundaries of the holes. This is different than the MAXAXISLEN attribute. Values are in map units.
COMPACT	A shape measure that indicates the compactness of the polygon. A circle is the most compact shape with a value of $1 / \pi$. The compactness value of a square is $1 / 2(\sqrt{\pi})$. $COMPACT = \sqrt{4 * AREA / \pi} / \text{outer contour length}$
CONVEXITY	Polygons are either convex or concave. This attribute measures the convexity of the polygon. The convexity value for a convex polygon with no holes is 1.0, while the value for a concave polygon is less than 1.0. $CONVEXITY = \text{length of convex hull} / LENGTH$
SOLIDITY	A shape measure that compares the area of the polygon to the area of a convex hull surrounding the polygon. The solidity value for a convex polygon with no holes is 1.0, and the value for a concave polygon is less than 1.0. $SOLIDITY = AREA / \text{area of convex hull}$
ROUNDNESS	A shape measure that compares the area of the polygon to the square of the maximum diameter of the polygon. The "maximum diameter" is the length of the major axis of an oriented bounding box enclosing the polygon. The roundness value for a circle is 1, and the value for a square is $4 / \pi$. $ROUNDNESS = 4 * (AREA) / (\pi * MAXAXISLEN^2)$
FORMFACTOR	A shape measure that compares the area of the polygon to the square of the total perimeter. The form factor value of a circle is 1, and the value of a square is $\pi / 4$. $FORMFACTOR = 4 * \pi * (AREA) / (\text{total perimeter})^2$
ELONGATION	A shape measure that indicates the ratio of the major axis of the polygon to the minor axis of the polygon. The major and minor axes are derived from an oriented bounding box containing the polygon. The elongation value for a square is 1.0, and the value for a rectangle is greater than 1.0. $ELONGATION = MAXAXISLEN / MINAXISLEN$

RECT_FIT	<p>A shape measure that indicates how well the shape is described by a rectangle. This attribute compares the area of the polygon to the area of the oriented bounding box enclosing the polygon. The rectangular fit value for a rectangle is 1.0, and the value for a non-rectangular shape is less than 1.0.</p> $\text{RECT_FIT} = \text{AREA} / (\text{MAXAXISLEN} * \text{MINAXISLEN})$
MAINDIR	<p>The angle subtended by the major axis of the polygon and the x-axis in degrees. The main direction value ranges from 0 to 180 degrees. 90 degrees is North/South, and 0 to 180 degrees is East/West.</p>
MAJAXISLEN	<p>The length of the major axis of an oriented bounding box enclosing the polygon. Values are map units of the pixel size. If the image is not georeferenced, then pixel units are reported.</p>
MINAXISLEN	<p>The length of the minor axis of an oriented bounding box enclosing the polygon. Values are map units of the pixel size. If the image is not georeferenced, then pixel units are reported.</p>
NUMHOLES	<p>The number of holes in the polygon. Integer value.</p>
HOLESOLRAT	<p>The ratio of the total area of the polygon to the area of the outer contour of the polygon. The hole solid ratio value for a polygon with no holes is 1.0.</p> $\text{HOLESOLRAT} = \text{AREA} / \text{outer contour area}$

Spectral Attributes

Attribute	Description
MINBAND_ <i>x</i>	Minimum value of the pixels comprising the region in band <i>x</i> .
MAXBAND_ <i>x</i>	Maximum value of the pixels comprising the region in band <i>x</i> .
AVGBAND_ <i>x</i>	Average value of the pixels comprising the region in band <i>x</i> .
STDBAND_ <i>x</i>	Standard deviation value of the pixels comprising the region in band <i>x</i> .

Texture Attributes

Attribute	Description
TX_RANGE	<p>Average data range of the pixels comprising the region inside the kernel. A kernel is an array of pixels used to constrain an operation to a subset of pixels. Refer to the Texture Kernel Size preference (see "ENVI Feature Extraction Preferences" on page 60).</p>
TX_MEAN	<p>Average value of the pixels comprising the region inside the kernel.</p>

TX_VARIANCE	Average variance of the pixels comprising the region inside the kernel.
TX_ENTROPY	Average entropy value of the pixels comprising the region inside the kernel. ENVI Zoom computes entropy, in part, from the Max Bins in Histogram preference.

Band Ratio Attributes

Attribute	Description
BANDRATIO	Values range from -1.0 to 1.0. See “Band Ratio” on page 30.
HUE	Hue is often used as a color filter and is measured in degrees from 0 to 360. A value of 0 is red, 120 is green, and 240 is blue.
SATURATION	Saturation is often used as a color filter and is measured in floating-point values that range from 0 to 1.0.
INTENSITY	Intensity often provides a better measure of brightness than using the AVGBAND_x spectral attribute. Intensity is measured in floating-point values from 0 to 1.0.

Appendix C - Attributes Selected For Classification

Taken from “ENVI Feature Extraction Module User’s Guide (2008), ENVI Feature Extraction Preferences,” Copyright © ITT Visual Information Solutions.

Attribute	Description
AREA	Total area of the polygon, minus the area of the holes. Values are in map units.
LENGTH	The combined length of all boundaries of the polygon, including the boundaries of the holes. This is different than the MAXAXISLEN attribute. Values are in map units.
COMPACT	A shape measure that indicates the compactness of the polygon. A circle is the most compact shape with a value of $1 / \pi$. The compactness value of a square is $1 / 2(\sqrt{\pi})$. $COMPACT = \text{Sqrt}(4 * AREA / \pi) / \text{outer contour length}$
CONVEXITY	Polygons are either convex or concave. This attribute measures the convexity of the polygon. The convexity value for a convex polygon with no holes is 1.0, while the value for a concave polygon is less than 1.0. $CONVEXITY = \text{length of convex hull} / LENGTH$
ROUNDNESS	A shape measure that compares the area of the polygon to the square of the maximum diameter of the polygon. The "maximum diameter" is the length of the major axis of an oriented bounding box enclosing the polygon. The roundness value for a circle is 1, and the value for a square is $4 / \pi$. $ROUNDNESS = 4 * (AREA) / (\pi * MAXAXISLEN^2)$
ELONGATION	A shape measure that indicates the ratio of the major axis of the polygon to the minor axis of the polygon. The major and minor axes are derived from an oriented bounding box containing the polygon. The elongation value for a square is 1.0, and the value for a rectangle is greater than 1.0. $ELONGATION = MAXAXISLEN / MINAXISLEN$
RECT_FIT	A shape measure that indicates how well the shape is described by a rectangle. This attribute compares the area of the polygon to the area of the oriented bounding box enclosing the polygon. The rectangular fit value for a rectangle is 1.0, and the value for a non-rectangular shape is less than 1.0. $RECT_FIT = AREA / (MAXAXISLEN * MINAXISLEN)$
MAINDIR	The angle subtended by the major axis of the polygon and the x-axis in degrees. The main direction value ranges from 0 to 180 degrees. 90 degrees is North/South, and 0 to 180 degrees is East/West.

MAJAXISLEN	The length of the major axis of an oriented bounding box enclosing the polygon. Values are map units of the pixel size. If the image is not georeferenced, then pixel units are reported.
MINAXISLEN	The length of the minor axis of an oriented bounding box enclosing the polygon. Values are map units of the pixel size. If the image is not georeferenced, then pixel
HOLESOLRAT	The ratio of the total area of the polygon to the area of the outer contour of the polygon. The hole solid ratio value for a polygon with no holes is 1.0. $\text{HOLESOLRAT} = \text{AREA} / \text{outer contour area}$
MINBAND_x	Minimum value of the pixels comprising the region in band <i>x</i> .
MAXBAND_x	Maximum value of the pixels comprising the region in band <i>x</i> .
AVGBAND_x	Average value of the pixels comprising the region in band <i>x</i> .
STDBAND_x	Standard deviation value of the pixels comprising the region in band <i>x</i> .
TX_MEAN	Average value of the pixels comprising the region inside the kernel.
TX_VARIANCE	Average variance of the pixels comprising the region inside the kernel.
BANDRATIO	Values range from -1.0 to 1.0. See “Band Ratio” on page 30.
HUE	Hue is often used as a color filter and is measured in degrees from 0 to 360. A value of 0 is red, 120 is green, and 240 is blue.
SATURATION	Saturation is often used as a color filter and is measured in floating-point values that range from 0 to 1.0.
INTENSITY	Intensity often provides a better measure of brightness than using the AVGBAND_x spectral attribute. Intensity is measured in floating-point values from 0 to 1.0.

Appendix D - Procedures for using the ENVI Zoom 4.5 *Feature Extraction Module*

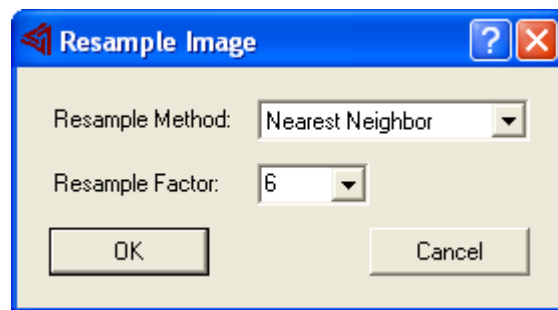
1. Imagery Collection

To obtain aerial imagery for Kansas Counties go to www.kansasgis.org. Click on the 'Browse and Download' data tap, this will prompt a new window where the 'Imagery' Tab should be selected. Look for the 2008 NAIP Imagery tab and select it. 105 zip folders labeled with Kansas County abbreviation will appear, select the county of interest and download the zip folder. Inside the zip folder will be a .jp2 CCM of the county selected. Unzip the folder and save the contents.

2. Image Preprocessing

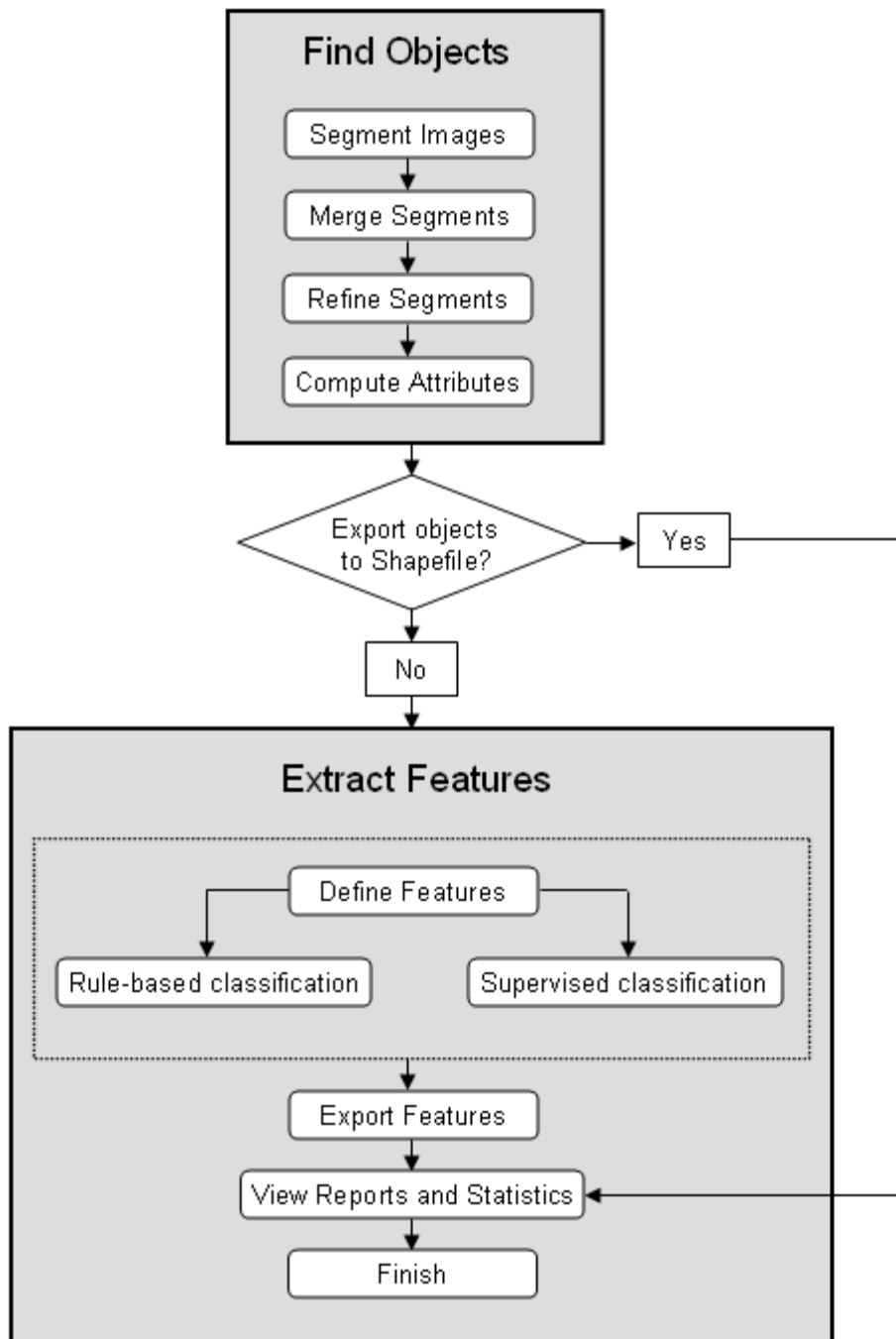
Because ENVI Zoom 4.5 *Feature Extraction Module* does not recognize .jp2 file formats the NAIP imagery must be converted to a compatible file format. To convert files to .tiff which the software will recognize the imagery must be reduced to less than 4GB.

Load the imagery into ArcGIS 9.3 and display bands 1,2, and 3. This will produce a true color composite. Next select the **Feature Analyst** tab → **Raster Tools** → **Resample Images**. A pop up window will appear next. Set the resample Method to Nearest Neighbor and the Resample factor to 6.



When the resampling algorithm has finished export the resulting image to .tiff format in ArcGIS 9.3. To do this, right click on the image file name in the Layers contents box and select 'Export Data.' In the window that appears name the file and save it as file type .tiff.

3. ENVI Zoom 4.5 Feature Extraction Work Flow

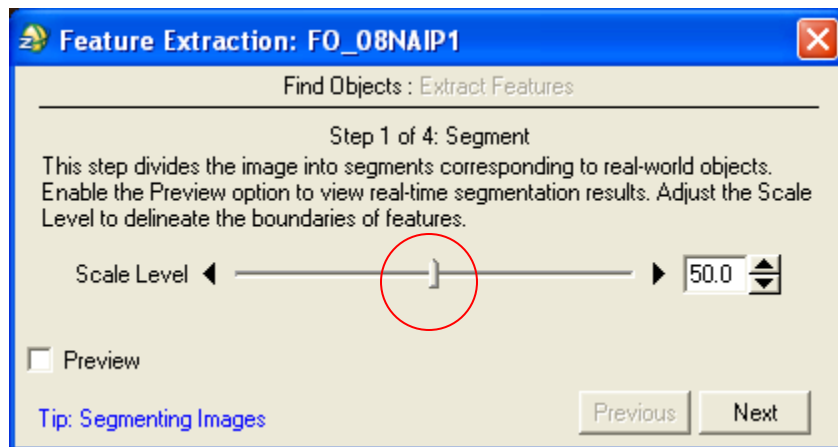


Source: ENVI Zoom *Feature Extraction Module* Users Guide (2008)

4. Image Segmentation, Merging, and Thresholding

Launch ENVI Zoom 4.5. Click on the 'File' tab and select 'Open...' Locate the resampled imagery and select the .tiff file. Click the 'Data Manager' button located just below the 'Edit' tab in the upper right corner of the display window. In the resulting dialog box begin by selecting the Red, Green, and Blue bands for display, this will ensure that you have a true color image to view during image processing (Note: information from the NRI band will be analyzed even if it is not displayed in the data view screen).

With the image displayed properly select **Processing** → **Feature Extraction**, in the resulting window select the .tiff image file for processing, click OK. Next a pop up window like the one below will appear (if the imagery changes color which it will reload the red, green, and blue bands as outlined earlier).



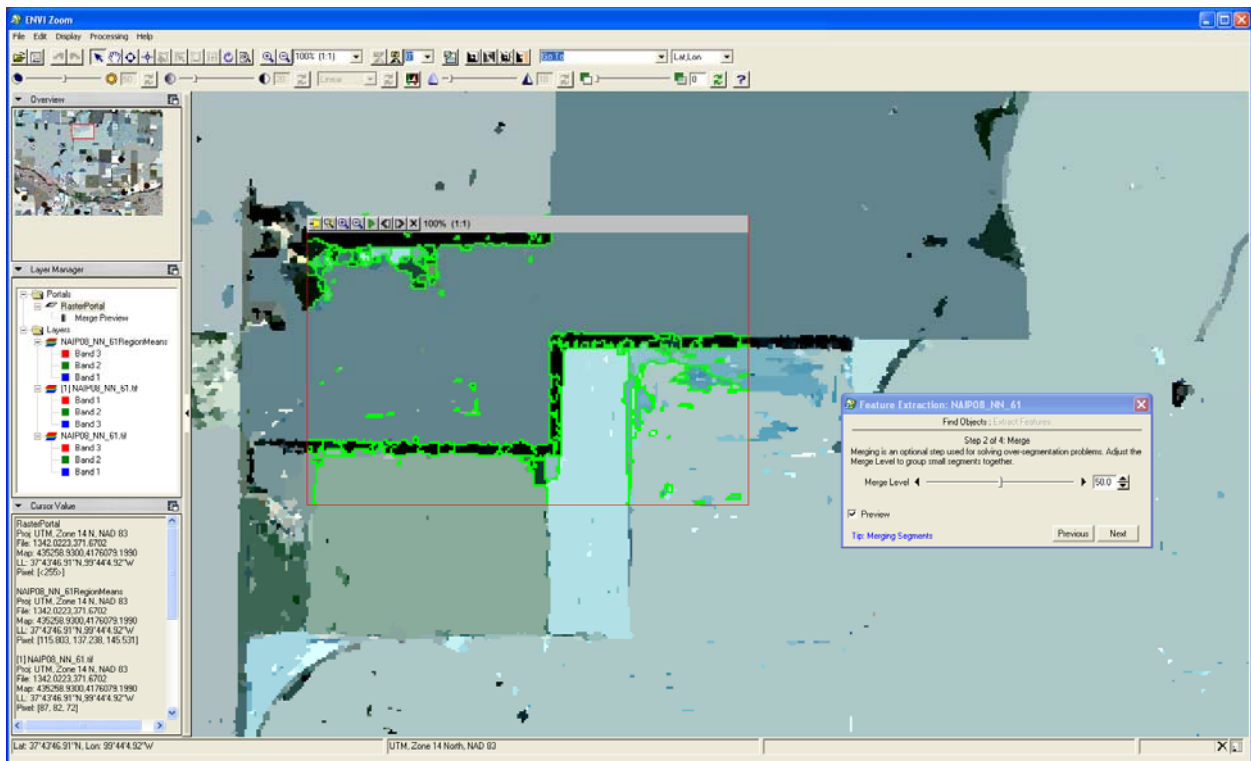
This is the segmentation parameter setting window. Move the slider bar circled in red to adjust scale level/parameter. Scale parameter is an area measure that determines how large of objects to select. Scale parameter values range from 0-100 with objects increasing as values move toward 100. For Ford County a Scale level of 78 was used. Click the preview box in the bottom left of the segmentation parameter setting box. A viewing portal outlined in red will appear in the middle of the data view screen. In this window segmentation results can be viewed 'on the fly.' Move the viewing portal throughout the imagery to ensure that the scale level settings are isolating windbreaks from neighboring fields throughout the image. The features outlined in green below will be objects created after the segmentation algorithm runs. When the desired scale level settings are set click the 'Next' button in the Segmentation parameter setting window.



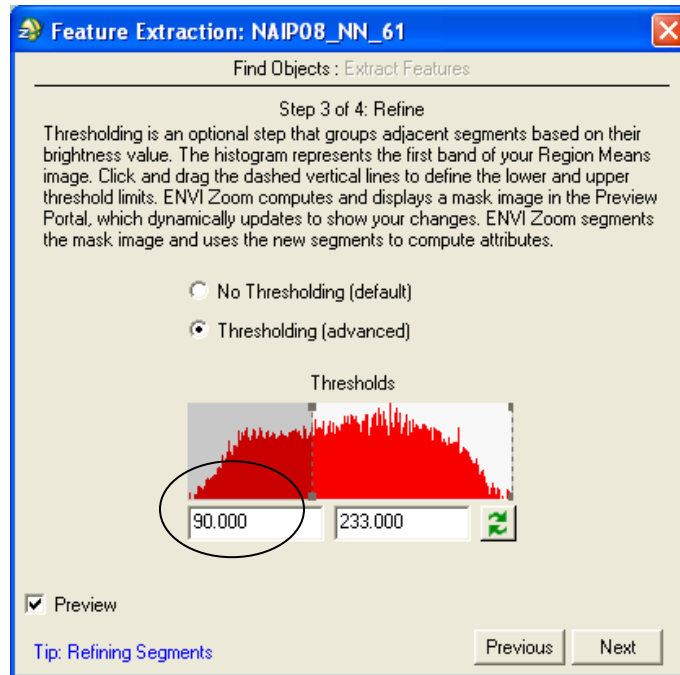
Once the segmentation process has completed a 'Merge Segments' window will appear as well as a 'Region Means' image. The Region Means objects contain mean BV's for all of the objects created in the segmentation process. The Merge Segments option allows smaller segments to be merged together with larger segments having similar spectral values. A merge factor of 50 was used to grasp the overall homogeneity of windbreaks in Ford County. (Depending on the nature of windbreaks in other counties, the merge factor may need to be reduced or increased)



Use the slider bar to adjust Merge Level just like in the Segmentation process. Notice how the object sizes have increased as the Merge level was placed at 50 in the image below. Click next in the Merge level window when the desired setting has been established.

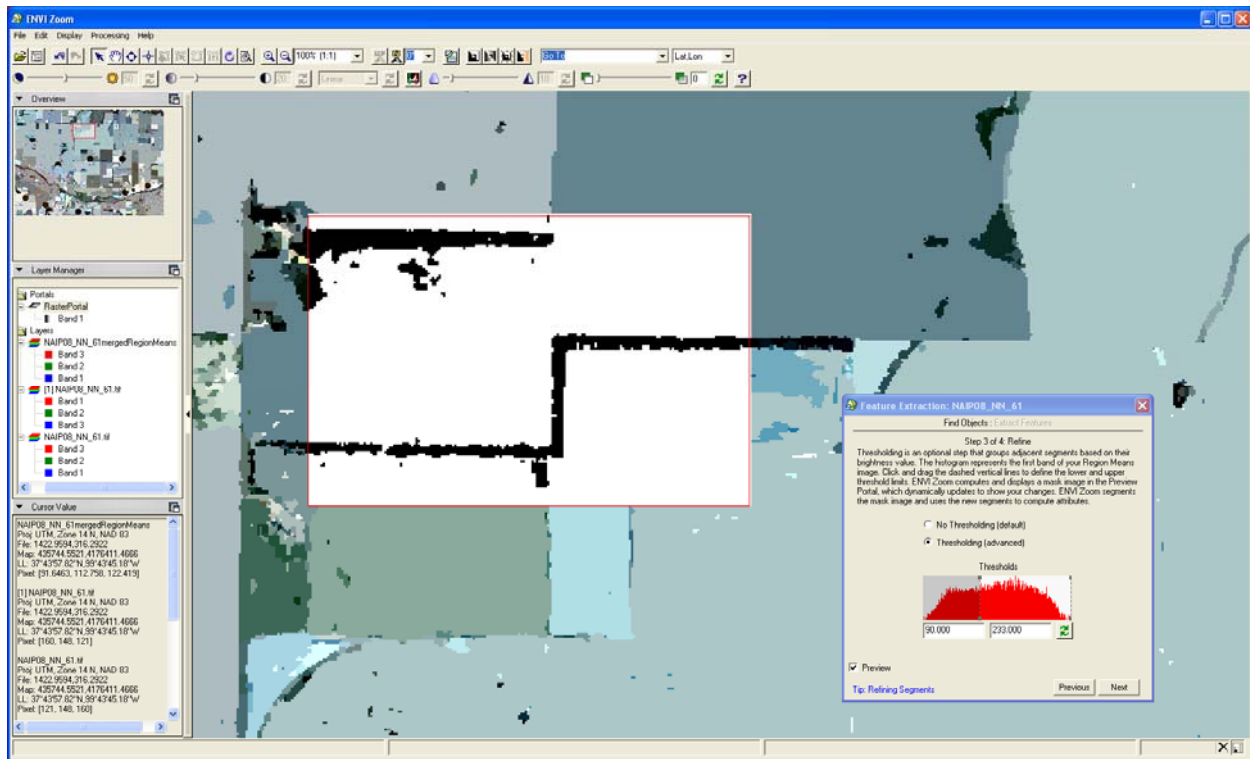


After merging is complete the option for 'Thresholding.' This options allows superfluous objects to be eliminated based on their 'Region Means' values.



Click the circle next to the Thresholding (advanced) option as seen in the image above.

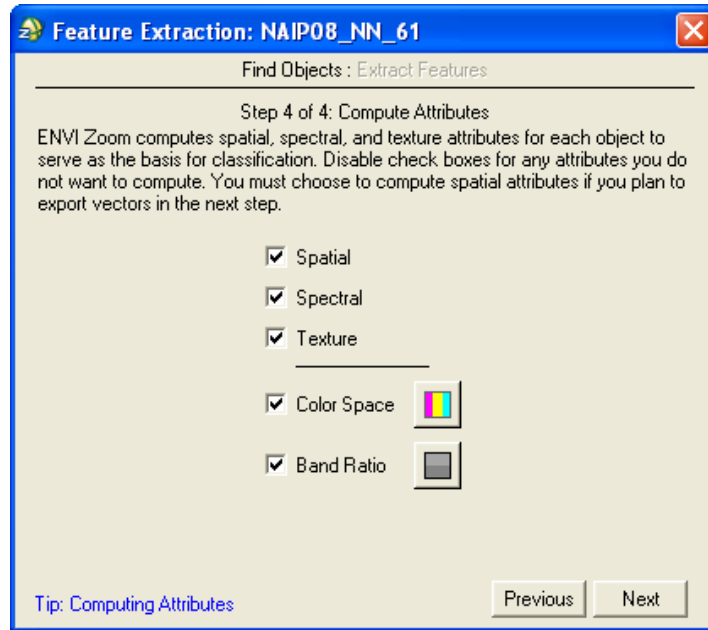
Increasing the minimum Region Means threshold will eliminate most impervious features such as roads, parking lots, buildings etc... all things that can cause confusion in future classification steps and slow down processing time. A minimum threshold value of 90 was use in Ford County, however this setting may need to be adjusted for other Counties just like the Scale level and Merge level parameters.



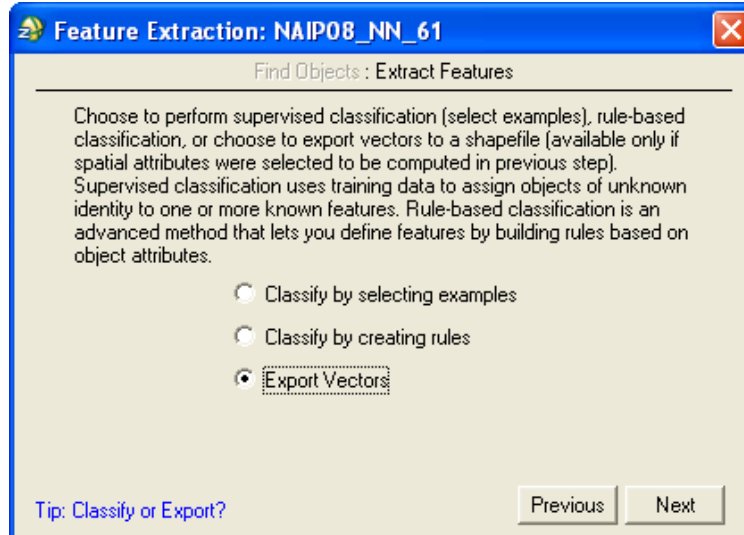
After setting the minimum threshold value, areas that will be masked from further analysis can be seen in white in the viewing portal. The black objects will remain. Note that the upper threshold limits should not be decreased, this could cause vegetative features to be eliminated. When the desired minimum threshold value has been established click Next. After Thresholding has processed the only remaining objects should be vegetative features.

5. Calculate Attributes

When the Threshold process is complete a 'Compute Attributes' window will appear. In this step select all of boxes next to the attribute options as seen in the image below. (Spatial, Spectral, Texture, Color Space, and Band Ratio) This step will calculate for all objects the attributes outlined in Appendix B. After selecting all the boxes click Next and the 'Compute Attributes' process will begin.

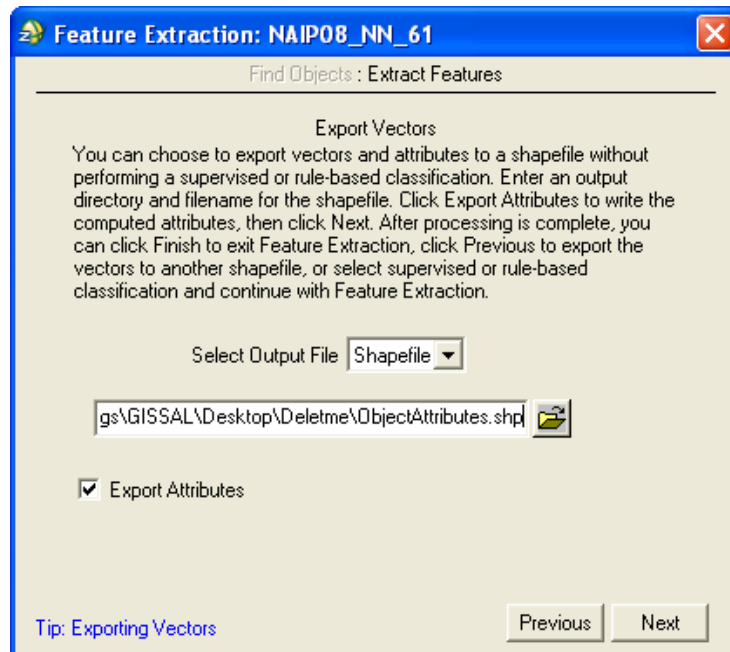


Next a window will appear with the option to 'Classify by selecting examples,' 'Classify by creating rules,' and 'Export Vector.' Select Export vectors as seen below and click Next.

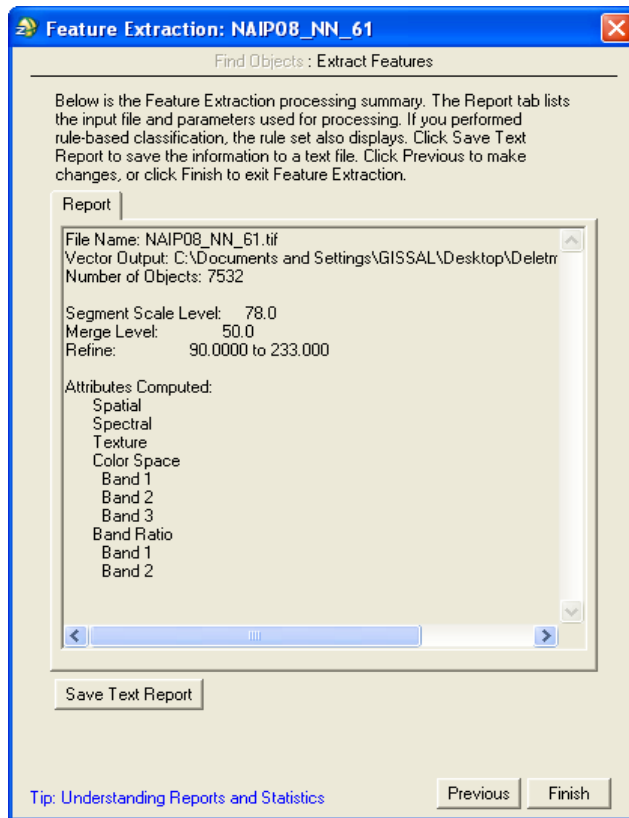


The *Feature Extraction Module* will not export the attributes that have been calculated after classifying the object in future steps. These attributes are only used within the software for classification, which is why it is very important to export the unclassified vectors that contain this information to ensure that a spatial data file will exist with such information. Click Next

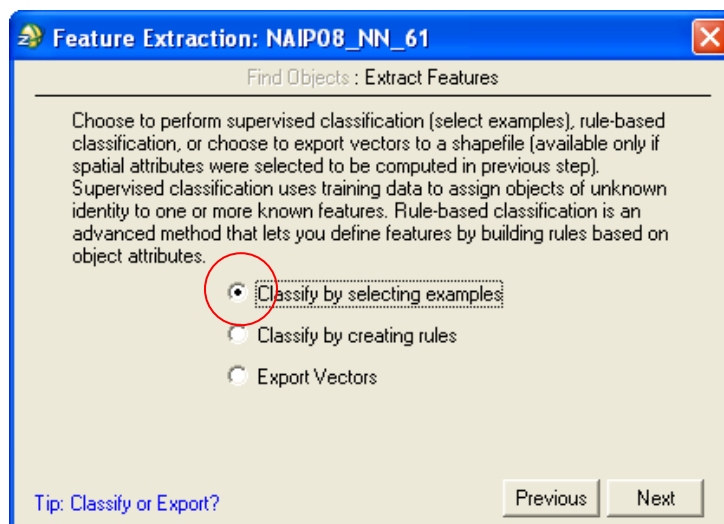
after selection 'Export Vectors.' A new window will appear, in the 'Select Output File' dialog box select 'Shapefile' from the dropdown menu. Choose the appropriate directory and name the file something like "object attributes." Also, Make sure to select the 'Export Attributes' box in the bottom left of this window. Click Next.



After the objects have been exported with their associated attributes the window below will appear. Select the 'Previous' tab.

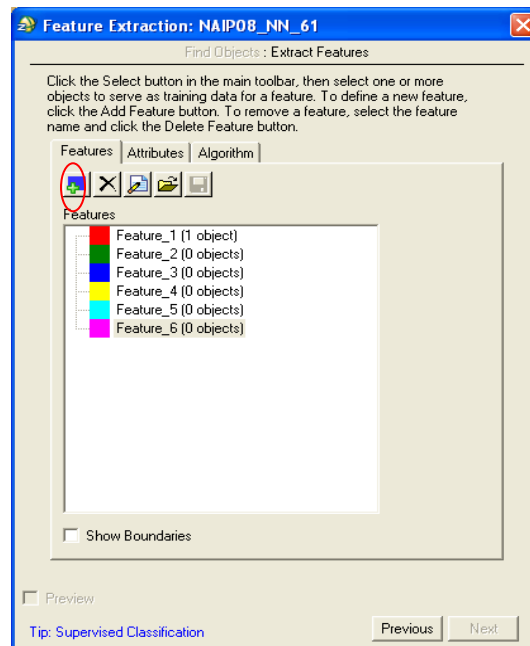


In the next window select the 'Previous' Tab on the bottom right again. After that the window offering the option to 'Classify by selection examples' will reappear. Select 'Classify by selecting examples' and click Next.

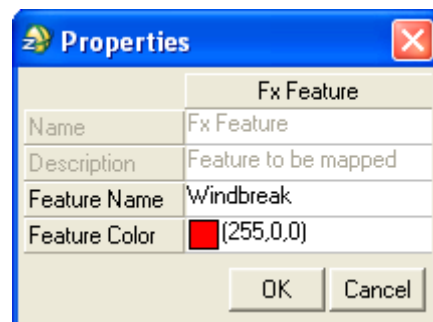


6. Supervised Classification of Objects

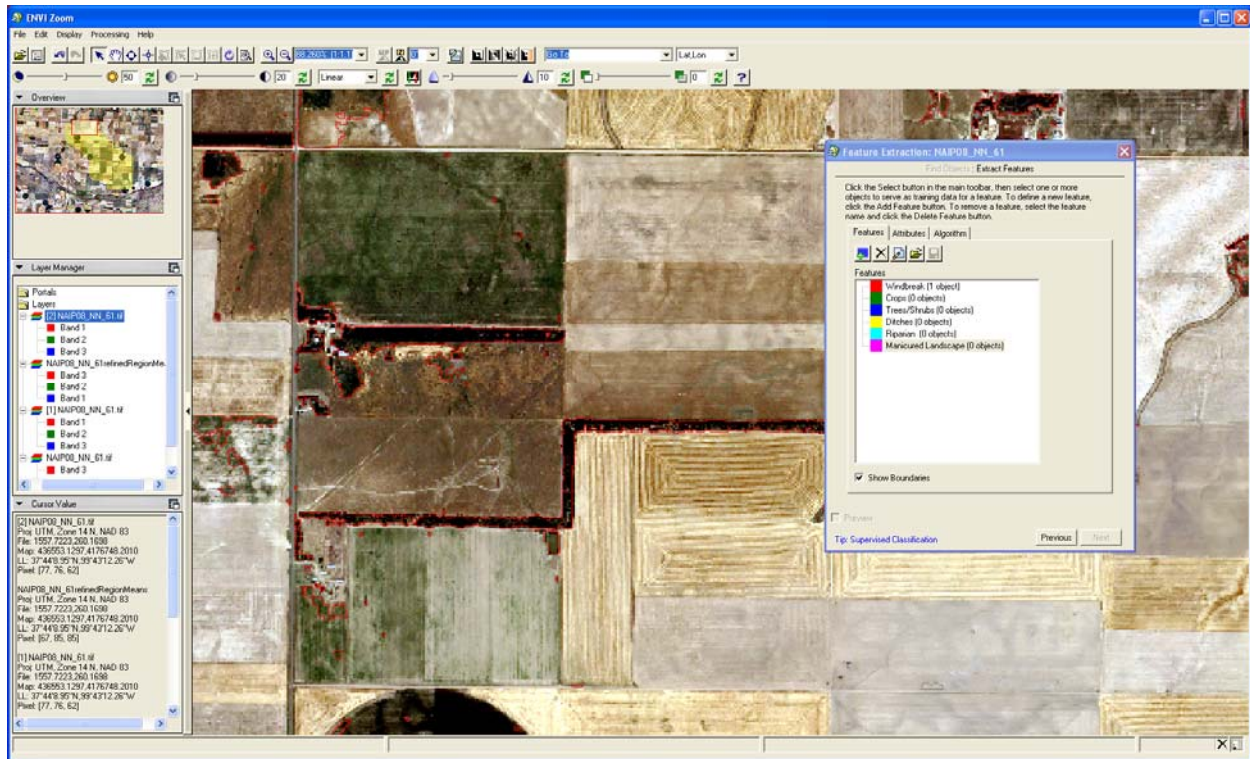
Next a Supervised Classification window will appear in which object classes must be established based on their underlying landcover/landuse. In Ford County 6 remaining land cover classes were identified after thresholding (Windbreak, Riparian Areas, Individual Tree/Shrub Stands, Manicured Landscapes, Crops, and Ditches). Additional classes may need to added or removed in different counties. In the window below click the ‘Add Feature’ button circled in red 6 times to establish 6classes.



To label the classes right click on the class labeled ‘Feature_1(1Object).’ The ‘Properties window of that feature will appear. In the ‘Feature Name’ dialog box type “Windbreak” and click OK. Repeat this step to label all the feature classes with their appropriate landcover name.

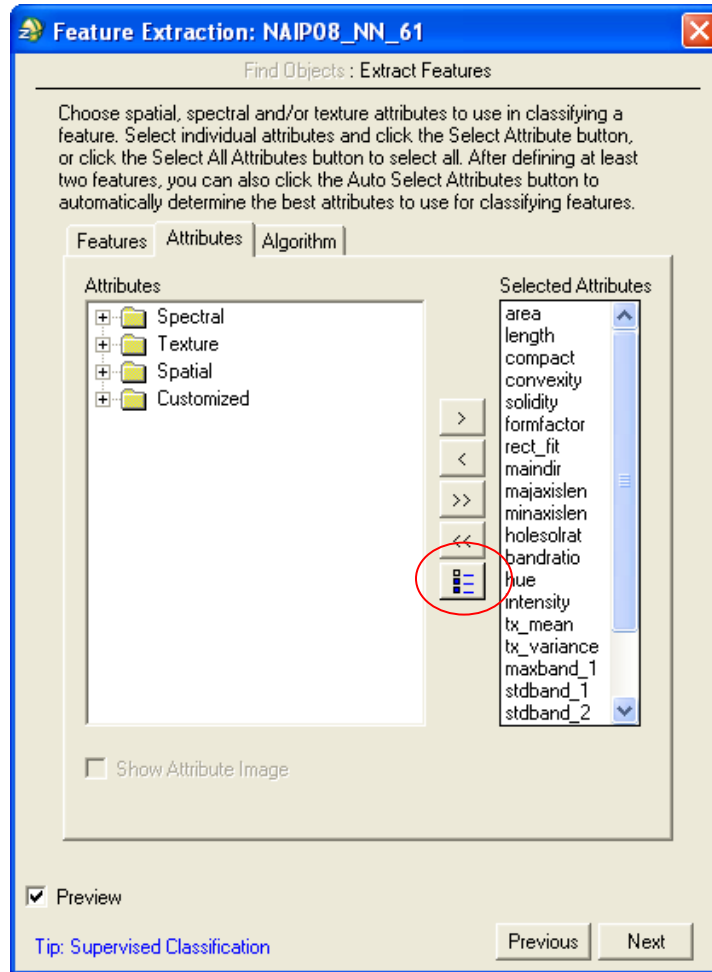


Next click the 'Show Boundaries' box in the bottom right of Supervised classification window.



The object boundaries will now be displayed in red and ready to be selected as training sites. To select training sites click on a landcover class in the Supervised Classification window then using the mouse pointer click on the features in the image that correspond with said landcover class. Select at least 10 training sites per feature class.

Once training sites have been selected click the 'Attributes' tab in the Supervised classification window. Select the 'Auto Select Attributes' button in the circled in red in the image below. This option statistically tests how well any given attribute can distinguish between a set of features then measures the significance of each attributes ability to distinguish between classes.



After classification attributes have been selected click the ‘Algorithm’ tab to the right of the ‘Attributes’ tab in the Supervised Classification window.

In the ‘Classification Algorithm’ dropdown menu select ‘Support Vector Machine’ (SVM) then in the ‘Kernel Type’ dropdown dialog box select ‘Radial Basis Function.’ Accept the rest of the default values concerning the SVM algorithm and click Next at the bottom the Supervised Classification window.

When the objects have all been classified a final window will appear, this is the Export Classification Results window (See Below). Select the ‘Export Vector Results’ and ‘Export features to a single layer’ box. Additionally make sure to select ‘Polygon’ as the feature type and

‘Shapefile’ as the output file format. Name the file something like “SVM_AllVectors” and save it in the appropriate directory.

